

AD-A047 289

NAVAL UNDERWATER SYSTEMS CENTER NEW LONDON CONN NEW --ETC F/G 17/2
OPERATING CHARACTERISTICS FOR DETECTION OF A FADING SIGNAL WITH--ETC(U)
OCT 77 A H NUTTALL
NUSC-TR-5739

UNCLASSIFIED

NL

1 of 2
ADA047289



NUSC Technical Report 5739

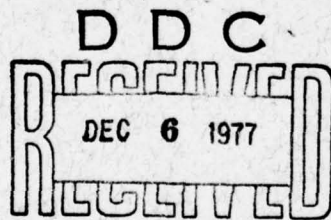
NUSC Technical Report 5739



AD A 0 4 7 2 8 9

Operating Characteristics for Detection of a Fading Signal With K Dependent Fades and D-Fold Diversity in M Alternative Locations

Albert H. Nuttall
Special Projects Department



25 October 1977

NUSC

NAVAL UNDERWATER SYSTEMS CENTER
Newport, Rhode Island • New London, Connecticut

AD NO. —
DDC FILE COPY

Approved for public release; distribution unlimited.

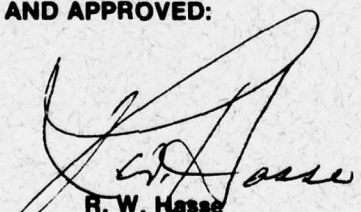
PREFACE

This research was conducted under NUSC Project No. A-616-05, "IACS Signal Design," Principal Investigator--C. D. Mason (Code 325), Subproject and Task No. S0252-CC, 17695, Program Manager--J. F. Calabrese (NAVSEA, SEA-661E); also, this research was conducted under NUSC Project No. A-752-05, "Applications of Statistical Communication Theory to Acoustic Signal Processing," Principal Investigator--Dr. A. H. Nuttall (Code 313), Navy Subproject and Task No. ZR-00-001, Program Manager: J. H. Probus (MAT 035), Naval Material Command.

The Technical Reviewer for this report was C. D. Mason (Code 325).

61152N

REVIEWED AND APPROVED:



R. W. Hasse

Head: Special Projects Department

The author of this report is located at the New London
Laboratory, Naval Underwater Systems Center,
New London, Connecticut 06320.

REPORT DOCUMENTATION PAGE		READ INSTRUCTIONS BEFORE COMPLETING FORM
1. REPORT NUMBER TR 5739 ✓	2. GOVT ACCESSION NO.	3. RECIPIENT'S CATALOG NUMBER 9
4. TITLE (and Subtitle) OPERATING CHARACTERISTICS FOR DETECTION OF A FADING SIGNAL WITH K DEPENDENT FADES AND D-FOLD DIVERSITY IN M ALTERNATIVE LOCATIONS.		4. TYPE OF REPORT & PERIOD COVERED Technical rept.
7. AUTHOR(s) Albert H. Nuttall		5. PERFORMING ORG. REPORT NUMBER
9. PERFORMING ORGANIZATION NAME AND ADDRESS Naval Underwater Systems Center ✓ New London Laboratory New London, CT 06320		6. CONTRACT OR GRANT NUMBER(s)
11. CONTROLLING OFFICE NAME AND ADDRESS Naval Sea Systems Command (SEA-661E) Washington, DC 20362	11	10. PROGRAM ELEMENT, PROJECT, TASK AREA & WORK UNIT NUMBERS A-616-05 A-752-05
14. MONITORING AGENCY NAME & ADDRESS (if different from Controlling Office) 14 NUSC-TR-5739		12. REPORT DATE 25 October 1977
		13. NUMBER OF PAGES 100
		15. SECURITY CLASS. (of this report) UNCLASSIFIED
		15a. DECLASSIFICATION/DOWNGRADING SCHEDULE
16. DISTRIBUTION STATEMENT (of this Report) Approved for public release; distribution unlimited		1298p.
17. DISTRIBUTION STATEMENT (of the abstract entered in Block 20, if different from Report) 16 S0252, 2R00001 17 S0252CC		
18. SUPPLEMENTARY NOTES		
19. KEY WORDS (Continue on reverse side if necessary and identify by block number) Correct-Decision Probability Multiple Alternatives Dependent Signal Fading Operating Characteristics Detection of Fading Signal Optimum Processor Diversity Partially Dependent Fading False-Alarm Probability		
20. ABSTRACT (Continue on reverse side if necessary and identify by block number) The probabilities of correct decision and false alarm for a fading signal with K dependent fades and D-fold diversity in M alternative locations are derived and numerically evaluated for a variety of values of K, M, and D, and for a wide range of signal-energy-to-noise-density ratio. It is found that the degradation in performance relative to that for K = 1 (NUSC Technical Report 4793) is given by approximately 3.5 log(K) dB, in terms of required additional input signal-to-noise ratio to maintain the same error probabilities.		

↙ The form of the optimum processor for $K = 2$ is derived; although it is not difficult to implement, it needs knowledge about the absolute levels of signal and noise and is very difficult to analyze in terms of error probabilities.

For partially dependent signal fading and general K , the characteristic function of the decision variables is derived in closed form; however, no numerical evaluations are attempted for this generalization.



ACCESSION for	
NTIS	White Section <input checked="" type="checkbox"/>
DDC	Buff Section <input type="checkbox"/>
UNANNOUNCED	<input type="checkbox"/>
JUSTIFICATION.....	
BY.....	
DISTRIBUTION/AVAILABILITY CODES	
Dist.	AVAIL. and/or SPECIAL
A	

DDC
RECEIVED
DEC 6 1977
D

TABLE OF CONTENTS

	Page
LIST OF ILLUSTRATIONS	ii
LIST OF SYMBOLS	iv
INTRODUCTION	1
PROBLEM DEFINITION AND PERFORMANCE CALCULATIONS	2
PERFORMANCE RESULTS	5
OPTIMUM PROCESSOR	7
PARTIALLY DEPENDENT SIGNAL FADING	8
SUMMARY	10
APPENDIX A - DERIVATION OF $P_1(\Lambda)$	A-1
APPENDIX B - ALTERNATIVE INTERPRETATION OF R	B-1
APPENDIX C - DERIVATION OF OPTIMUM PROCESSOR	C-1
APPENDIX D - DERIVATION OF CHARACTERISTIC FUNCTION FOR PARTIALLY DEPENDENT SIGNAL FADING	D-1
REFERENCES	R-1

LIST OF ILLUSTRATIONS

Figure		Page
1	Time-Frequency Occupancy Pattern	2
2	Detection Characteristics for $K = 2, M = 1, P_{FA} = 10^{-2}$. .	11
3	Detection Characteristics for $K = 2, M = 1, P_{FA} = 10^{-3}$. .	12
4	Detection Characteristics for $K = 2, M = 1, P_{FA} = 10^{-4}$. .	13
5	Detection Characteristics for $K = 2, M = 1, P_{FA} = 10^{-6}$. .	14
6	Detection Characteristics for $K = 2, M = 1, P_{FA} = 10^{-8}$. .	15
7	Detection Characteristics for $K = 2, M = 16, P_{FA} = 10^{-2}$. .	16
8	Detection Characteristics for $K = 2, M = 16, P_{FA} = 10^{-3}$. .	17
9	Detection Characteristics for $K = 2, M = 16, P_{FA} = 10^{-4}$. .	18
10	Detection Characteristics for $K = 2, M = 16, P_{FA} = 10^{-6}$. .	19
11	Detection Characteristics for $K = 2, M = 16, P_{FA} = 10^{-8}$. .	20
12	Detection Characteristics for $K = 2, M = 256, P_{FA} = 10^{-2}$. .	21
13	Detection Characteristics for $K = 2, M = 256, P_{FA} = 10^{-3}$. .	22
14	Detection Characteristics for $K = 2, M = 256, P_{FA} = 10^{-4}$. .	23
15	Detection Characteristics for $K = 2, M = 256, P_{FA} = 10^{-6}$. .	24
16	Detection Characteristics for $K = 2, M = 256, P_{FA} = 10^{-8}$. .	25
17	Detection Characteristics for $K = 3, M = 1, P_{FA} = 10^{-2}$. .	26
18	Detection Characteristics for $K = 3, M = 1, P_{FA} = 10^{-3}$. .	27
19	Detection Characteristics for $K = 3, M = 1, P_{FA} = 10^{-4}$. .	28
20	Detection Characteristics for $K = 3, M = 1, P_{FA} = 10^{-6}$. .	29
21	Detection Characteristics for $K = 3, M = 1, P_{FA} = 10^{-8}$. .	30
22	Detection Characteristics for $K = 3, M = 16, P_{FA} = 10^{-2}$. .	31
23	Detection Characteristics for $K = 3, M = 16, P_{FA} = 10^{-3}$. .	32
24	Detection Characteristics for $K = 3, M = 16, P_{FA} = 10^{-4}$. .	33
25	Detection Characteristics for $K = 3, M = 16, P_{FA} = 10^{-6}$. .	34
26	Detection Characteristics for $K = 3, M = 16, P_{FA} = 10^{-8}$. .	35
27	Detection Characteristics for $K = 3, M = 256, P_{FA} = 10^{-2}$. .	36
28	Detection Characteristics for $K = 3, M = 256, P_{FA} = 10^{-3}$. .	37
29	Detection Characteristics for $K = 3, M = 256, P_{FA} = 10^{-4}$. .	38
30	Detection Characteristics for $K = 3, M = 256, P_{FA} = 10^{-6}$. .	39
31	Detection Characteristics for $K = 3, M = 256, P_{FA} = 10^{-8}$. .	40
32	Detection Characteristics for $K = 4, M = 16, P_{FA} = 10^{-2}$. .	41
33	Detection Characteristics for $K = 4, M = 16, P_{FA} = 10^{-3}$. .	42
34	Detection Characteristics for $K = 4, M = 16, P_{FA} = 10^{-4}$. .	43
35	Detection Characteristics for $K = 4, M = 16, P_{FA} = 10^{-6}$. .	44
36	Detection Characteristics for $K = 4, M = 16, P_{FA} = 10^{-8}$. .	45
37	Detection Characteristics for $K = 5, M = 16, P_{FA} = 10^{-2}$. .	46
38	Detection Characteristics for $K = 5, M = 16, P_{FA} = 10^{-3}$. .	47
39	Detection Characteristics for $K = 5, M = 16, P_{FA} = 10^{-4}$. .	48
40	Detection Characteristics for $K = 5, M = 16, P_{FA} = 10^{-6}$. .	49
41	Detection Characteristics for $K = 5, M = 16, P_{FA} = 10^{-8}$. .	50

LIST OF ILLUSTRATIONS (Cont'd)

Figure		Page
42	Detection Characteristics for $K = 6$, $M = 16$, $P_{FA} = 10^{-2}$. . .	51
43	Detection Characteristics for $K = 6$, $M = 16$, $P_{FA} = 10^{-3}$. . .	52
44	Detection Characteristics for $K = 6$, $M = 16$, $P_{FA} = 10^{-4}$. . .	53
45	Detection Characteristics for $K = 6$, $M = 16$, $P_{FA} = 10^{-6}$. . .	54
46	Detection Characteristics for $K = 6$, $M = 16$, $P_{FA} = 10^{-8}$. . .	55
47	Detection Characteristics for $K = 8$, $M = 16$, $P_{FA} = 10^{-2}$. . .	56
48	Detection Characteristics for $K = 8$, $M = 16$, $P_{FA} = 10^{-3}$. . .	57
49	Detection Characteristics for $K = 8$, $M = 16$, $P_{FA} = 10^{-4}$. . .	58
50	Detection Characteristics for $K = 8$, $M = 16$, $P_{FA} = 10^{-6}$. . .	59
51	Detection Characteristics for $K = 8$, $M = 16$, $P_{FA} = 10^{-8}$. . .	60
52	Detection Characteristics for $K = 10$, $M = 16$, $P_{FA} = 10^{-2}$. . .	61
53	Detection Characteristics for $K = 10$, $M = 16$, $P_{FA} = 10^{-3}$. . .	62
54	Detection Characteristics for $K = 10$, $M = 16$, $P_{FA} = 10^{-4}$. . .	63
55	Detection Characteristics for $K = 10$, $M = 16$, $P_{FA} = 10^{-6}$. . .	64
56	Detection Characteristics for $K = 10$, $M = 16$, $P_{FA} = 10^{-8}$. . .	65
57	Additional Input Signal-to-Noise Ratio Necessary as a Function of K	66

LIST OF SYMBOLS*

K	Number of statistically dependent signal samples
s_d	Receiver output signal complex envelope on d-th branch
$n_{dk}^{(m)}$	Noise complex envelope sample
$e_j(\Lambda)$	Partial exponential series (equation (8))
R	Signal-to-noise ratio
\overline{E}_S	Average received signal energy on one diversity branch during one individual processing interval
$\alpha_{dk}^{(m)}$	Normalized envelope-squared sample (equation (16))
$\lambda_k^{(x)}$	Eigenvalues (equation (24))

*This list of symbols is supplementary to that in reference 1, to which this report is a sequel.

OPERATING CHARACTERISTICS FOR DETECTION
OF A FADING SIGNAL WITH K DEPENDENT FADES
AND D-FOLD DIVERSITY IN M ALTERNATIVE LOCATIONS

INTRODUCTION

The probabilities of correct decision and false alarm for a fading signal with D -fold diversity in M alternative locations were derived and evaluated numerically in reference 1 for a wide range of values of D , M and the signal-energy-to-noise-density ratio. It was assumed in that report that all the M decision variables were statistically independent of each other. In addition, the DM individual diversity-branch outputs were assumed to be statistically independent of each other.

In this report, we want to generalize the situation to include the possibility of having K signal samples (within each diversity branch) that are completely statistically dependent on each other. A possible communication scheme that could lead to this circumstance is illustrated in figure 1. For this example, there are two alternative locations ($M = 2$) for the signal, and there are three separated tones transmitted simultaneously ($D = 3$). However, instead of building narrowband filters of duration T for each diversity branch at the receiver to include all the received signal energy in each diversity branch, two narrowband filters of duration $T/2$ are used in each diversity branch, and their envelopes-squared are summed. Although the two noise segments (for $K = 2$) are independent (for white noise), because they do not overlap in time, the amplitudes of the signal fades can be completely dependent if T is significantly less than the correlation time of the channel. It is of interest to know the degradation in performance caused by this suboptimum processing technique. The results in reference 1 correspond to $K = 1$.

This report is a generalization of reference 1. To avoid duplication, that report is referenced for the physical motivation and application, background information, and interpretations. In addition, the definitions of the error probabilities of interest, the decision-making scheme, and the signal and noise models are documented in reference 1. In this report, knowledge of the material in the earlier report is assumed, and reference is made to the results, symbols, and notation in that report.

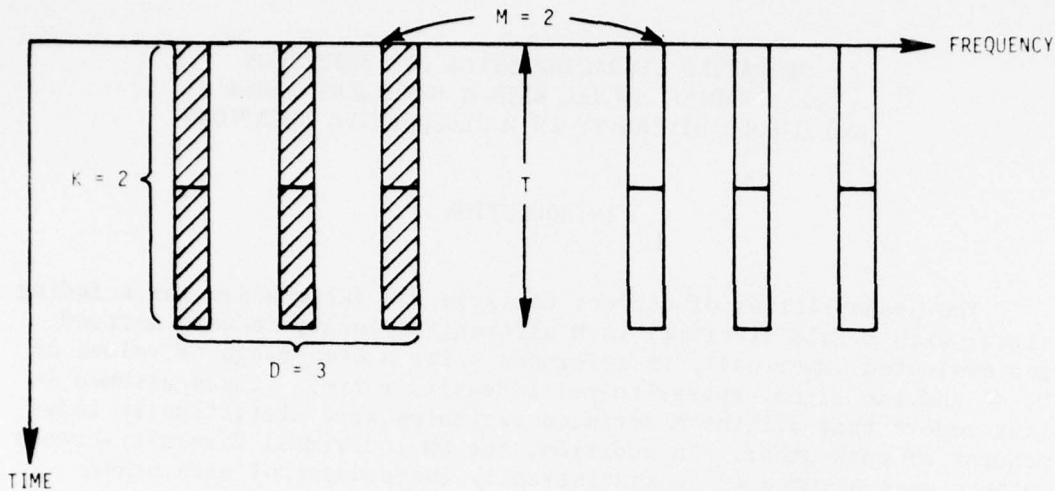


Figure 1. Time-Frequency Occupancy Pattern

PROBLEM DEFINITION AND PERFORMANCE CALCULATIONS

The signal diversity is D ; this is the number of statistically independent signal components (occupied frequency slots) per transmission. K is the number of independent noise samples per independent signal component. Hence, DK is the total number of independent noise components in one of the M alternative signal locations.

If a signal is present in alternative location 1 (without loss of generality), the M variables, on which decisions about signal absence or presence and identity must be made,* are given by (see reference 1, equations (24) and (B-1))

$$x_1 = \sum_{d=1}^D \sum_{k=1}^K \left| s_d + n_{dk}^{(1)} \right|^2, \quad (1)$$

$$x_m = \sum_{d=1}^D \sum_{k=1}^K \left| n_{dk}^{(m)} \right|^2, \quad 2 \leq m \leq M.$$

*The optimum processor is addressed in a later section. Here we consider the simple sum of envelopes-squared processor.

Here, s_d is the receiver output signal voltage complex envelope on the d -th diversity branch; notice that it is not dependent on k . The D random variables $\{s_d\}$ are all statistically independent of each other. The random variable $\{n_{dk}^{(m)}\}$ is the output noise complex envelope in the k -th sampling interval in the d -th diversity branch of the m -th alternative location. All DKM random variables $\{n_{dk}^{(m)}\}$ are statistically independent of each other and of the variables $\{s_d\}$.

It follows from the above that the M decision variables $\{x_m\}$ in equation (1) are statistically independent of each other. If the probability density function of x_m , $2 \leq m \leq M$ is denoted by p_0 , and that of x_1 by p_1 , then the probability of false alarm (see reference 1, page 4) is

$$P_{FA} = 1 - [P_0(\Lambda)]^M, \quad (2)$$

and the probability of correct decision is

$$P_{CD} = \int_{\Lambda}^{\infty} dx p_1(x) [P_0(x)]^{M-1}, \quad (3)$$

where Λ is a threshold.

From reference 1, equation (A-10), we have the upper and lower bounds on P_{CD} :

$$[1 - P_{FA}]^{\frac{M-1}{M}} [1 - P_1(\Lambda)] \leq P_{CD} \leq 1 - P_1(\Lambda). \quad (4)$$

Since $P_{FA} \ll 1$ for our applications, this is an exceedingly useful and tight bound for all M ; it requires only that we be able to evaluate the cumulative probability distribution P_1 , rather than perform the numerical integration indicated by equation (3).

The derivation of P_1 is given in appendix A. Two alternative forms are given by

$$\begin{aligned} 1 - P_1(\Lambda) &= \exp(-\Lambda) (1 - \gamma)^D \sum_{n=0}^{\infty} \binom{D+n-1}{n} \gamma^n e_{DK-1+n}(\Lambda) \\ &= 1 - (1 - \gamma)^D \sum_{n=0}^{\infty} \binom{D+n-1}{n} \gamma^n [1 - \exp(-\Lambda) e_{DK-1+n}(\Lambda)]. \end{aligned} \quad (5)$$

Reasons for choosing one form over the other and a method for accurate evaluation of equation (5) for large D are given in appendix A. The parameter

$$\gamma = \frac{KR}{1 + KR} \quad , \quad (6)$$

where

$$R = \frac{\sigma_s^2}{\sigma_n^2} = \frac{\overline{|s_d|^2}}{\overline{|n_{dk}^{(m)}|^2}} \quad (7)$$

is the signal-to-noise power ratio of an individual sample in equation (1). The quantity

$$e_j(\Lambda) = \sum_{k=0}^j \Lambda^k/k! = 1 + \Lambda + \dots + \Lambda^j/j! \quad (8)$$

is the first $j+1$ terms of the power series expansion of $\exp(\Lambda)$.

For zero signal-to-noise ratio, $R = 0$, we obtain from equation (5),

$$1 - P_0(\Lambda) = \exp(-\Lambda)e_{DK-1}(\Lambda) \quad , \quad (9)$$

and then equation (2) yields the false alarm probability,

$$P_{FA} = 1 - [1 - \exp(-\Lambda)e_{DK-1}(\Lambda)]^M \quad . \quad (10)$$

Given values of DK and M and a desired value for P_{FA} , equation (10) is solved for Λ . This value is substituted in equation (5), which is then evaluated as a function of R .

The parameter R in equation (7) can be interpreted differently for the model where the received signal is narrowband and deterministic (except for phase) and subject to slow Rayleigh fading. This consideration is taken up in appendix B, with the result that

$$R = \frac{\bar{E}_S}{N_0} = \frac{\bar{E}_T/N_0}{KD} , \quad (11)$$

and

$$\frac{\bar{E}_1}{N_0} = \frac{\bar{E}_T/N_0}{D} = RK , \quad (12)$$

where

\bar{E}_S is the average received signal energy on one diversity branch during one individual processing interval ($D = 1, K = 1$),

\bar{E}_T is the total average received signal energy over all diversity branches and processing intervals,

\bar{E}_1 is the average received signal energy on one diversity branch during all K processing intervals, and

N_0 is the (single-sided) noise density level.

The curves to follow will employ the signal-energy-to-noise-density ratio parameters in equations (11) and (12).

PERFORMANCE RESULTS

In figures 2 through 6, the probability of correct decision P_{CD} is plotted versus \bar{E}_1/N_0 in decibels,* with diversity D as a parameter (solid curves) for $M = 1, K = 2$, and $P_{FA} = 10^{-n}$, $n = 2, 3, 4, 6, 8$, respectively. The dashed curves in each figure connect points of equal average total received signal-energy-to-noise-density ratio, \bar{E}_T/N_0 .

In addition to the relevant observations made in reference 1, page 9, the following points are worth noting. For $P_{FA} = 10^{-2}$ in figure 2, the difference in minimum \bar{E}_T/N_0 required versus the $K = 1$ case (reference 1, figure 1) is 1.1 dB over a wide range of P_{CD} (above 0.9). Also, for a specified value of P_{CD} , the optimum order of diversity is the same for $K = 2$ as for $K = 1$. However, both \bar{E}_1/N_0 and \bar{E}_T/N_0 must be 1.1 dB greater.

*That is, $10 \log (\bar{E}_1/N_0)$.

For $P_{FA} = 10^{-8}$ in figure 6, the difference in required \bar{E}_T/N_0 between the $K = 2$ and $K = 1$ cases is 1.0 dB over a wide range of P_{CD} . Thus, the difference in required signal-to-noise ratio is relatively independent of P_{FA} , at least for $M = 1$.

In figures 7 through 11, the curves for $M = 16$, $K = 2$ are plotted. We find that the difference in required signal-to-noise ratio versus the $K = 1$ results (reference 1, figures 16 through 20) is approximately 1.0 dB over a wide range of P_{CD} and P_{FA} .

Continuing on to $M = 256$, $K = 2$ in figures 12 through 16, we find a difference in required signal-to-noise ratio of approximately 1.0 dB (0.9 dB for $P_{FA} = 10^{-8}$) between these results and those for $K = 1$. Thus, the degradation in performance is relatively insensitive to the values of M , P_{CD} , and P_{FA} .

The results for $K = 3$ are presented in figures 17 through 31, again for $M = 1$, 16, and 256. Once again, the same conclusions on invariance result, except that the degradation now is larger, 1.7 dB for $M = 16$, for example.

Finally, for M fixed at 16, curves for $K = 4, 5, 6, 8$, and 10 are presented in figures 32 through 56. They enable us to extract the degradation behavior with change in K that is plotted in figure 57. Namely, for $M = 16$, we find that additional signal-to-noise ratio, to the extent of approximately

$$3.5 \log(K) \text{decibels,} \quad (13)$$

is required, relative to the $K = 1$ case, to maintain the same performance, P_{FA} , P_{CD} . This is a rough rule-of-thumb; the exact values can be deduced from the curves in figures 2 through 56 or by modifying the program in appendix A to fit the user's case.

OPTIMUM PROCESSOR

With dependent fading, the optimum processing of random variables $\{x_{dk}^{(m)}\}$ (where we had, for the case in equation (1))

$$x_{dk}^{(m)} = \left\{ \begin{array}{l} |s_d + n_{dk}^{(1)}|^2, \quad m = 1 \\ |n_{dk}^{(m)}|^2, \quad 2 \leq m \leq M \end{array} \right\}, \quad (14)$$

is not simply to sum them. Rather, we find in appendix C that, for $K = 2$, we should consider the test

$$\max_{1 \leq m \leq M} \left\{ \sum_{d=1}^D (\alpha_{d1}^{(m)} + \alpha_{d2}^{(m)}) + \sum_{d=1}^D \ln I_0 \left(2 \sqrt{\alpha_{d1}^{(m)} \alpha_{d2}^{(m)}} \right) \right\} \geq \Lambda, \quad (15)$$

where

$$\alpha_{dk}^{(m)} \equiv \frac{R}{1 + 2R} \frac{x_{dk}^{(m)}}{\sigma_n^2} \quad (16)$$

can be interpreted as a scaled and normalized envelope-squared sample. Although equation (15) is not much more difficult to implement than the usual sum (which is proportional to the leading sum in equation (15)), the test (equation (15)) requires knowledge of the absolute levels of σ_s^2 and σ_n^2 . Also, the exact performance characteristics of equation (15) would be impossible to determine analytically.

For

$$\sqrt{\alpha_{d1}^{(m)} \alpha_{d2}^{(m)}} \ll 1, \quad (17)$$

since

$$I_0(x) \approx 1 + \frac{1}{2}x^2, \quad \ln I_0(x) \approx \frac{1}{2}x^2, \quad \text{for small } x, \quad (18)$$

the second sum of equation (15) is approximately

$$\sum_{d=1}^D \alpha_{d1}^{(m)} \alpha_{d2}^{(m)} \ll \sum_{d=1}^D \left(\alpha_{d1}^{(m)} + \alpha_{d2}^{(m)} \right) . \quad (19)$$

Thus, in case equation (17) is true, the processor (15) takes the form of a sum of two squared envelopes, which are then summed over the diversity branches.

For

$$\sqrt{\alpha_{d1}^{(m)} \alpha_{d2}^{(m)}} \gg 1 , \quad (20)$$

since

$$I_0(x) \approx \frac{\exp(x)}{\sqrt{2\pi x}}, \quad \ln I_0(x) \approx x, \quad \text{for large } x, \quad (21)$$

the processor (15) takes the form

$$\sum_{d=1}^D \left(\sqrt{\alpha_{d1}^{(m)}} + \sqrt{\alpha_{d2}^{(m)}} \right)^2 , \quad (22)$$

which is a sum of envelopes that are then squared and summed over the diversity branches. The likelihood of equation (17) or (20) occurring is discussed in appendix C. It is shown that if $R \ll 1$, the processor rule on the right side of equation (19) is substantially optimum, whereas if $R \gg 1$, the processor rule in equation (22) is substantially optimum.

PARTIALLY DEPENDENT SIGNAL FADING

When the rate of signal fading is neither faster nor slower than the rate of signaling (time T in figure 1), but the two are comparable, the signal complex amplitude s_d in equation (1) cannot be considered constant over all K samples. If we let the signal amplitude obey Rayleigh fading, we find (appendix D) that the characteristic function of the decision variable with signal present is given by

$$\left[\prod_{k=1}^K \{1 - i\xi(\sigma_n^2 + 2\lambda_k^{(x)})\} \right]^{-D} , \quad (23)$$

where $\{\lambda_k^{(x)}\}$ are the eigenvalues of the matrix

$$\left[\frac{x_k x_\ell}{x_k x_\ell} \right]_1^K \quad (24)$$

and where x_k is the real part of the Rayleigh-fading signal complex amplitude s_d at the k -th sampling instant.

For completely dependent fading, the elements of the matrix in equation (24) are all equal to $\sigma_x^2 = \sigma_s^2/2$, and

$$\lambda_k^{(x)} = \begin{cases} K\sigma_s^2/2, & k = 1 \\ 0, & 1 < k \end{cases} \quad (\text{dependent fading}), \quad (25)$$

in which case equation (23) reduces to equation (A-13). On the other hand, for completely independent fading, the matrix in equation (24) is $\frac{1}{2}\sigma_s^2 I$, and

$$\lambda_k^{(x)} = \frac{1}{2}\sigma_s^2, \quad \text{all } k \quad (\text{independent fading}), \quad (26)$$

in which case equation (23) reduces to $[1 - i\xi(\sigma_n^2 + \sigma_s^2)]^{-DK}$. This corresponds to the case studied in reference 1 for $K = 1$ (see, for example, reference 1, equation (B-3)).

For signal absent, the characteristic function in equation (23) reduces to the same result as that to which equation (A-13) would reduce. Therefore, the false alarm probability in equation (10) is applicable to this case as well.

A closed form for the probability density function corresponding to the general result, equation (23), is possible, but would be extremely tedious. Perhaps the best numerical procedure is straightforward Fourier transformation of equation (23) (see reference 2, for example). But, in any event, the results of this report and reference 1 furnish bounds on performance.

SUMMARY

The numerical results here for completely dependent fading, coupled with the results for independent fading in reference 1, serve to bound the performance in practical cases of partially dependent fading. This would be true whether the dependence is intentional, as, for example, sampling frequently in time in figure 1 (large K) or unintentional, as, for example, not being aware of the true rate of signal fading. If the losses indicated by figure 57 are too large for some larger values of K, it may be necessary to resort to the more exact result in equation (23), if the fading is fairly independent, to obtain a more exact result. The gains expected by doing optimum combination of individual samples is probably minimal and requires knowledge of signal and noise levels that often is not available.

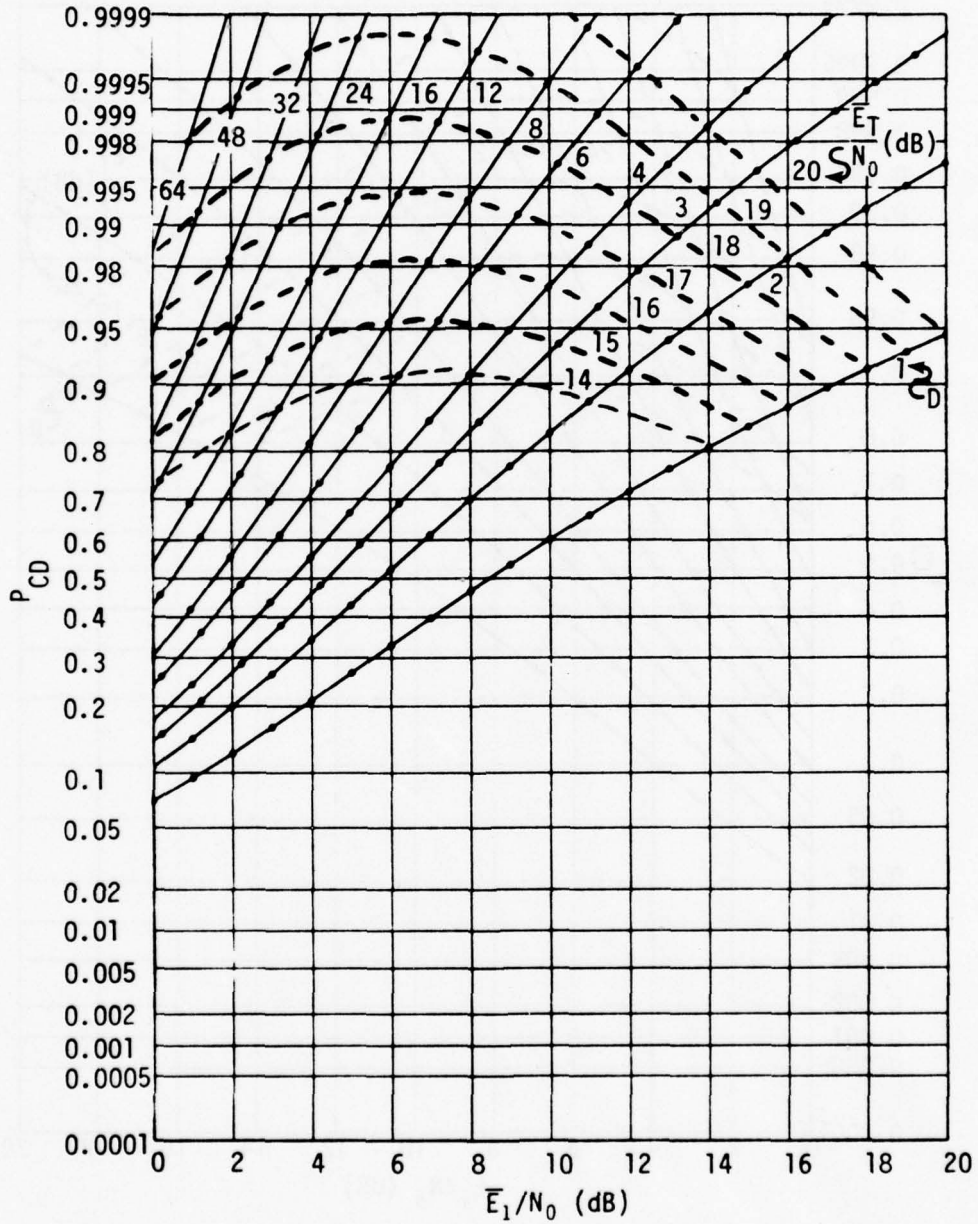


Figure 2. Detection Characteristics for $K = 2$, $M = 1$, $P_{FA} = 10^{-2}$

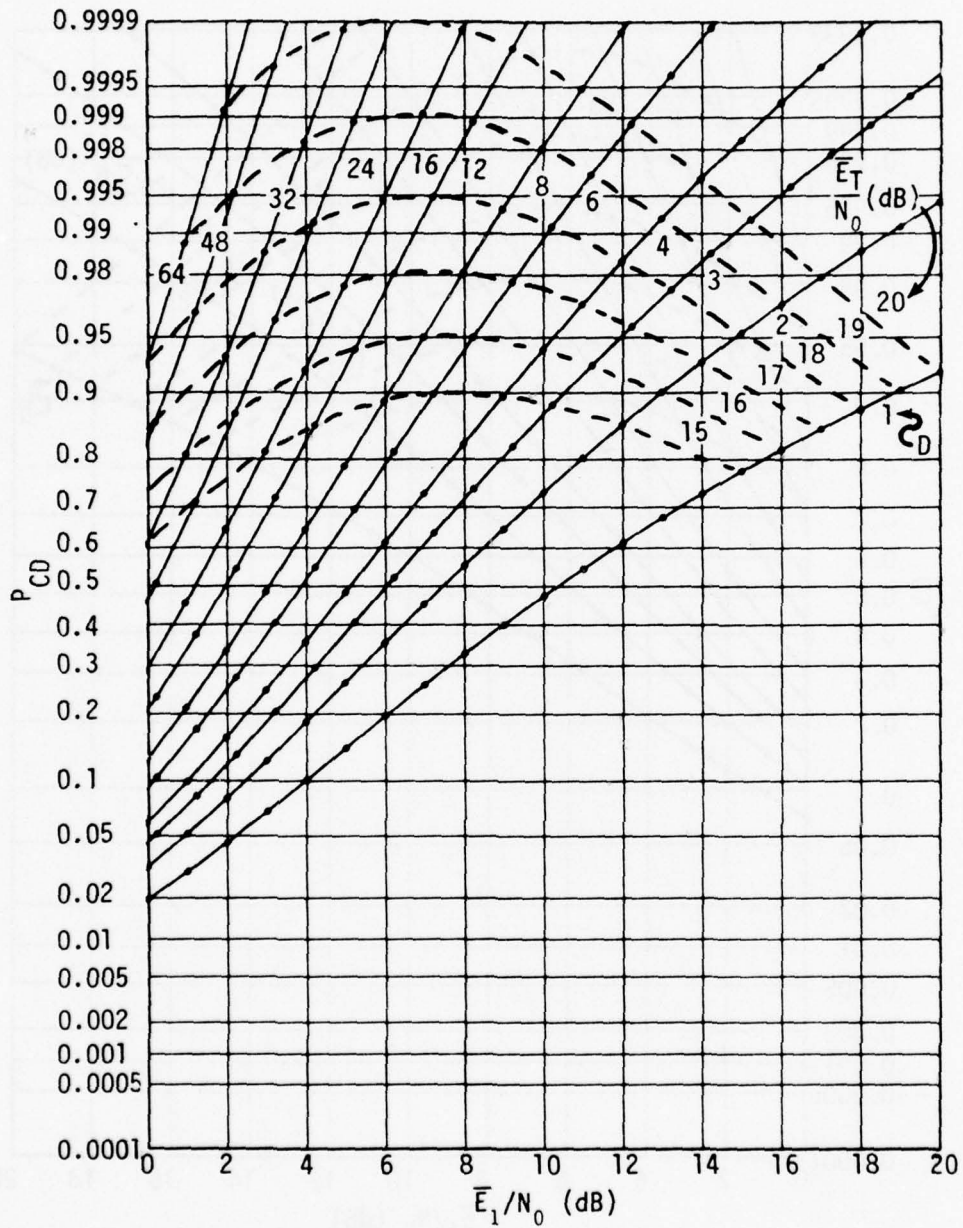


Figure 3. Detection Characteristics for $K = 2$, $M = 1$, $P_{FA} = 10^{-3}$

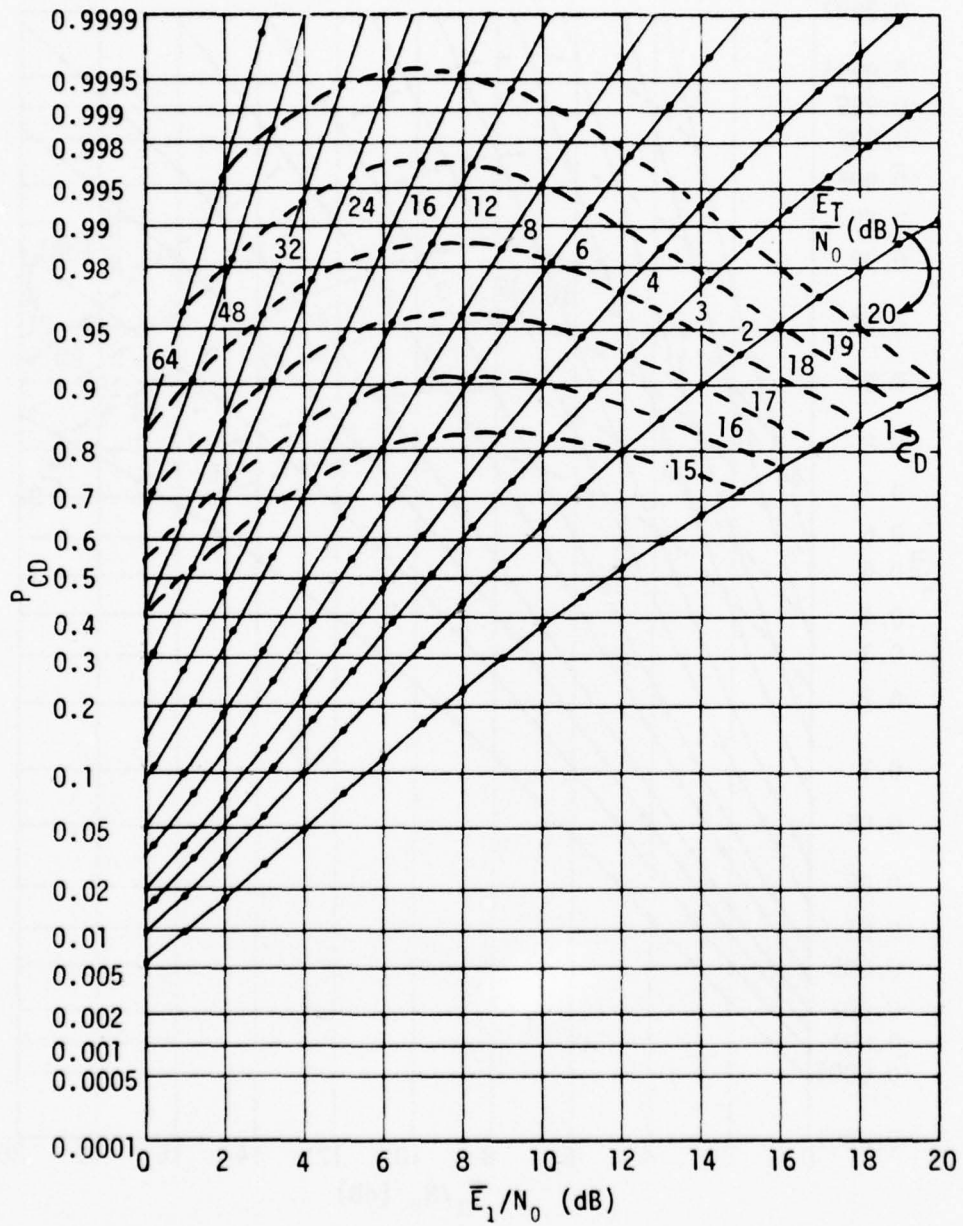


Figure 4. Detection Characteristics for $K = 2$, $M = 1$, $P_{FA} = 10^{-4}$

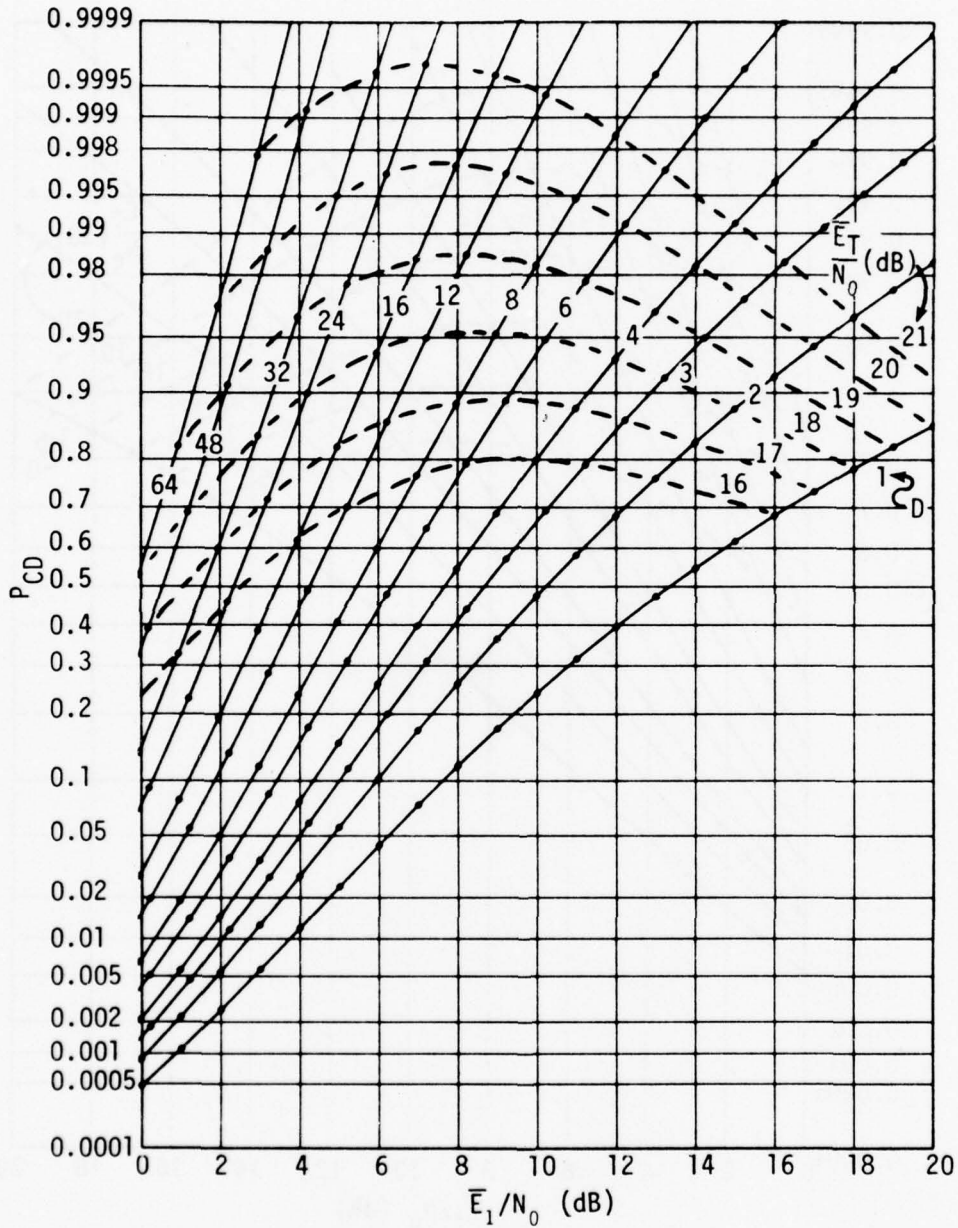


Figure 5. Detection Characteristics for $K = 2$, $M = 1$, $P_{FA} = 10^{-6}$

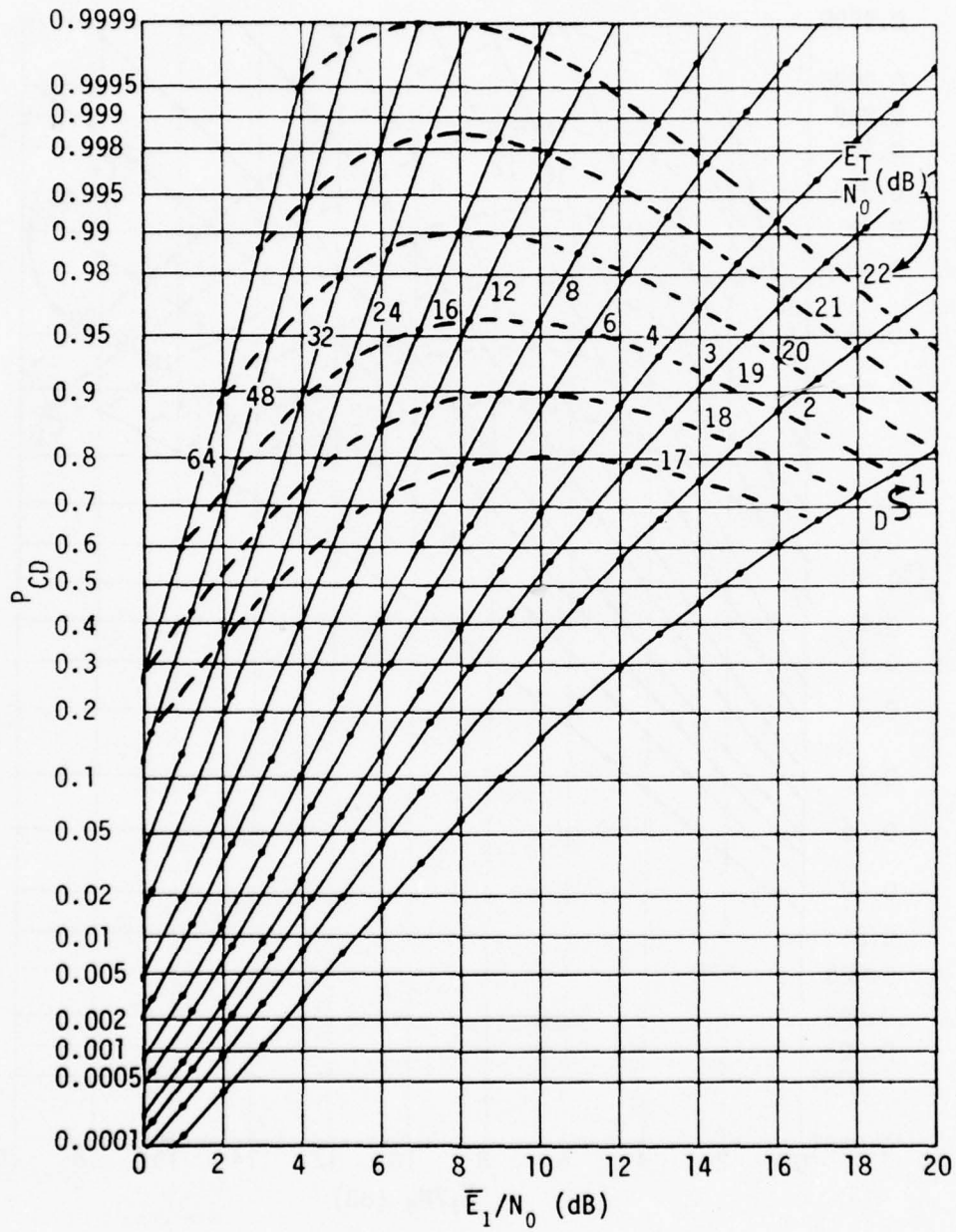


Figure 6. Detection Characteristics for $K = 2$, $M = 1$, $P_{FA} = 10^{-8}$

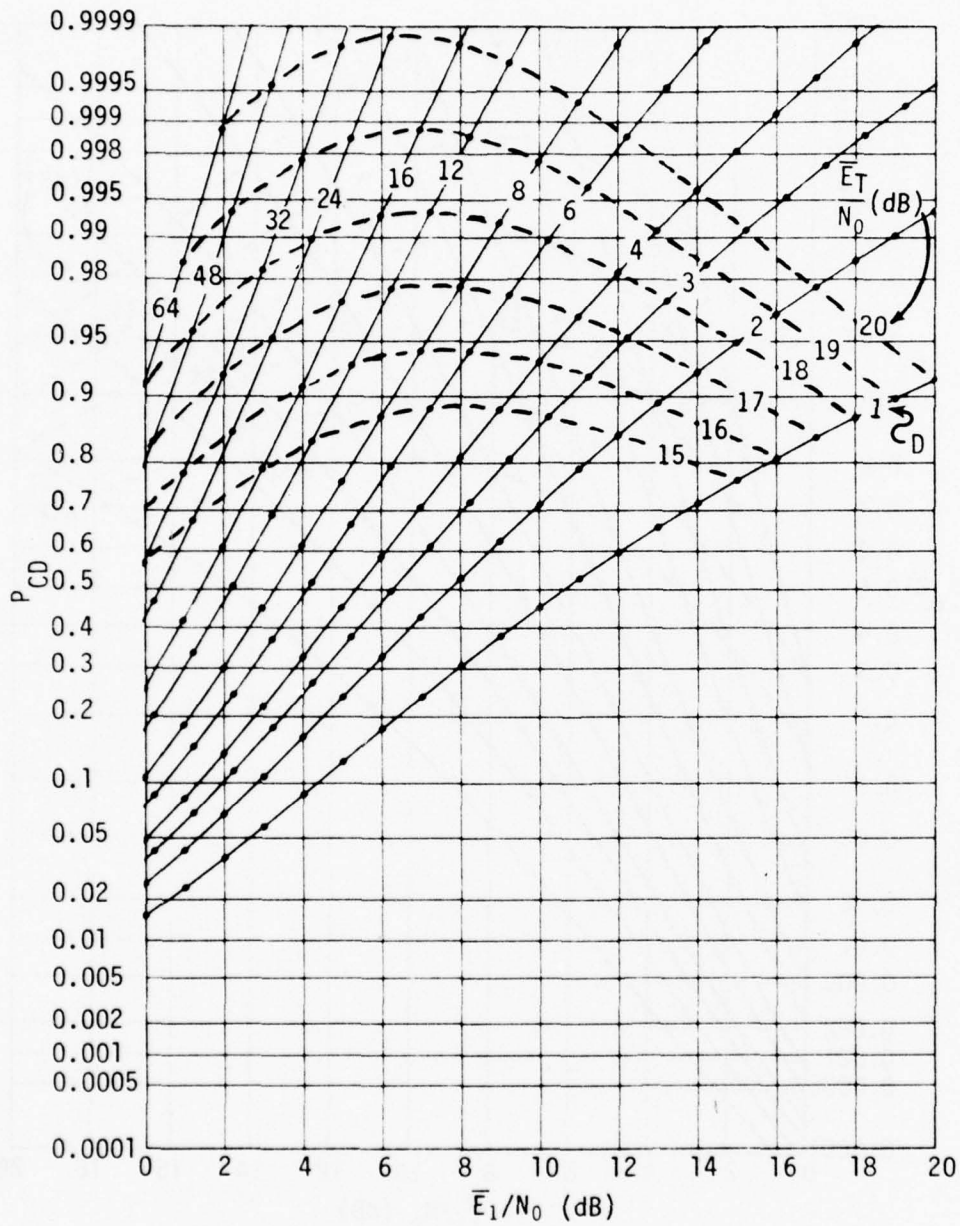


Figure 7. Detection Characteristics for $K = 2$, $M = 16$, $P_{FA} = 10^{-2}$

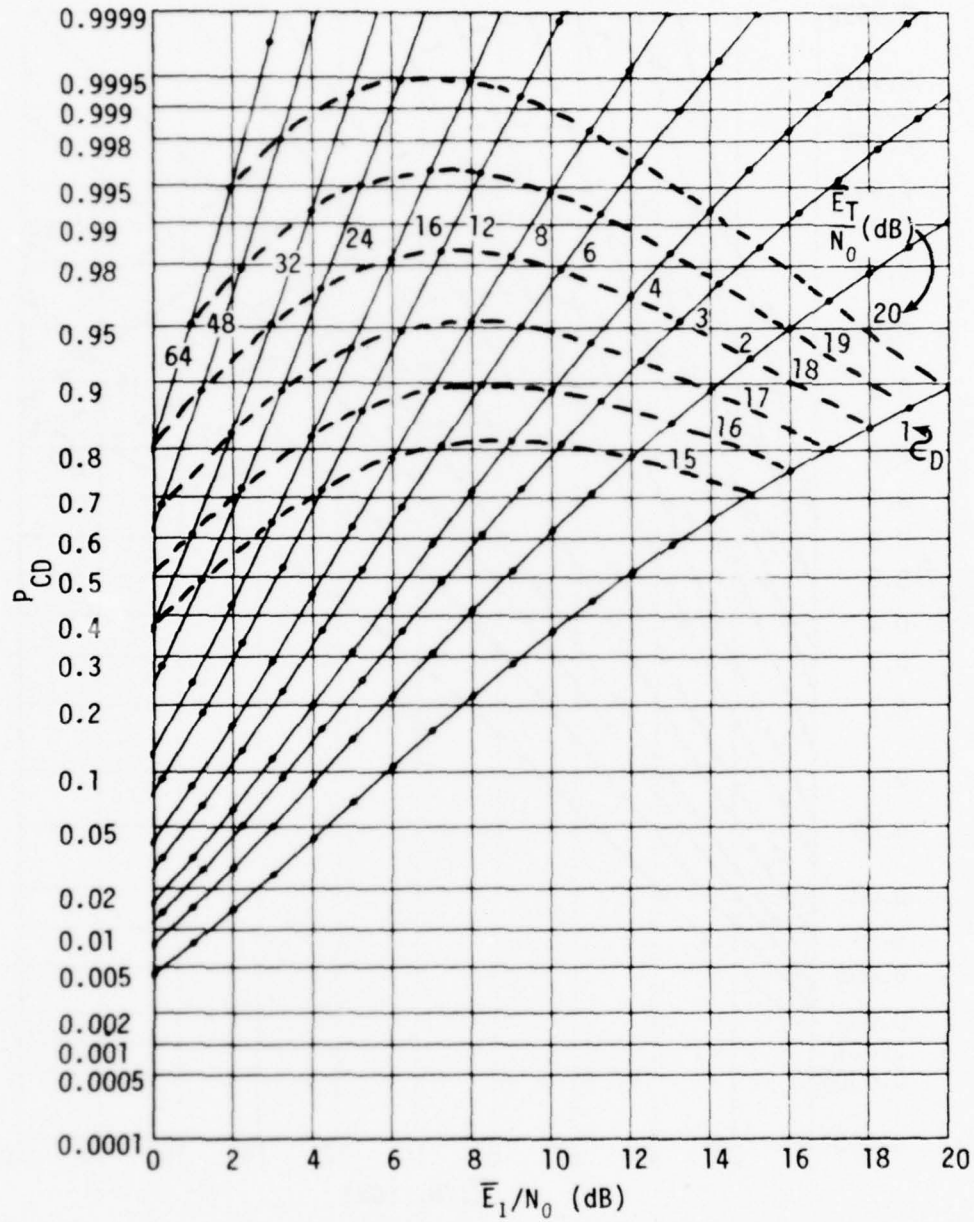


Figure 8. Detection Characteristics for $K = 2$, $M = 16$, $P_{FA} = 10^{-3}$

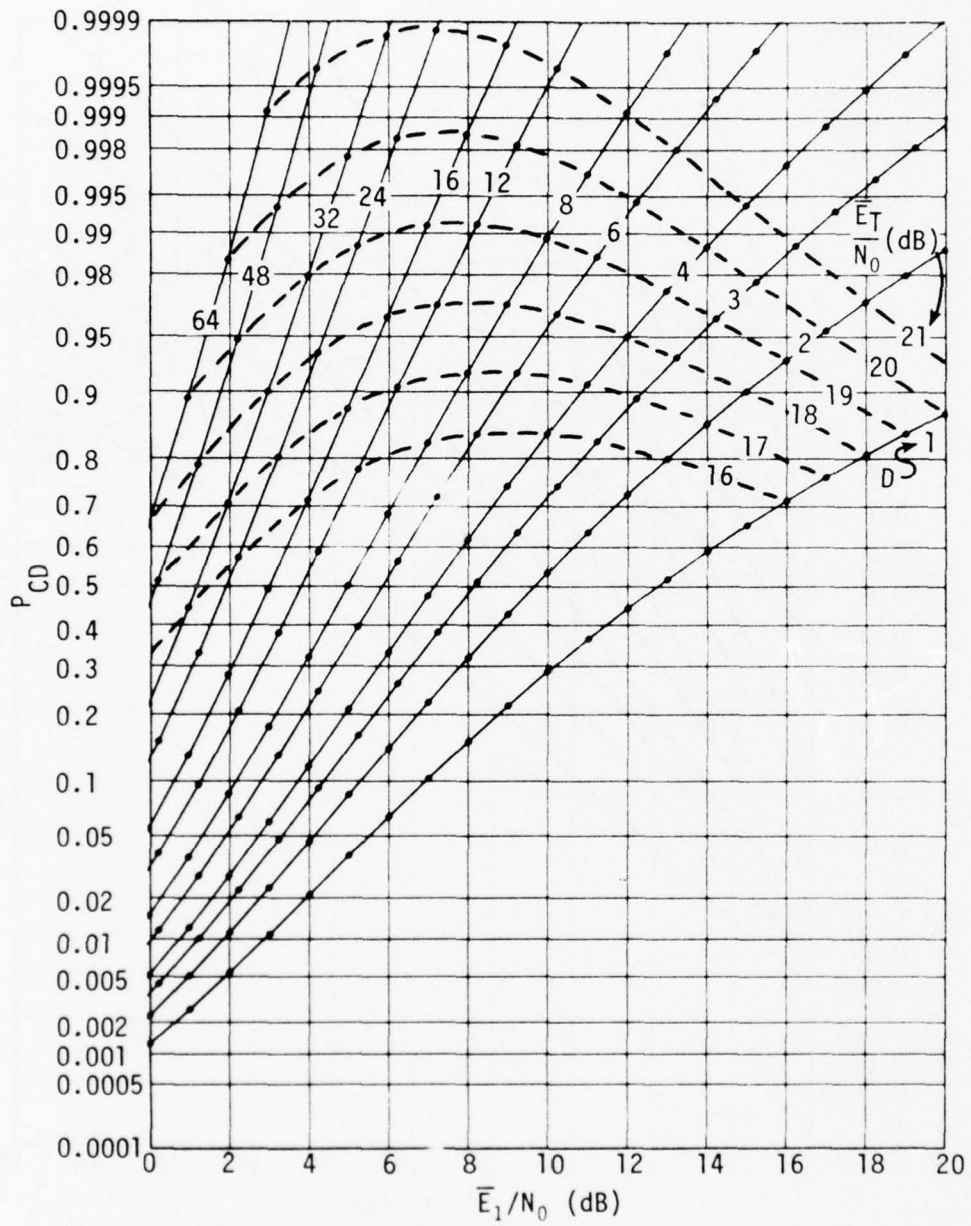


Figure 9. Detection Characteristics for $K = 2$, $M = 16$, $P_{FA} = 10^{-4}$

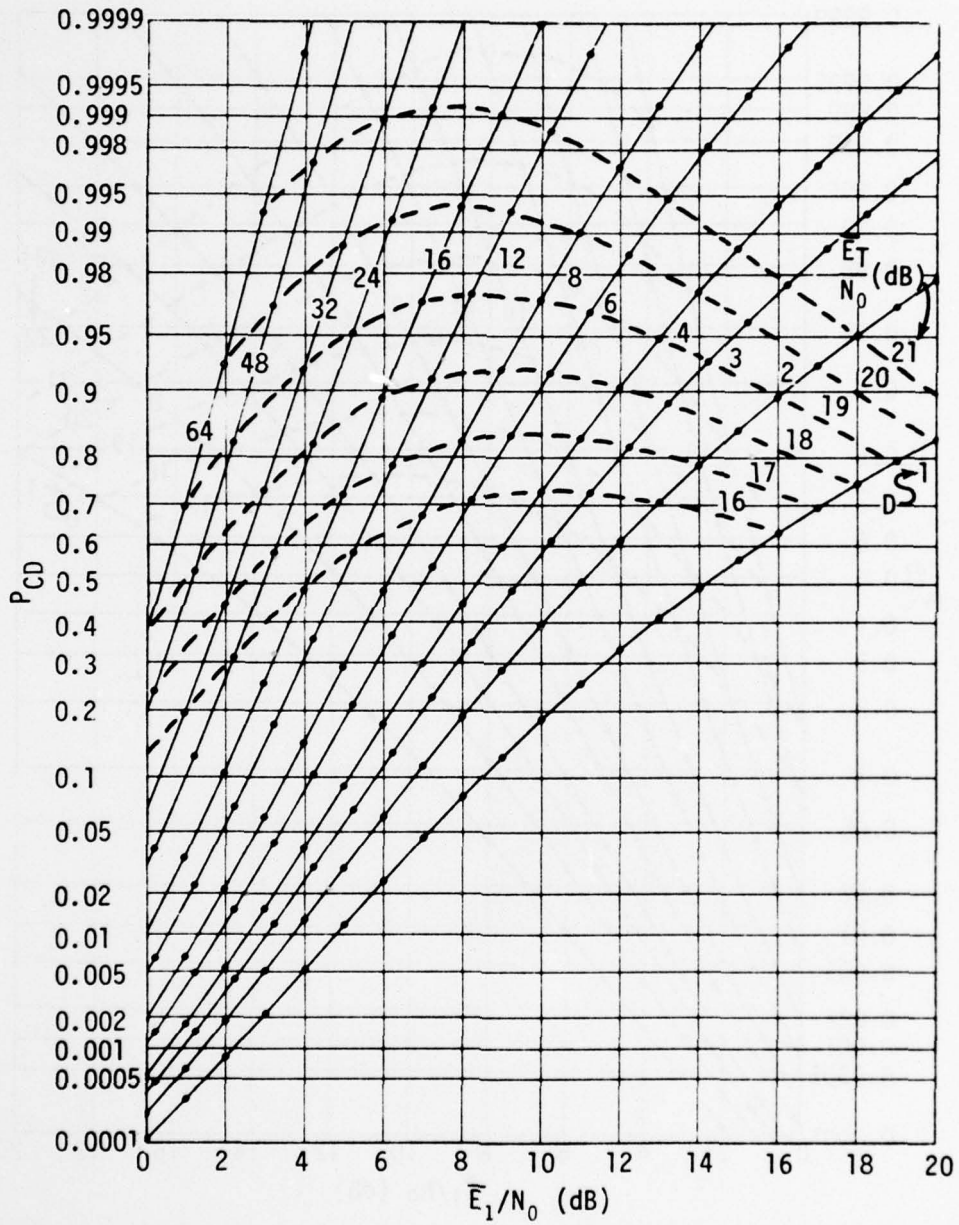


Figure 10. Detection Characteristics for $K = 2$, $M = 16$, $P_{FA} = 10^{-6}$

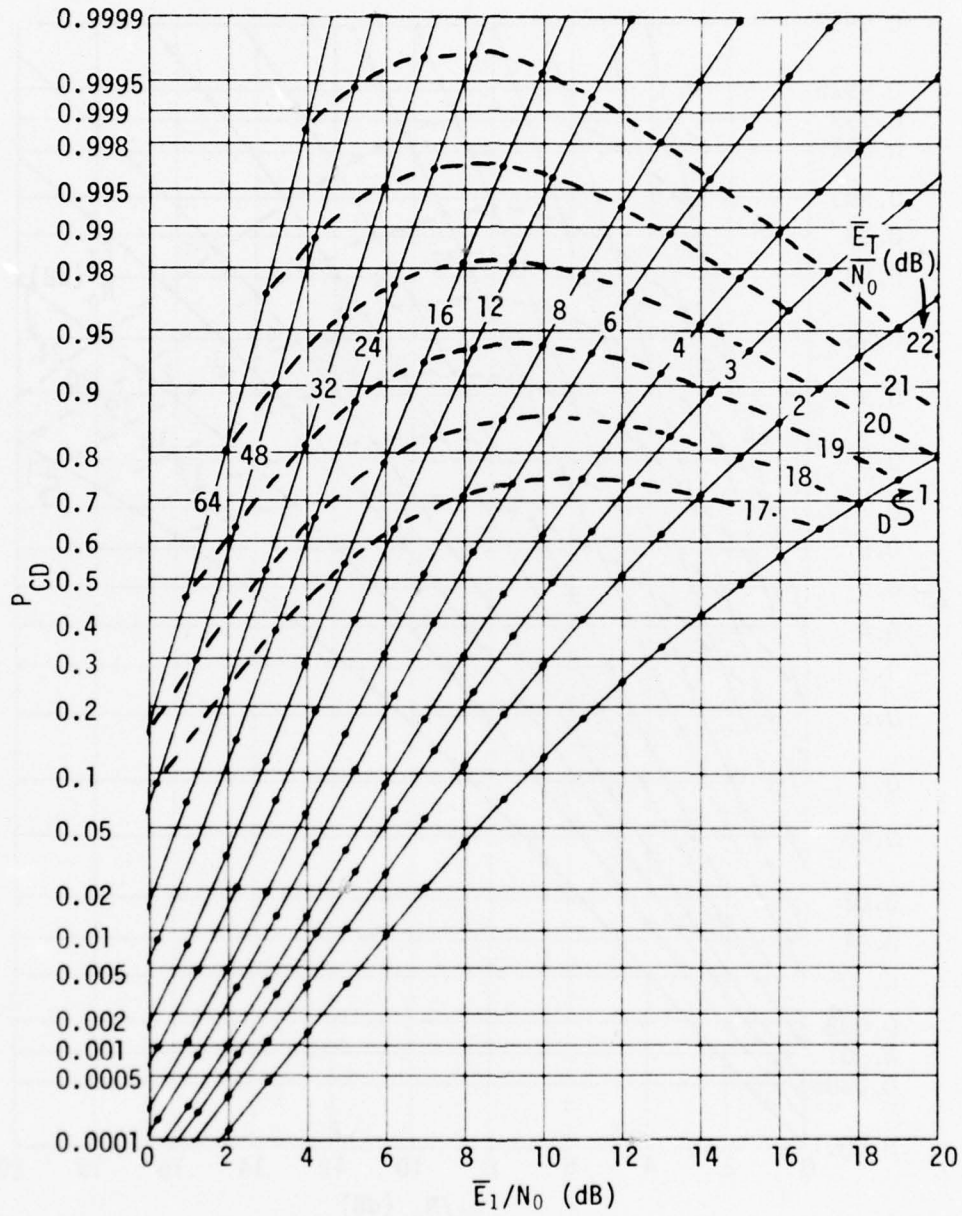


Figure 11. Detection Characteristics for $K = 2$, $M = 16$, $P_{FA} = 10^{-8}$

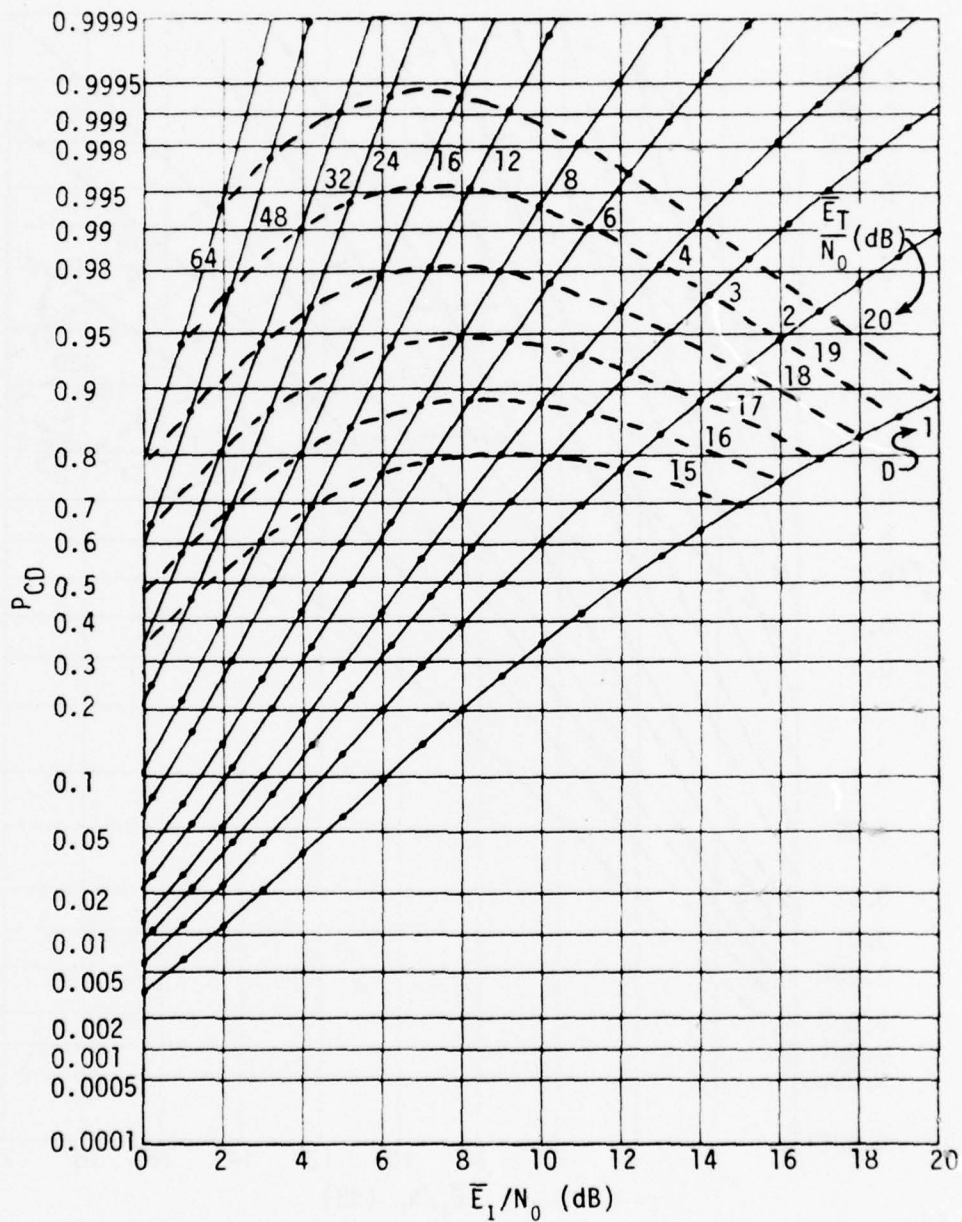


Figure 12. Detection Characteristics for $K = 2$, $M = 256$, $P_{FA} = 10^{-2}$

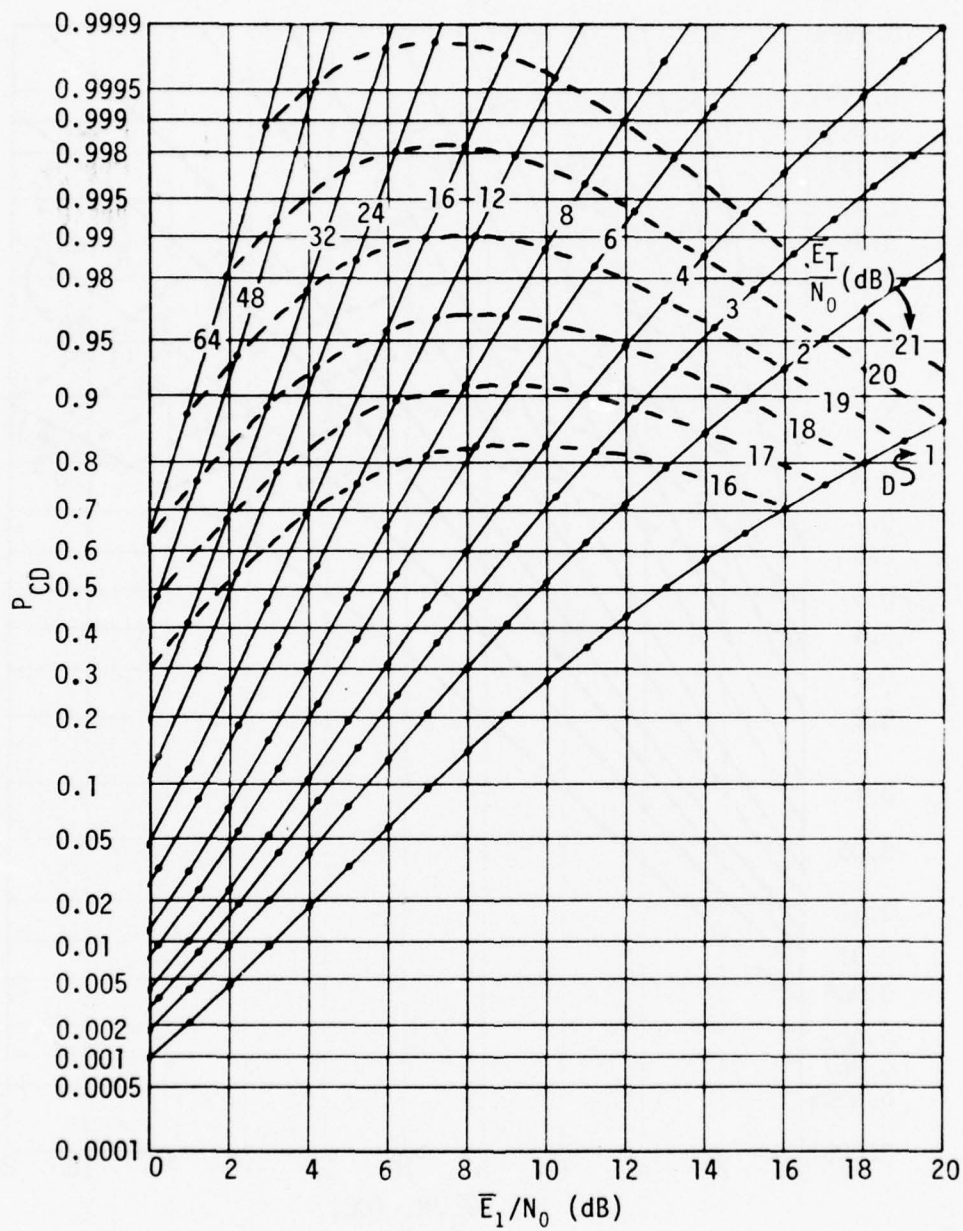


Figure 13. Detection Characteristics for $K = 2$, $M = 256$, $P_{FA} = 10^{-3}$

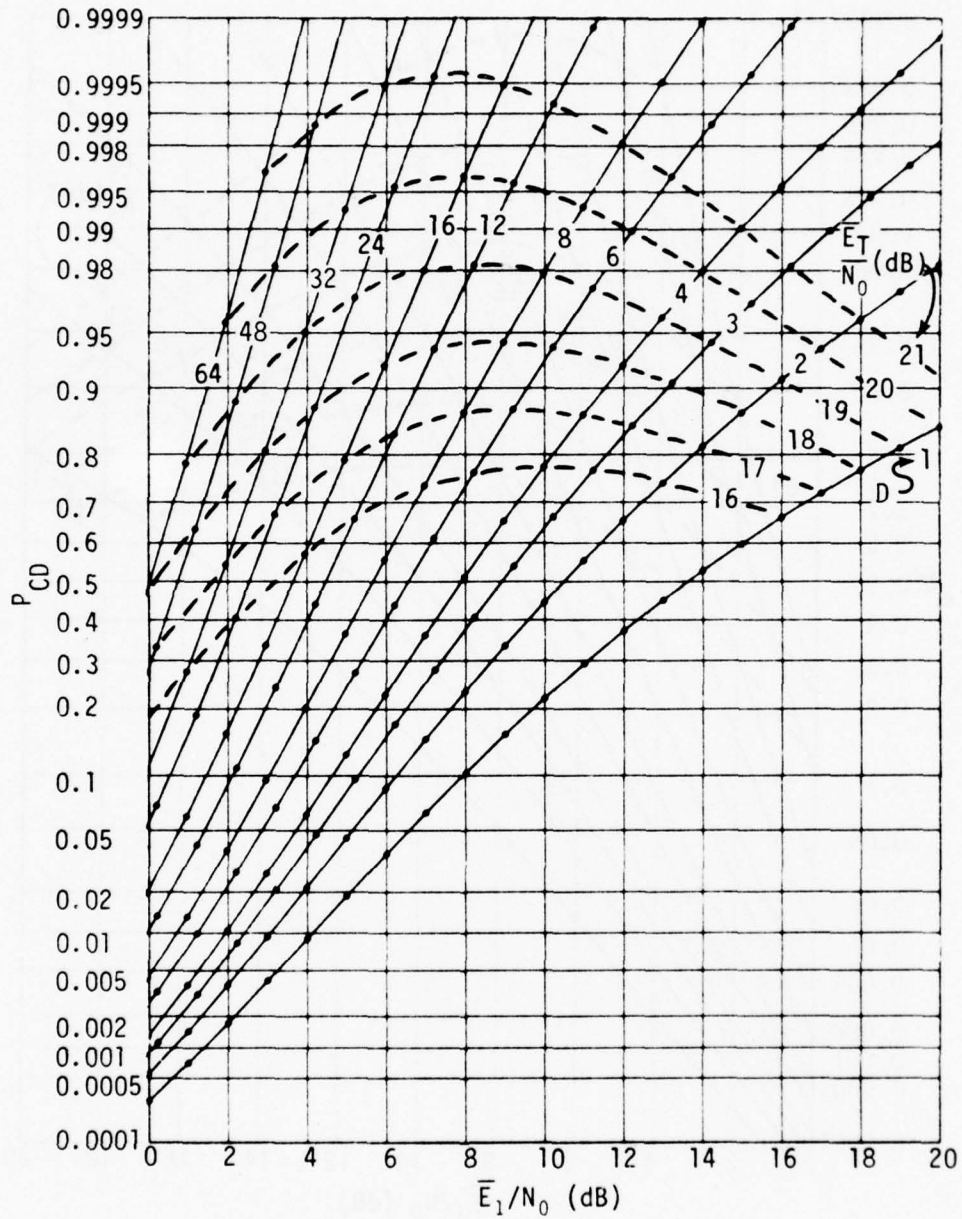


Figure 14. Detection Characteristics for $K = 2$, $M = 256$, $P_{FA} = 10^{-4}$

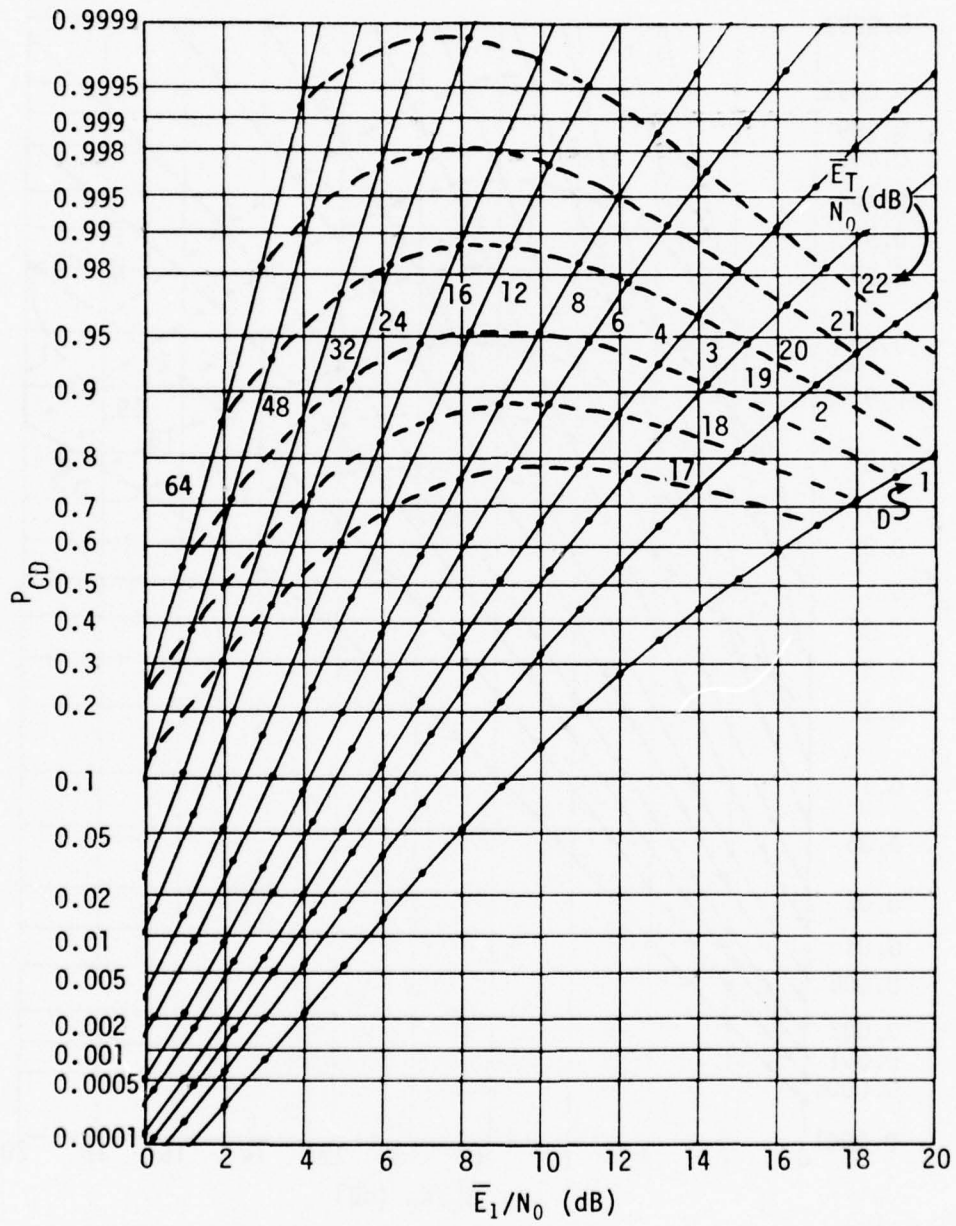


Figure 15. Detection Characteristics for $K = 2$, $M = 256$, $P_{FA} = 10^{-6}$

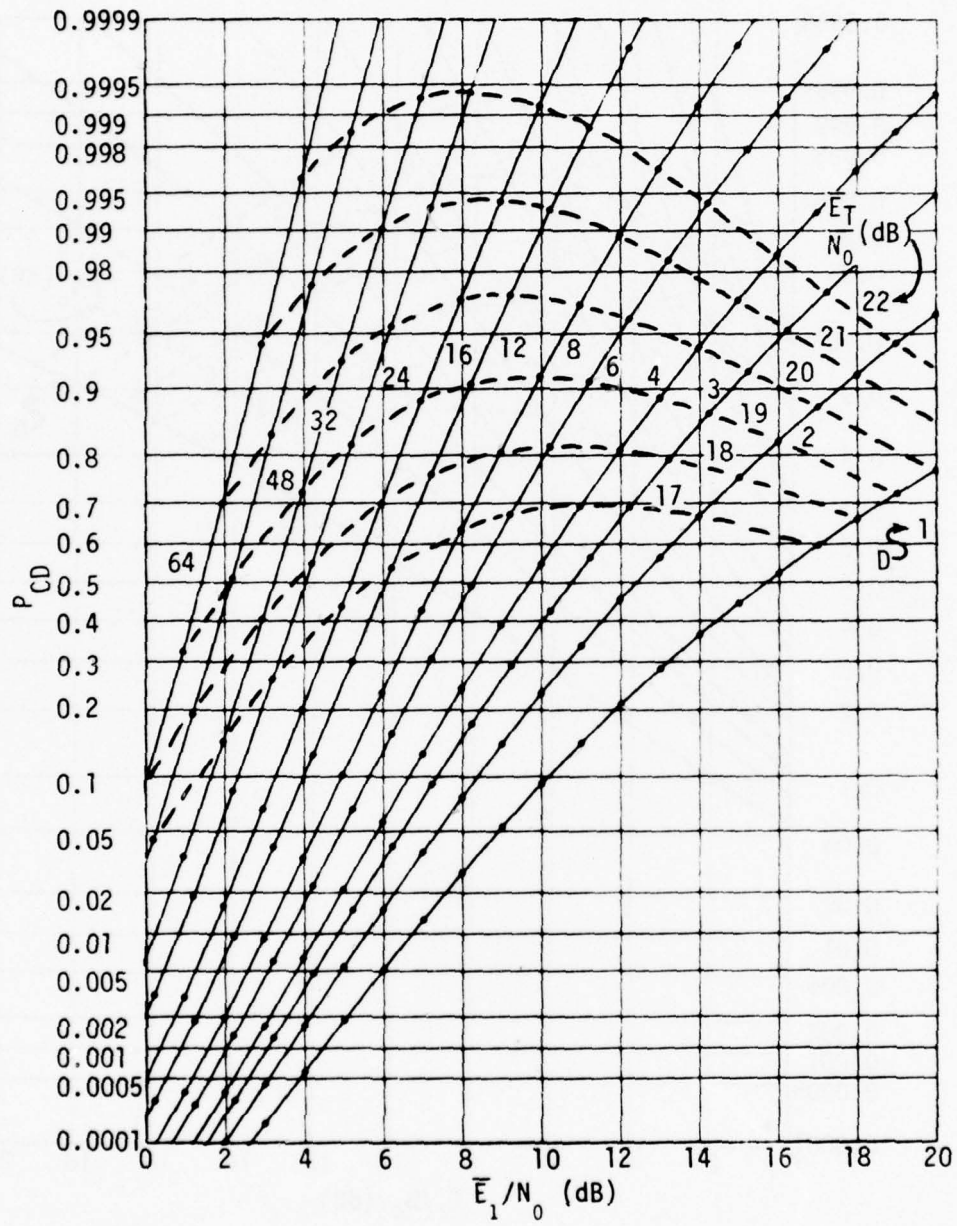


Figure 16. Detection Characteristics for $K = 2$, $M = 256$, $P_{FA} = 10^{-8}$

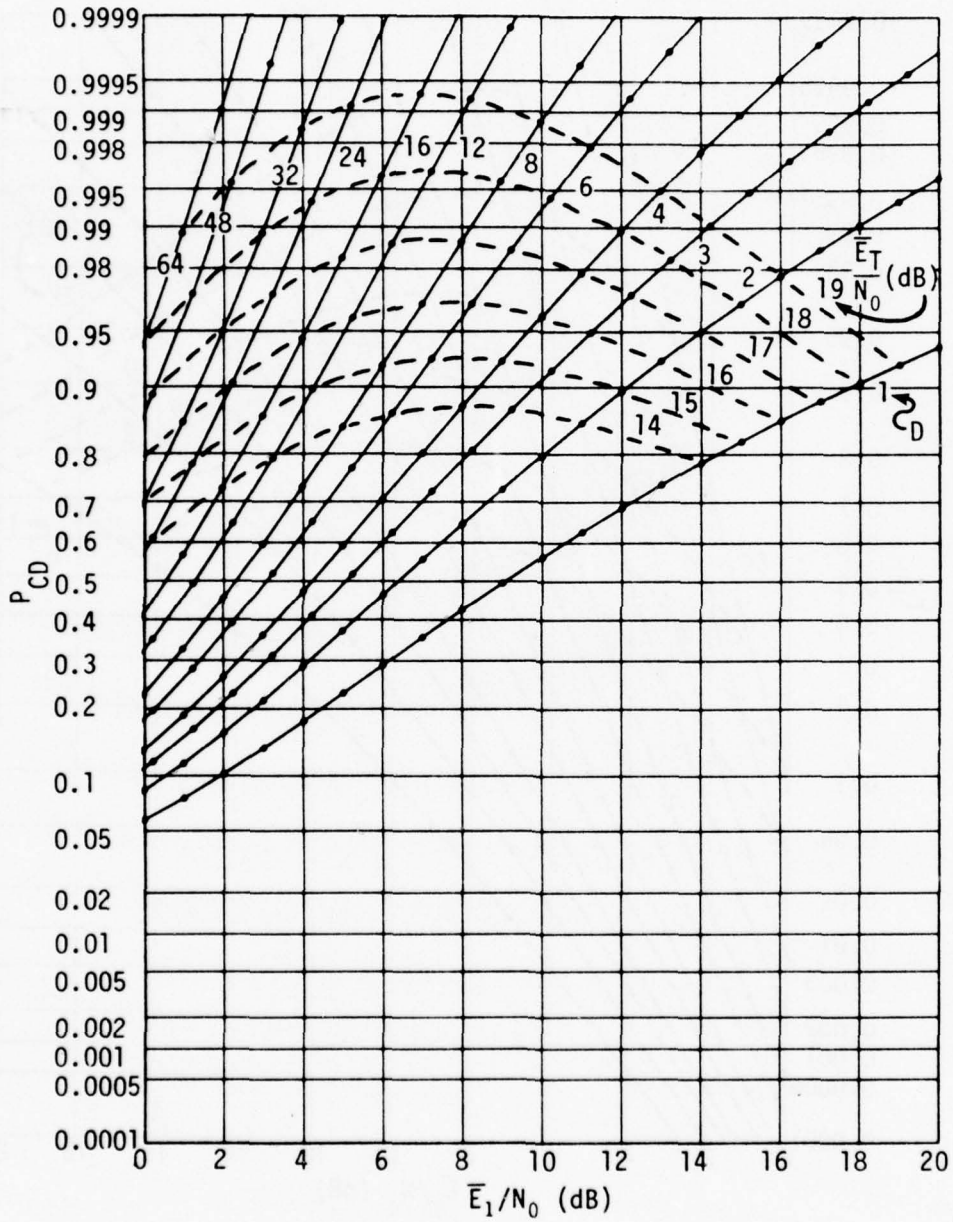


Figure 17. Detection Characteristics for $K = 3$, $M = 1$, $P_{FA} = 10^{-2}$

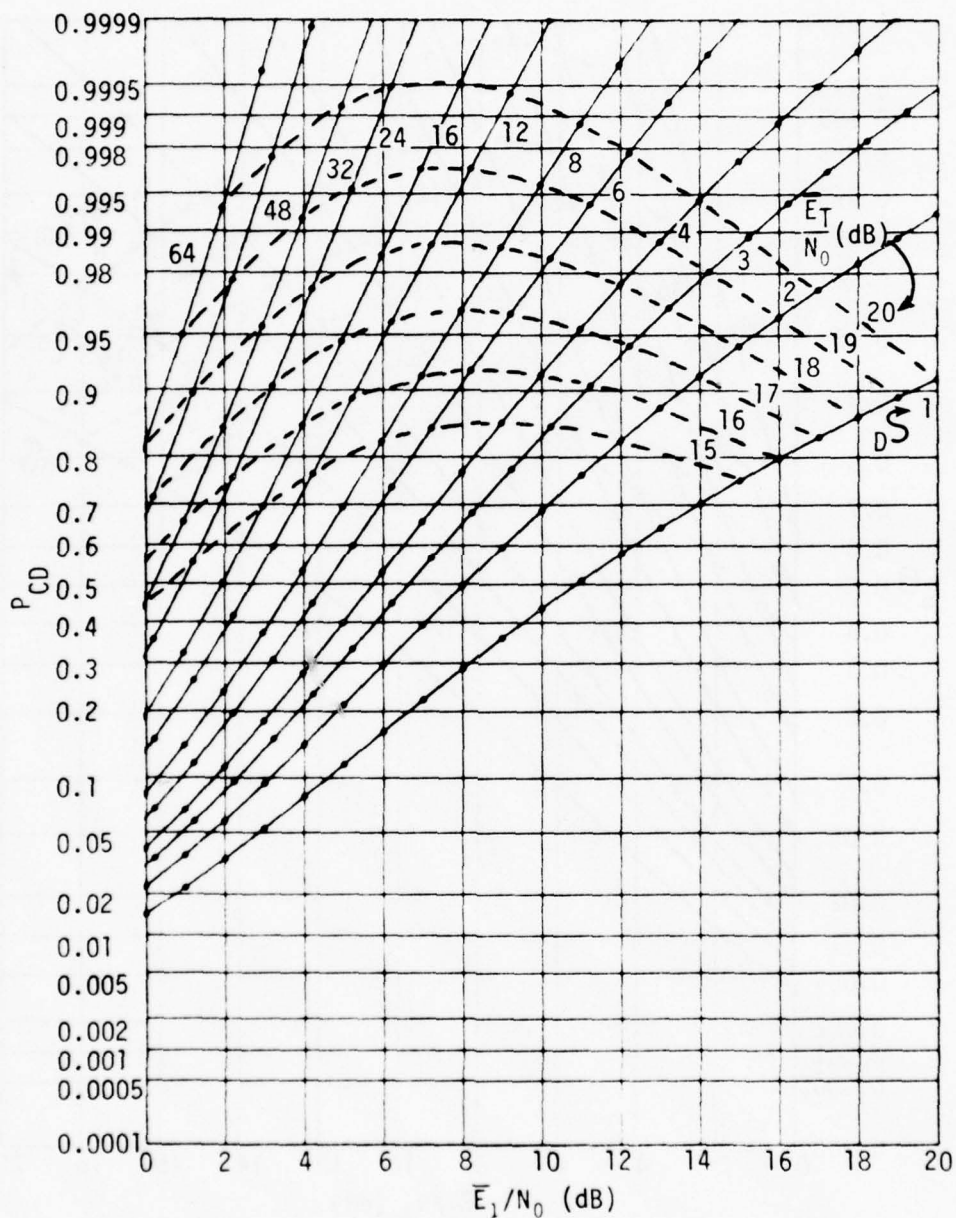


Figure 18. Detection Characteristics for $K = 3$, $M = 1$, $P_{FA} = 10^{-3}$

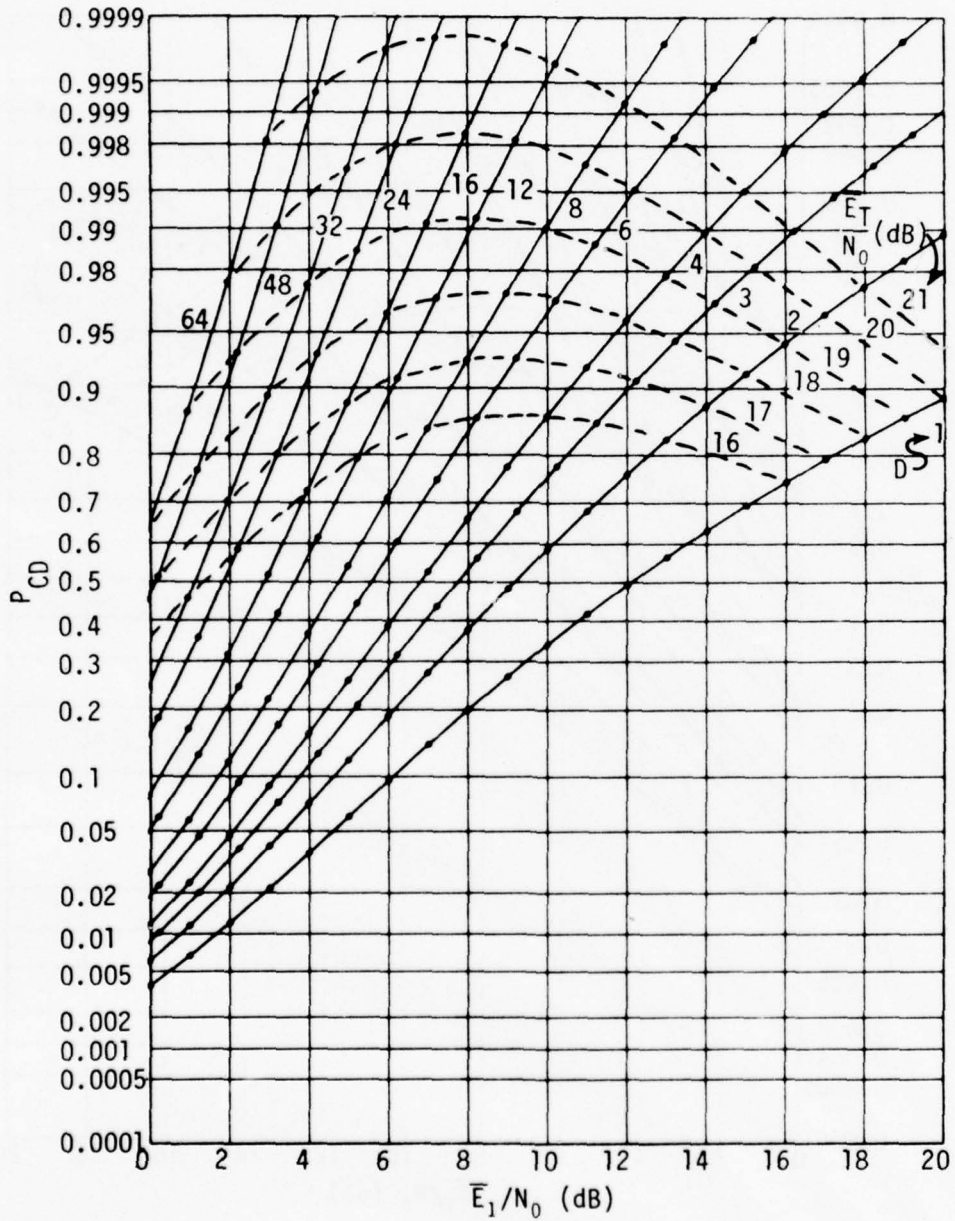


Figure 19. Detection Characteristics for $K = 3$, $M = 1$, $P_{FA} = 10^{-4}$

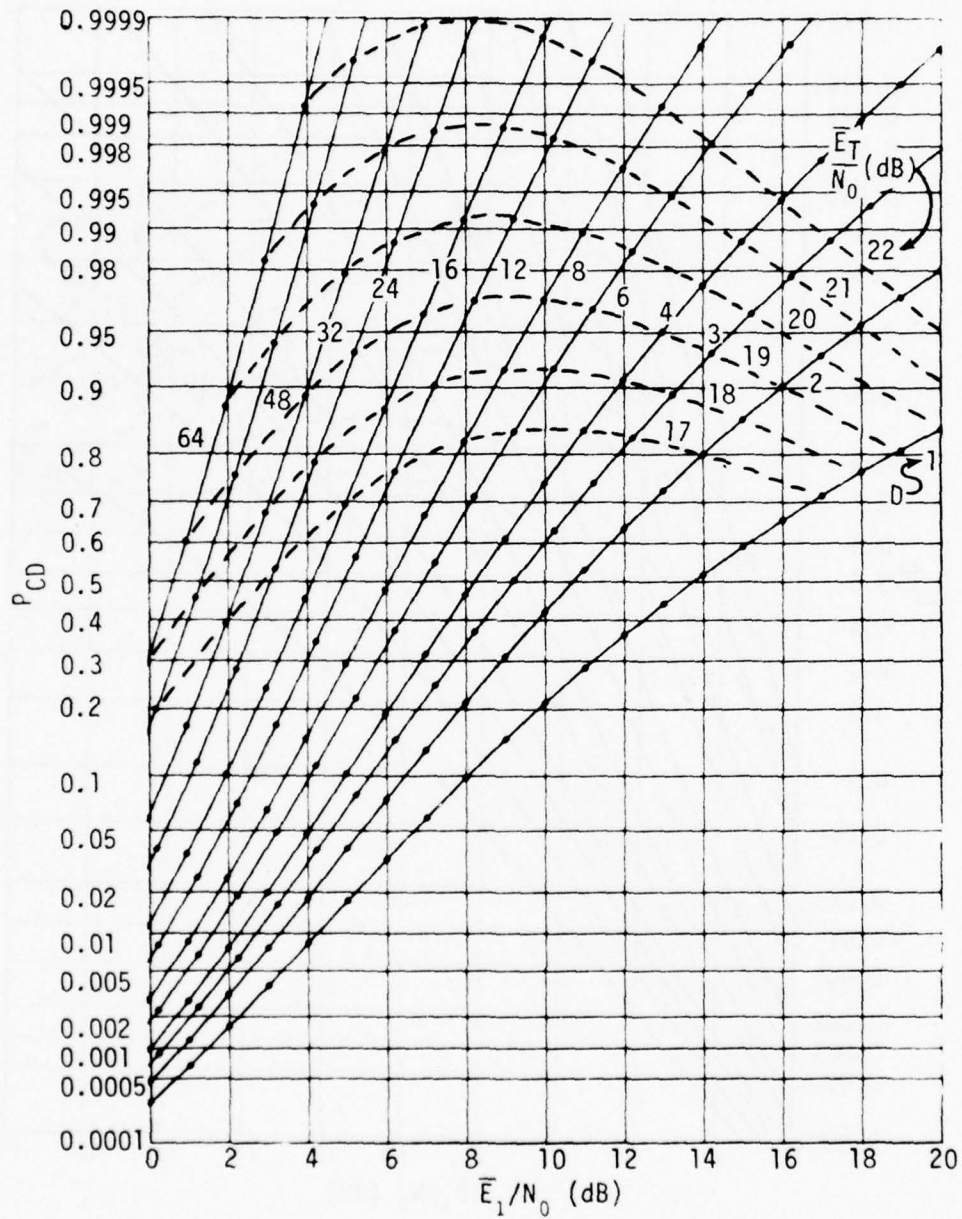


Figure 20. Detection Characteristics for $K = 3$, $M = 1$, $P_{FA} = 10^{-6}$

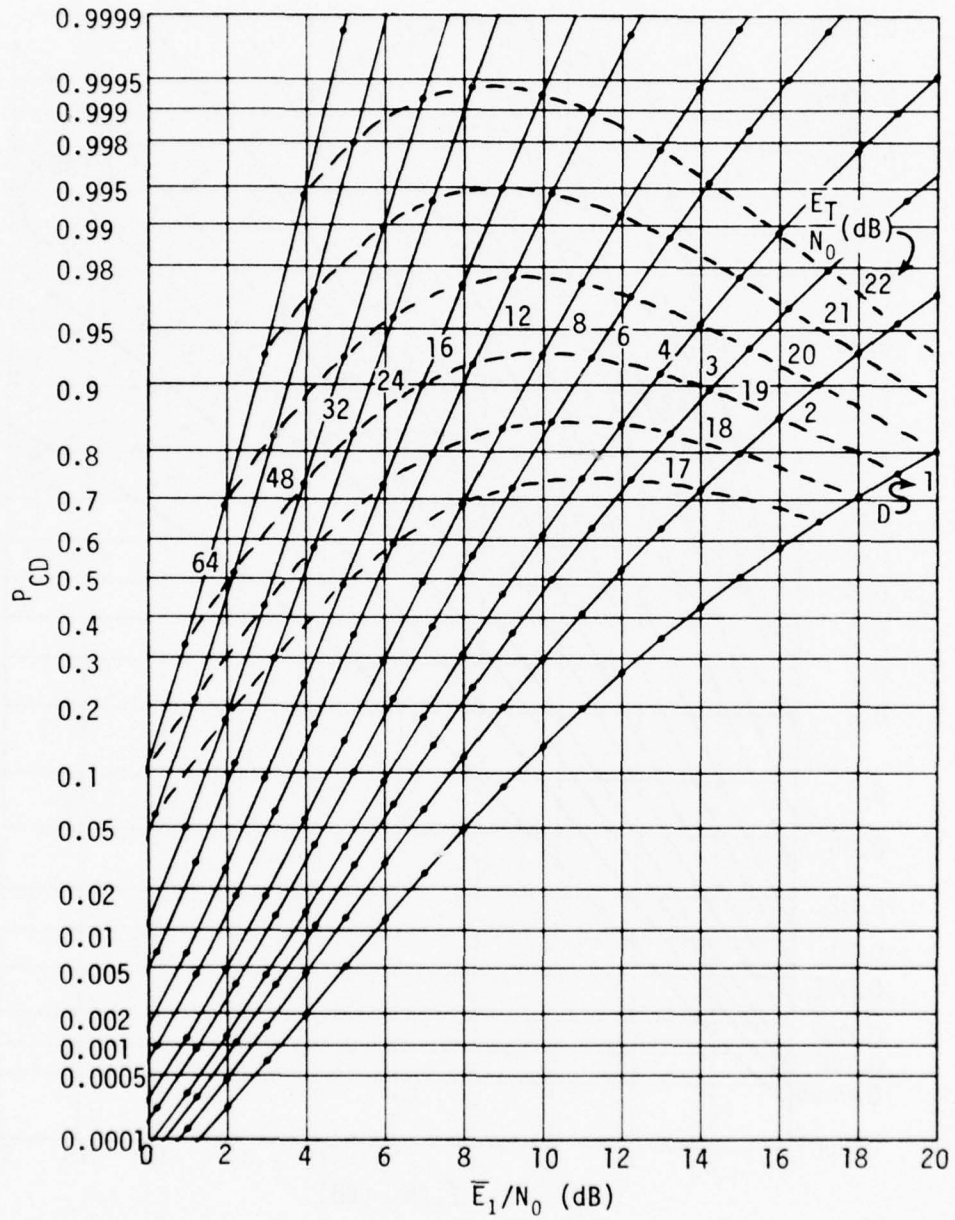


Figure 21. Detection Characteristics for $K = 3$, $M = 1$, $P_{FA} = 10^{-8}$

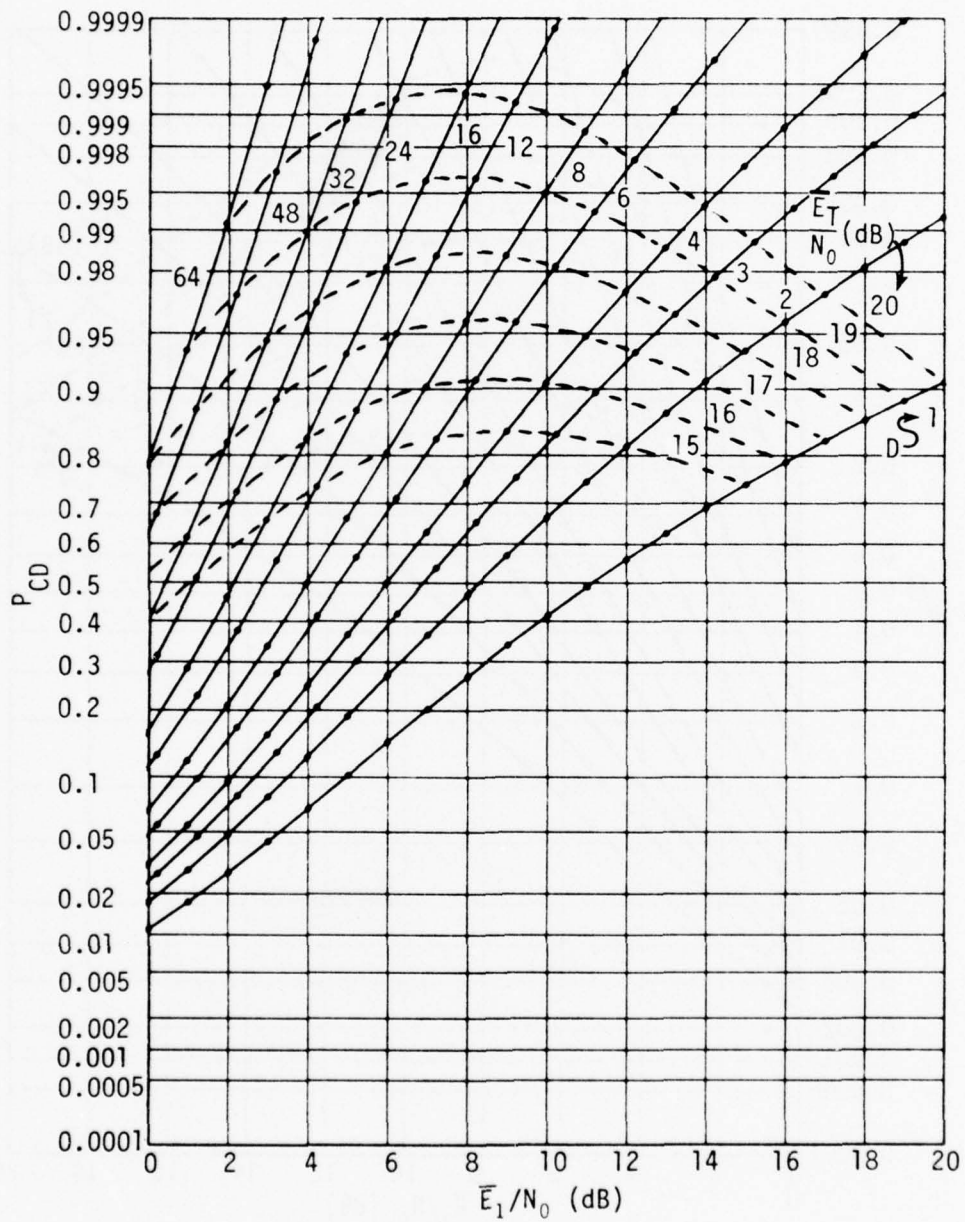


Figure 22. Detection Characteristics for $K = 3$, $M = 16$, $P_{FA} = 10^{-2}$

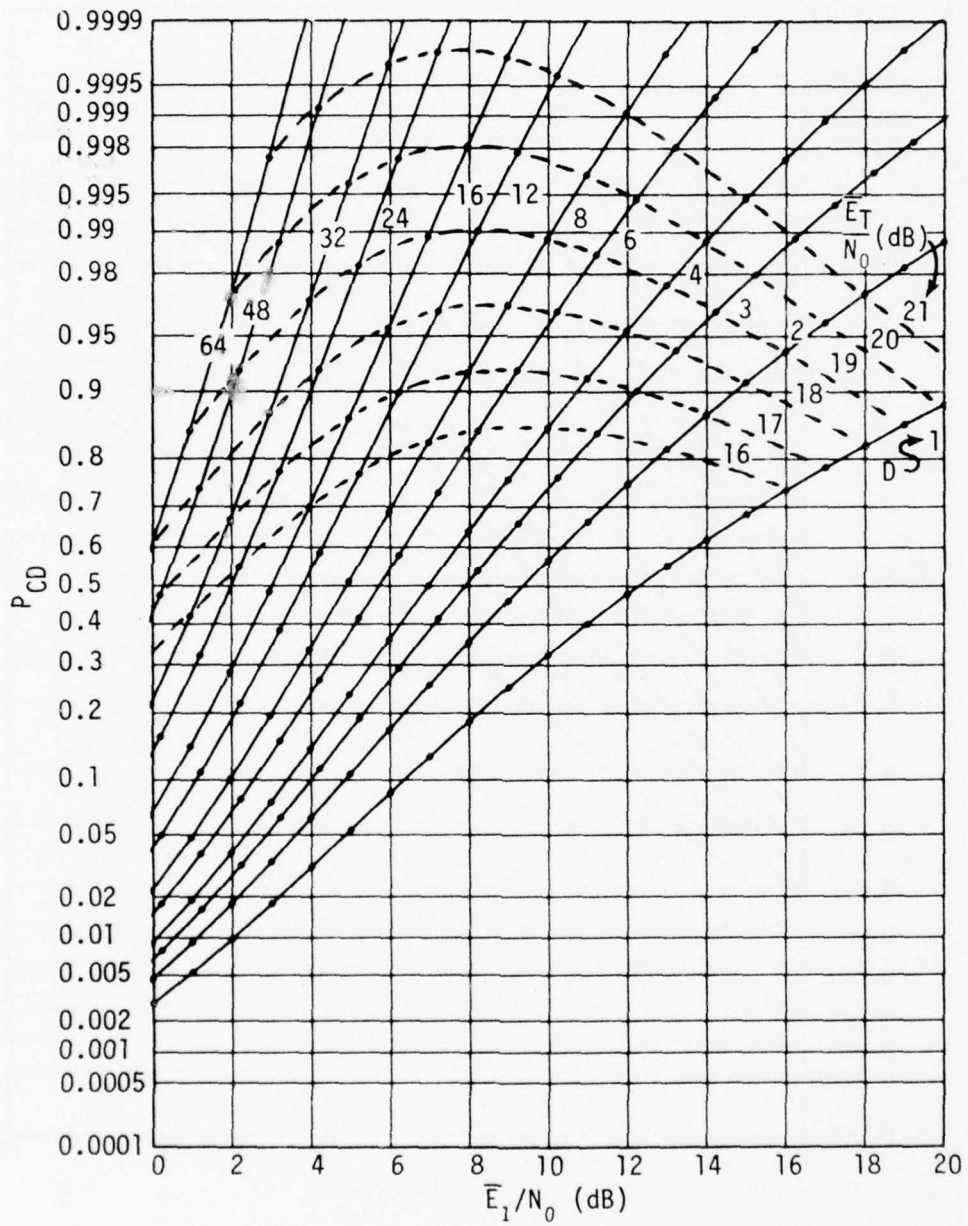


Figure 23. Detection Characteristics for $K = 3$, $M = 16$, $P_{FA} = 10^{-3}$

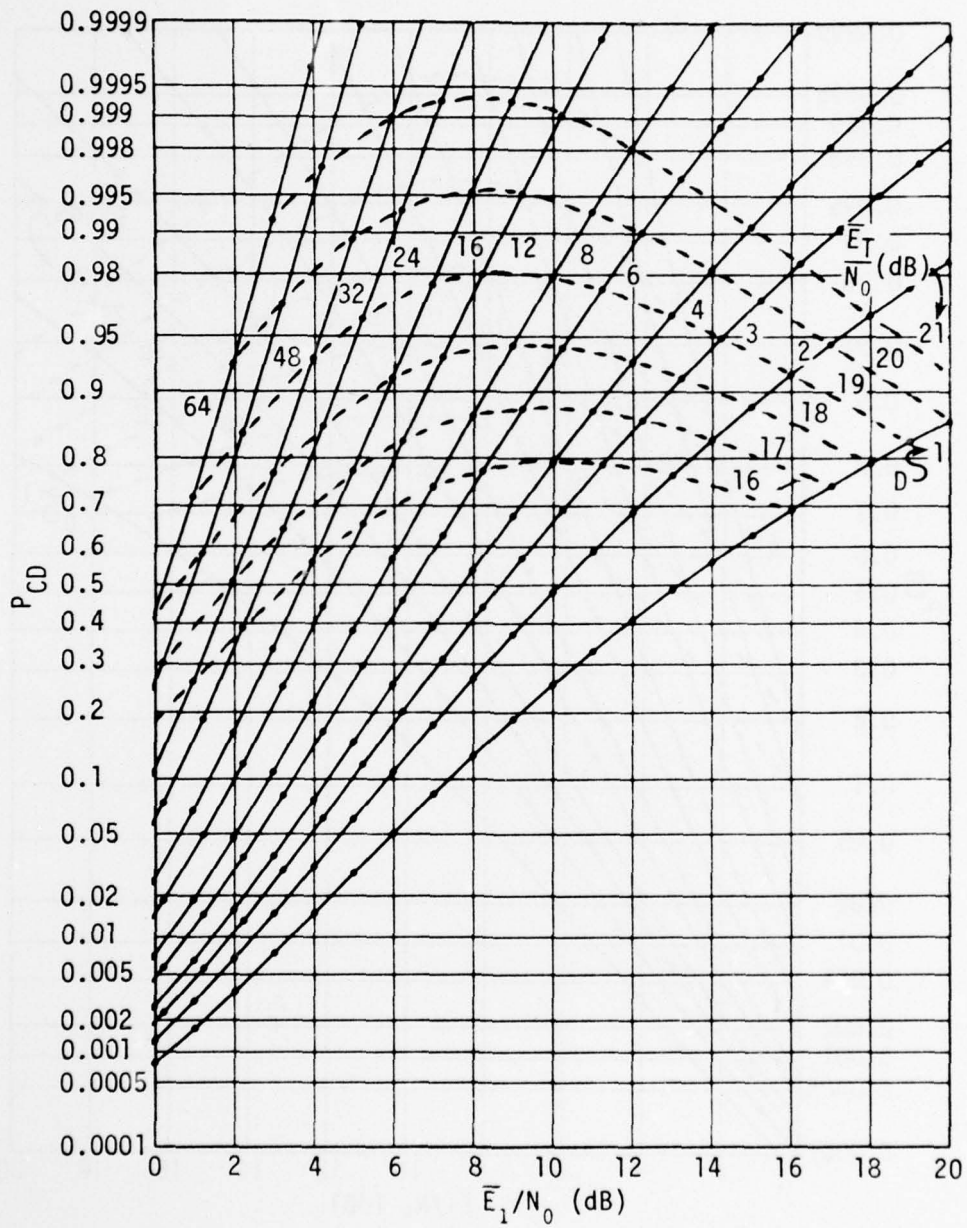


Figure 24. Detection Characteristics for $K = 3$, $M = 16$, $P_{FA} = 10^{-4}$

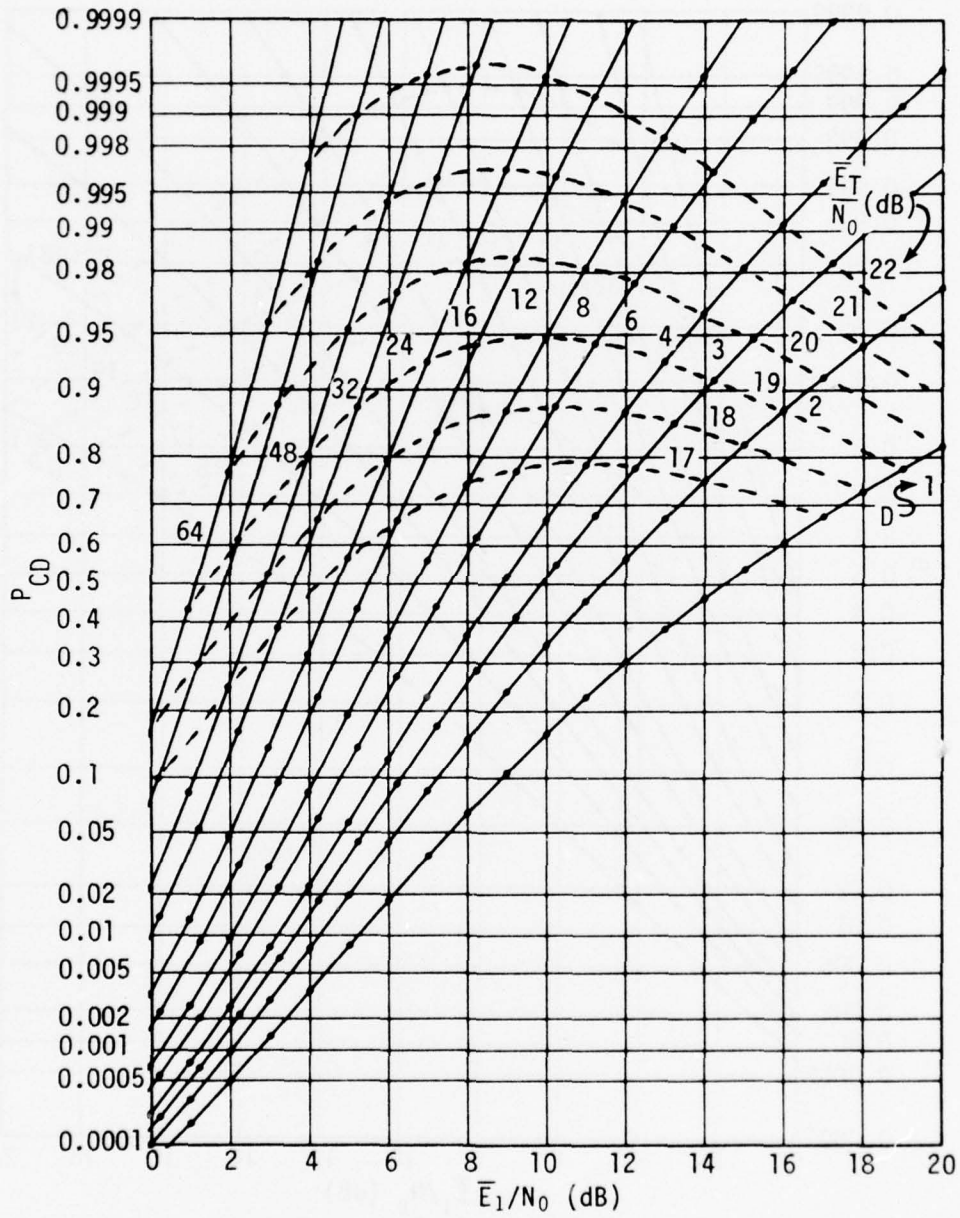


Figure 25. Detection Characteristics for $K = 3$, $M = 16$, $P_{FA} = 10^{-6}$

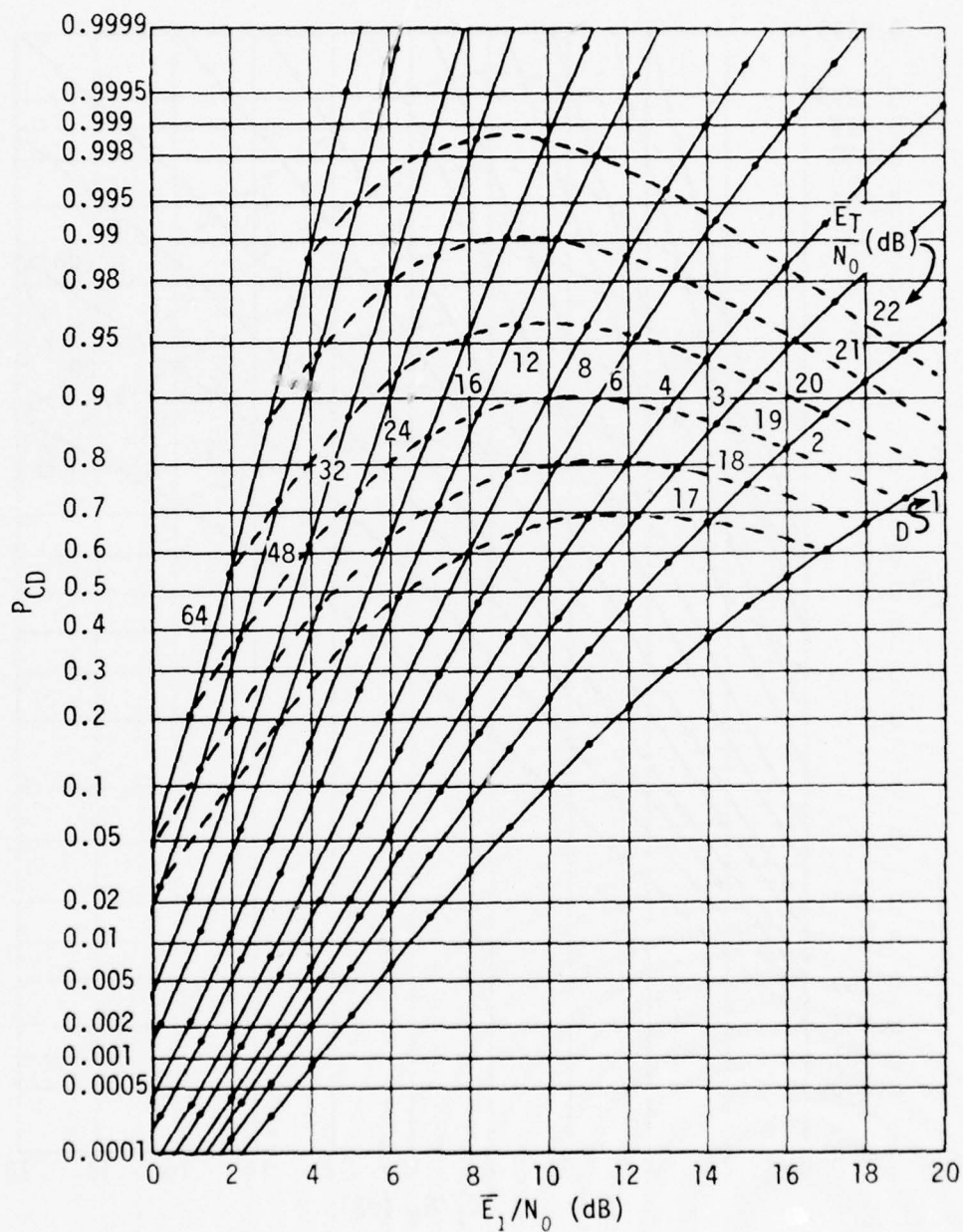


Figure 26. Detection Characteristics for $K = 3$, $M = 16$, $P_{FA} = 10^{-8}$

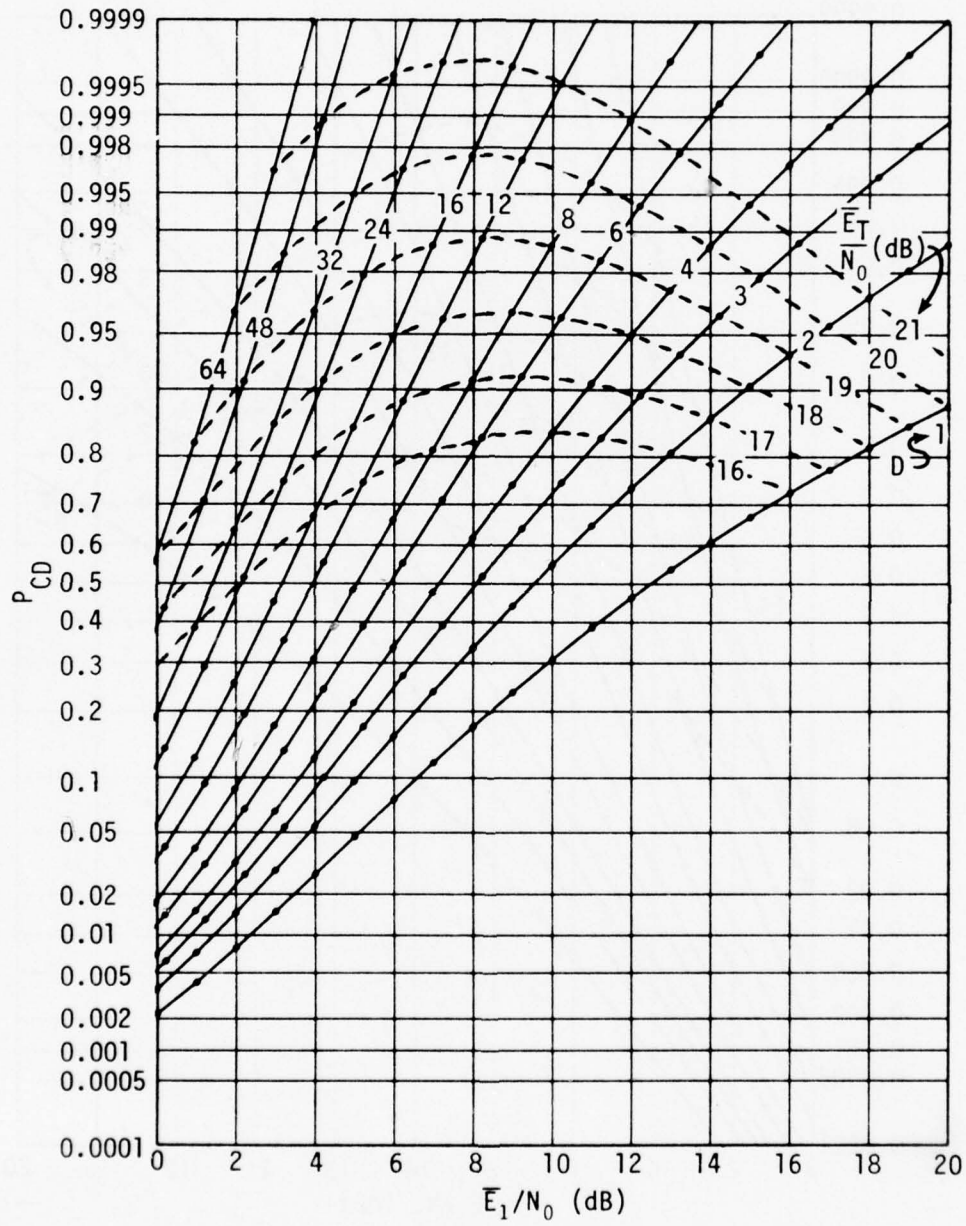


Figure 27. Detection Characteristics for $K = 3$, $M = 256$, $P_{FA} = 10^{-2}$

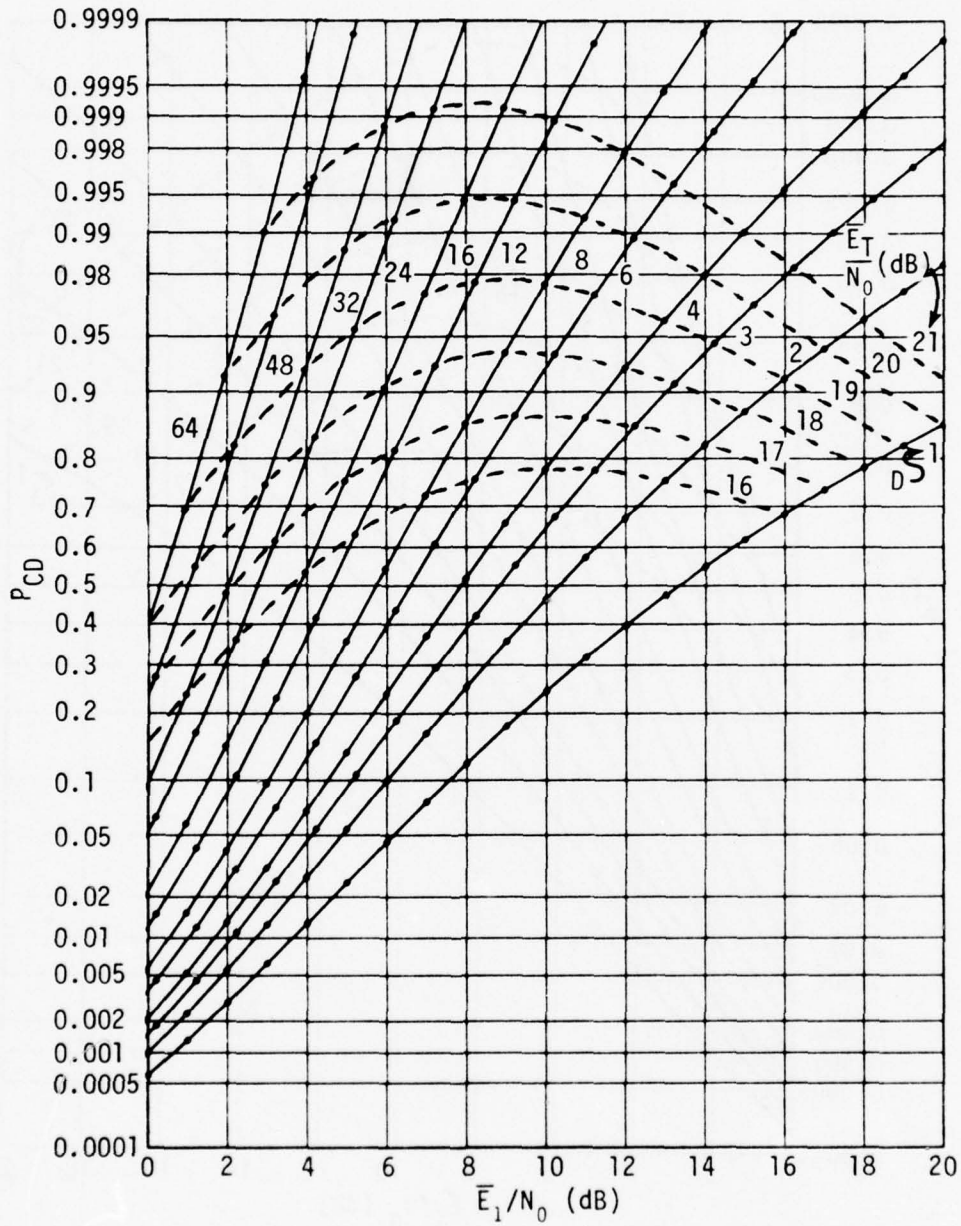


Figure 28. Detection Characteristics for $K = 3$, $M = 256$, $P_{FA} = 10^{-3}$

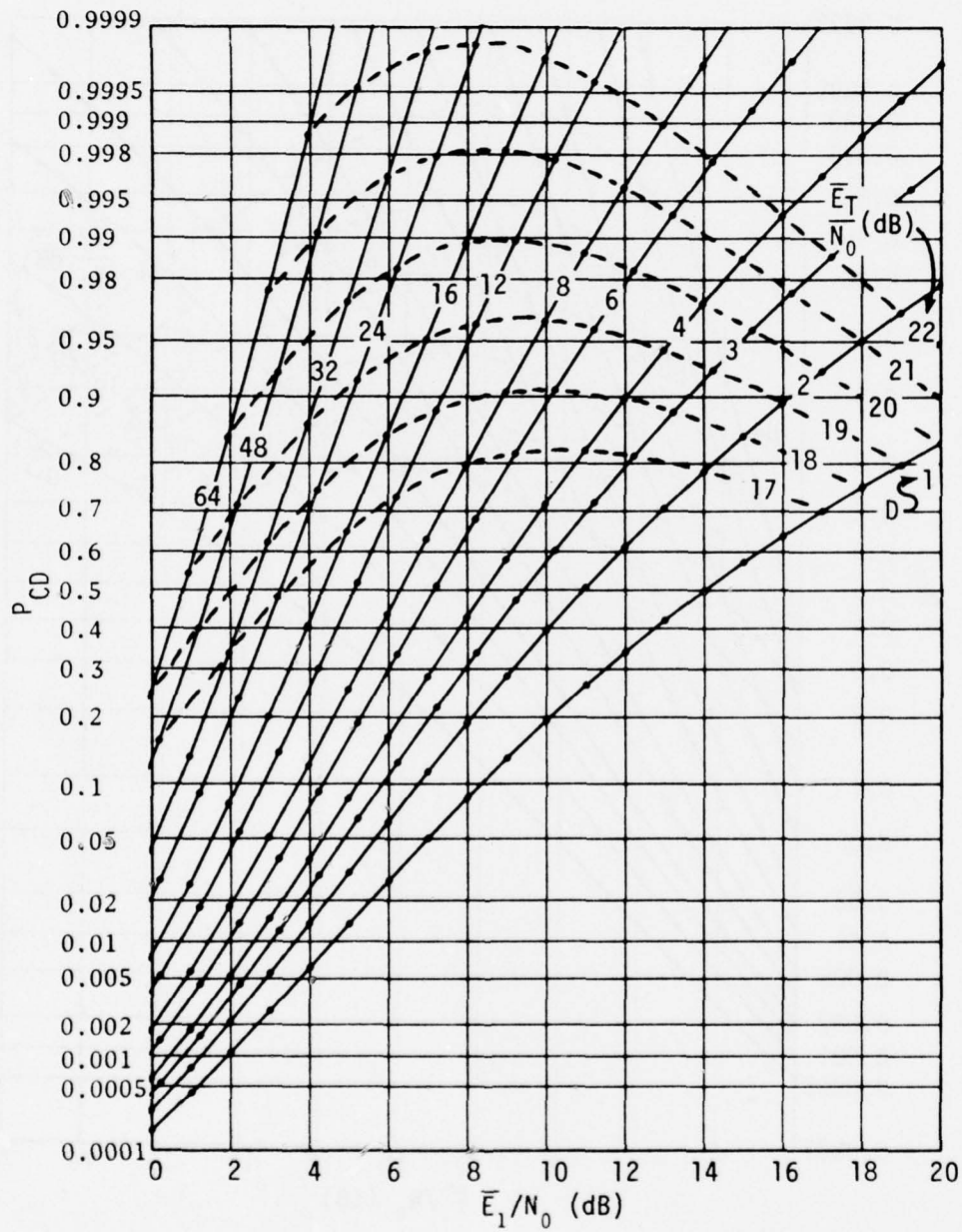


Figure 29. Detection Characteristics for $K = 3$, $M = 256$, $P_{FA} = 10^{-4}$

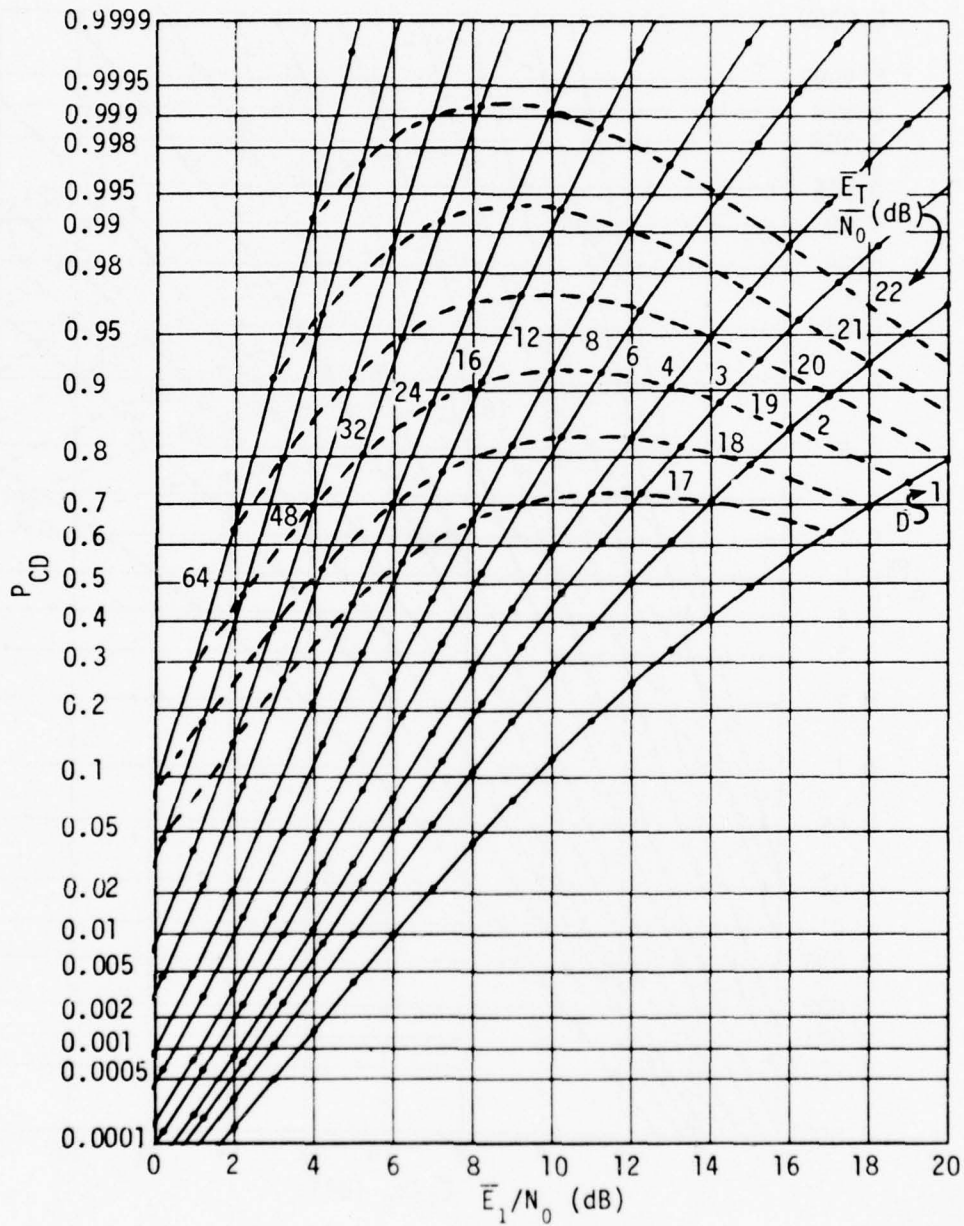


Figure 30. Detection Characteristics for $K = 3$, $M = 256$, $P_{FA} = 10^{-6}$

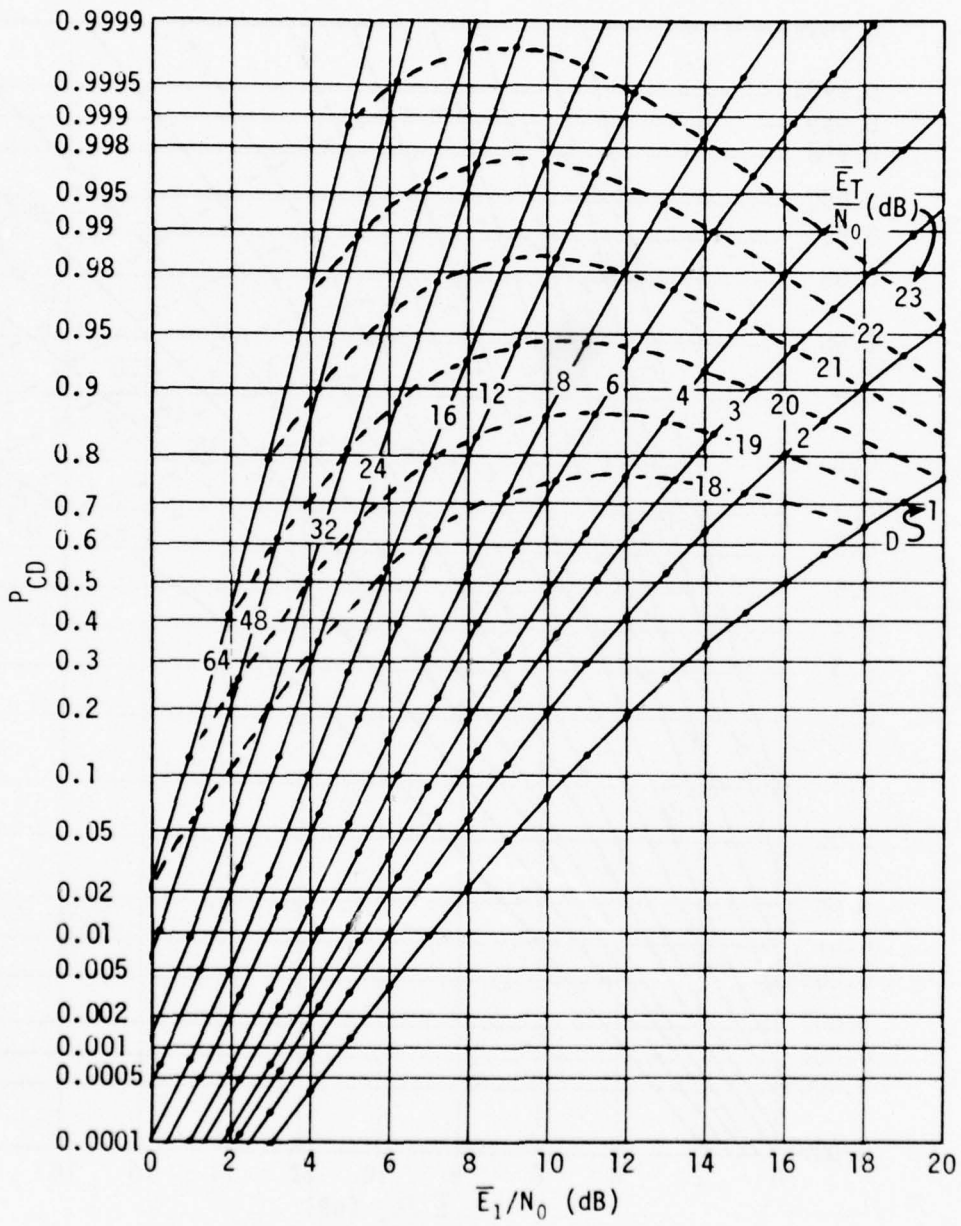


Figure 31. Detection Characteristics for $K = 3$, $M = 256$, $P_{FA} = 10^{-8}$

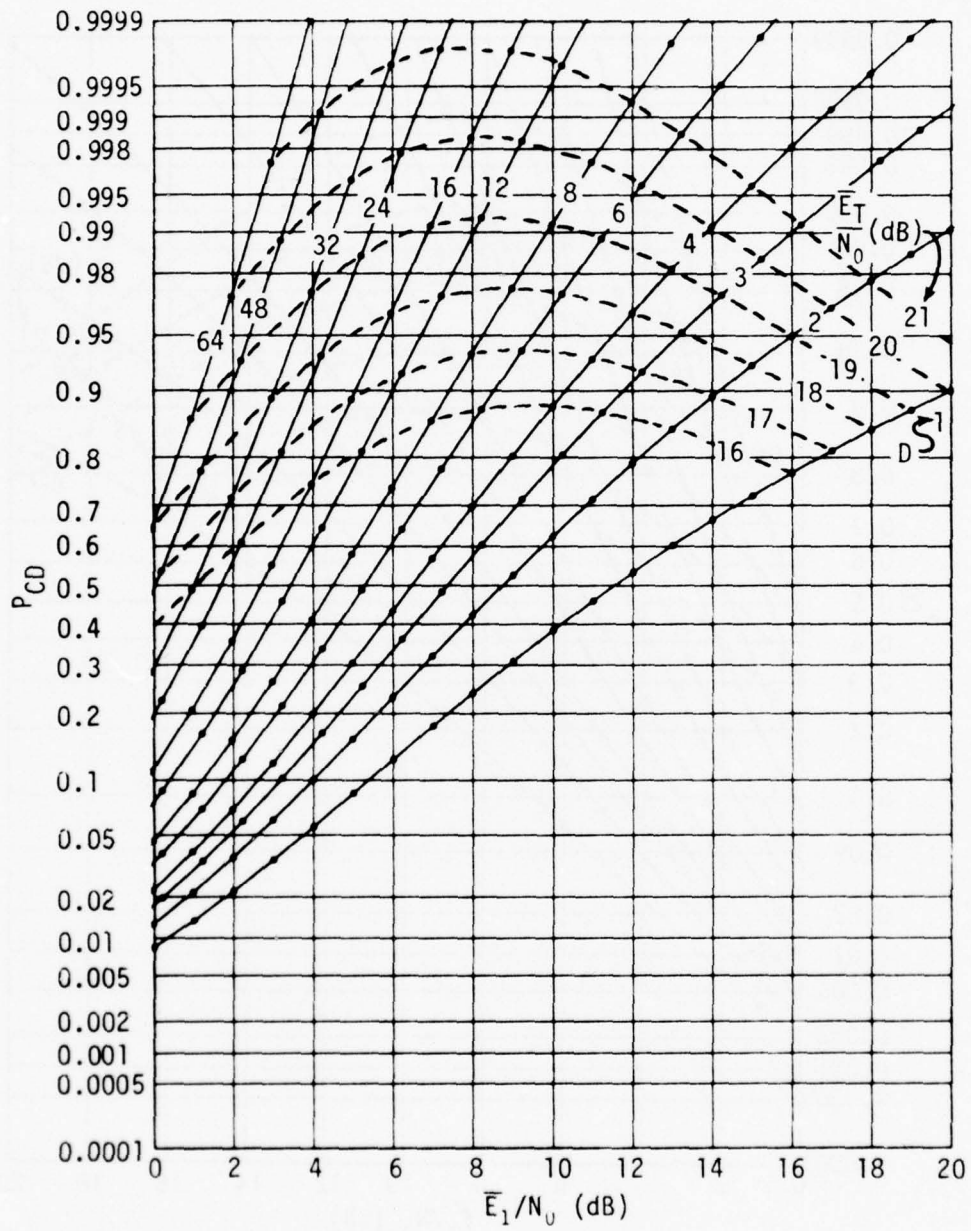


Figure 32. Detection Characteristics for $K = 4$, $M = 16$, $P_{FA} = 10^{-2}$

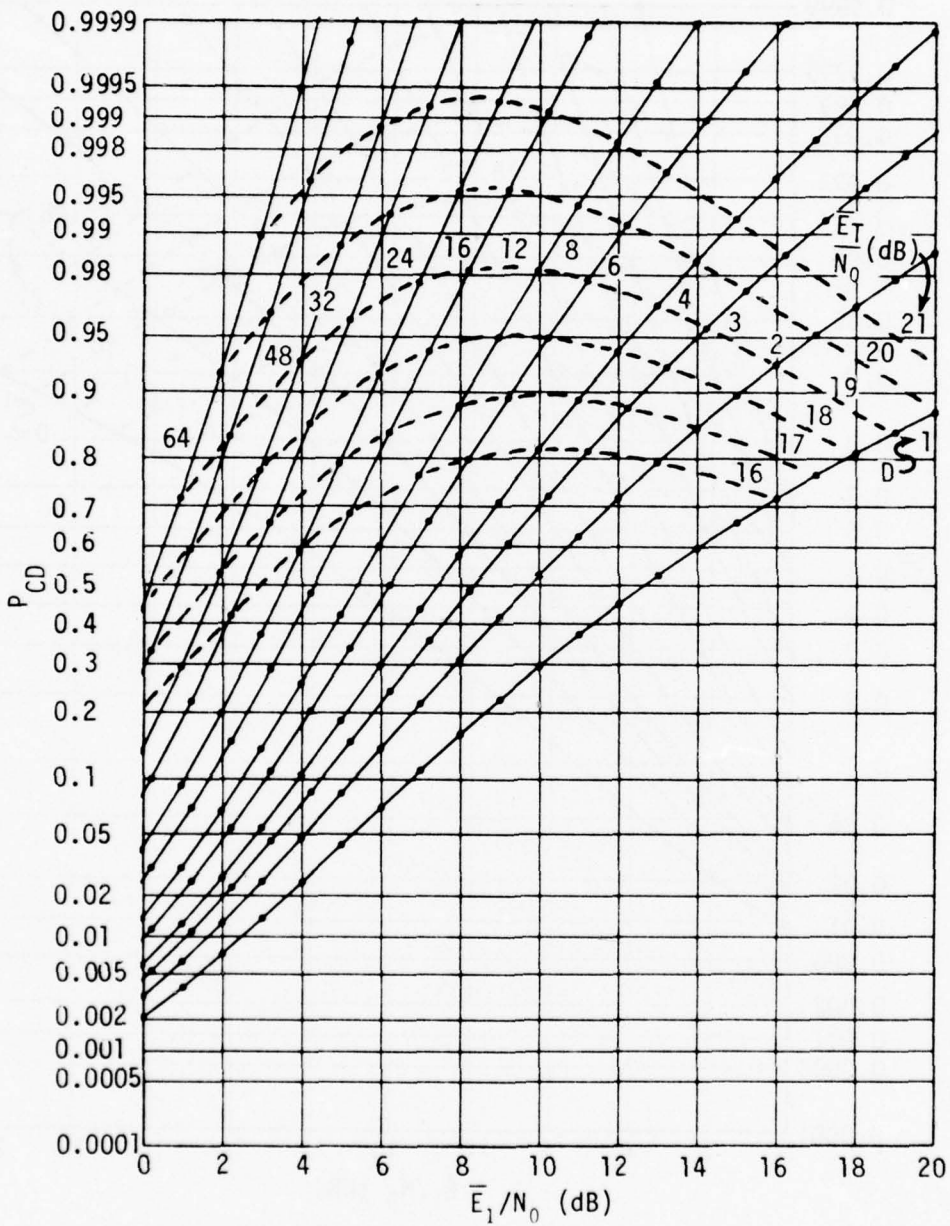


Figure 33. Detection Characteristics for $K = 4$, $M = 16$, $P_{FA} = 10^{-3}$

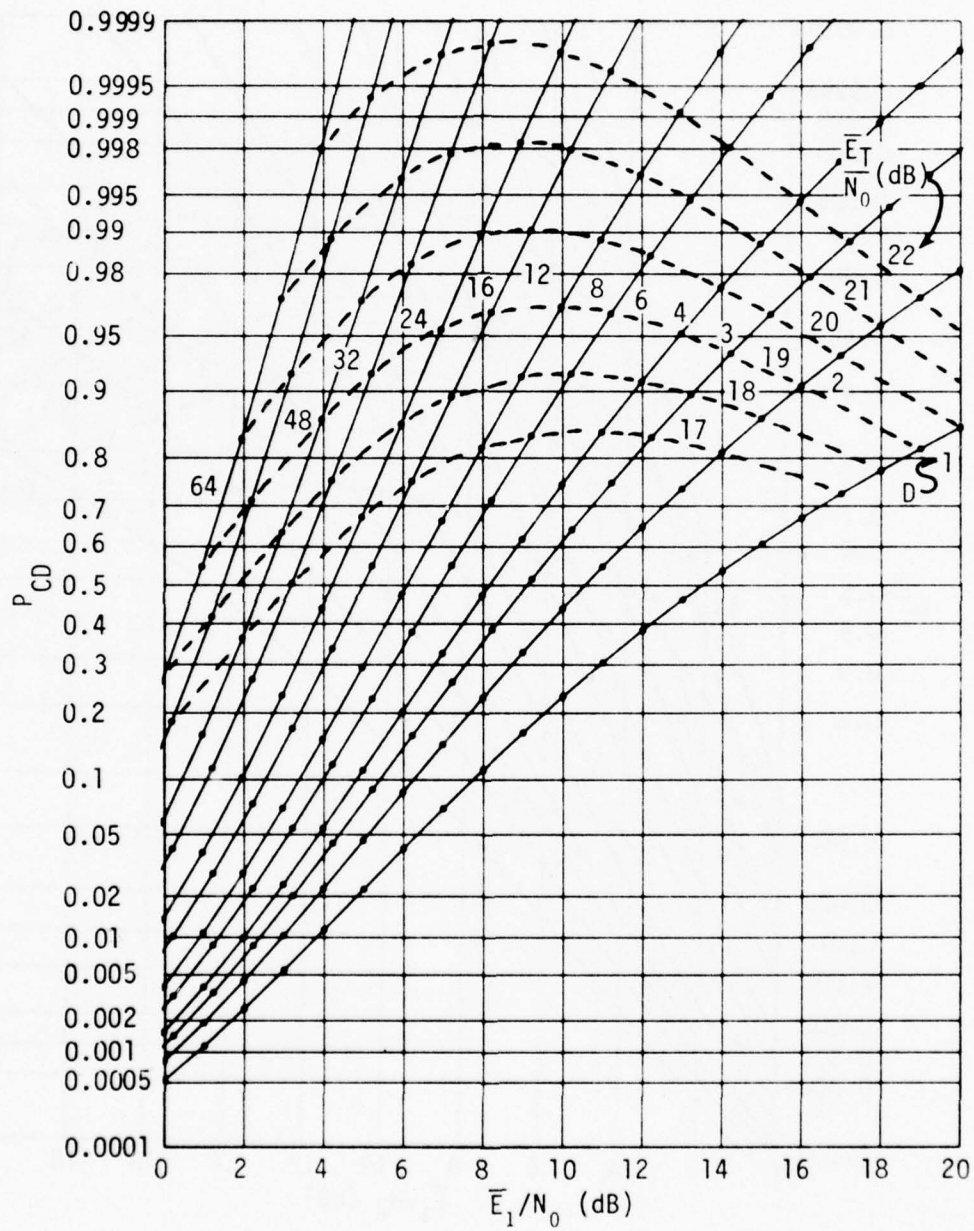


Figure 34. Detection Characteristics for $K = 4$, $M = 16$, $P_{FA} = 10^{-4}$

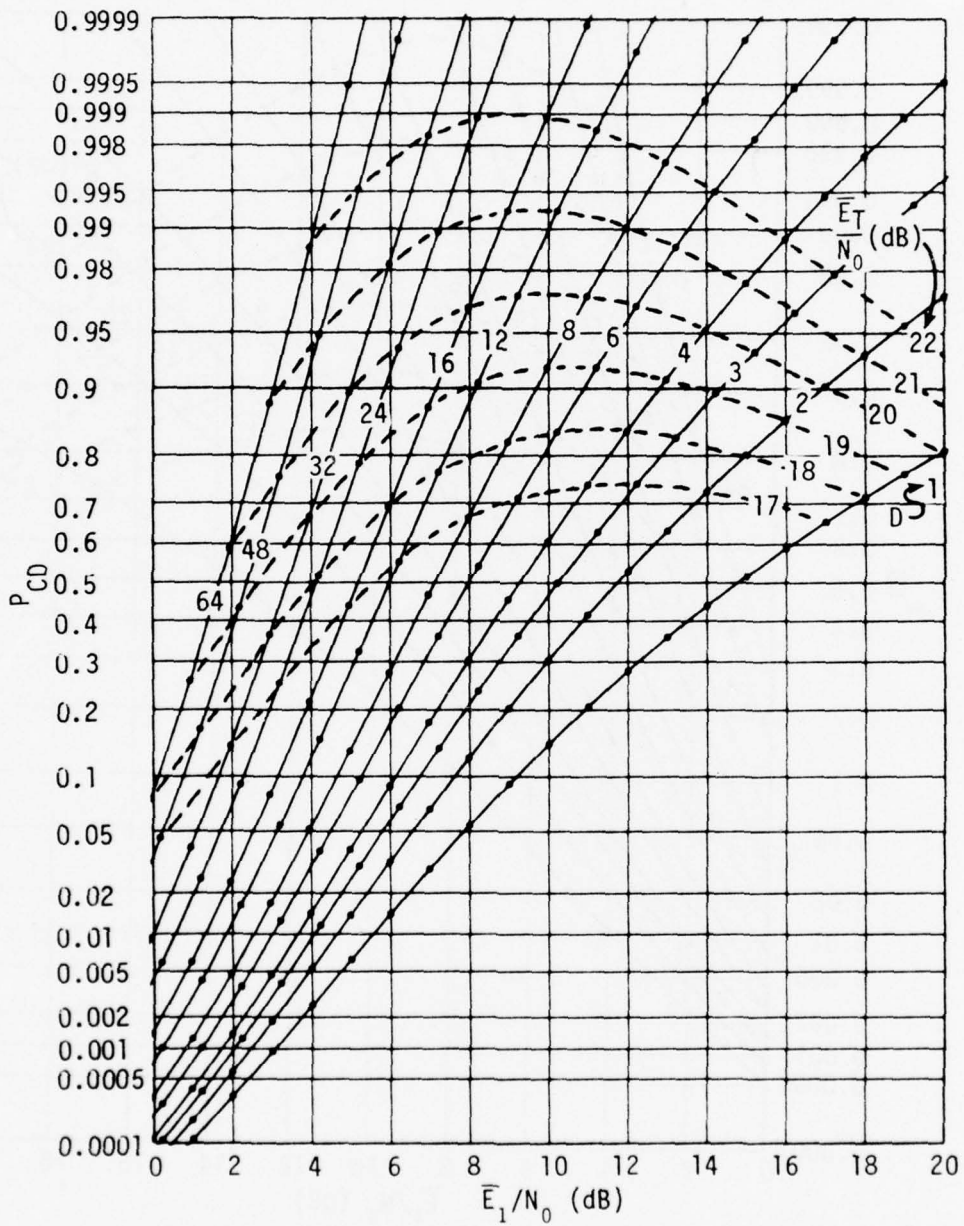


Figure 35. Detection Characteristics for $K = 4$, $M = 16$, $P_{FA} = 10^{-6}$

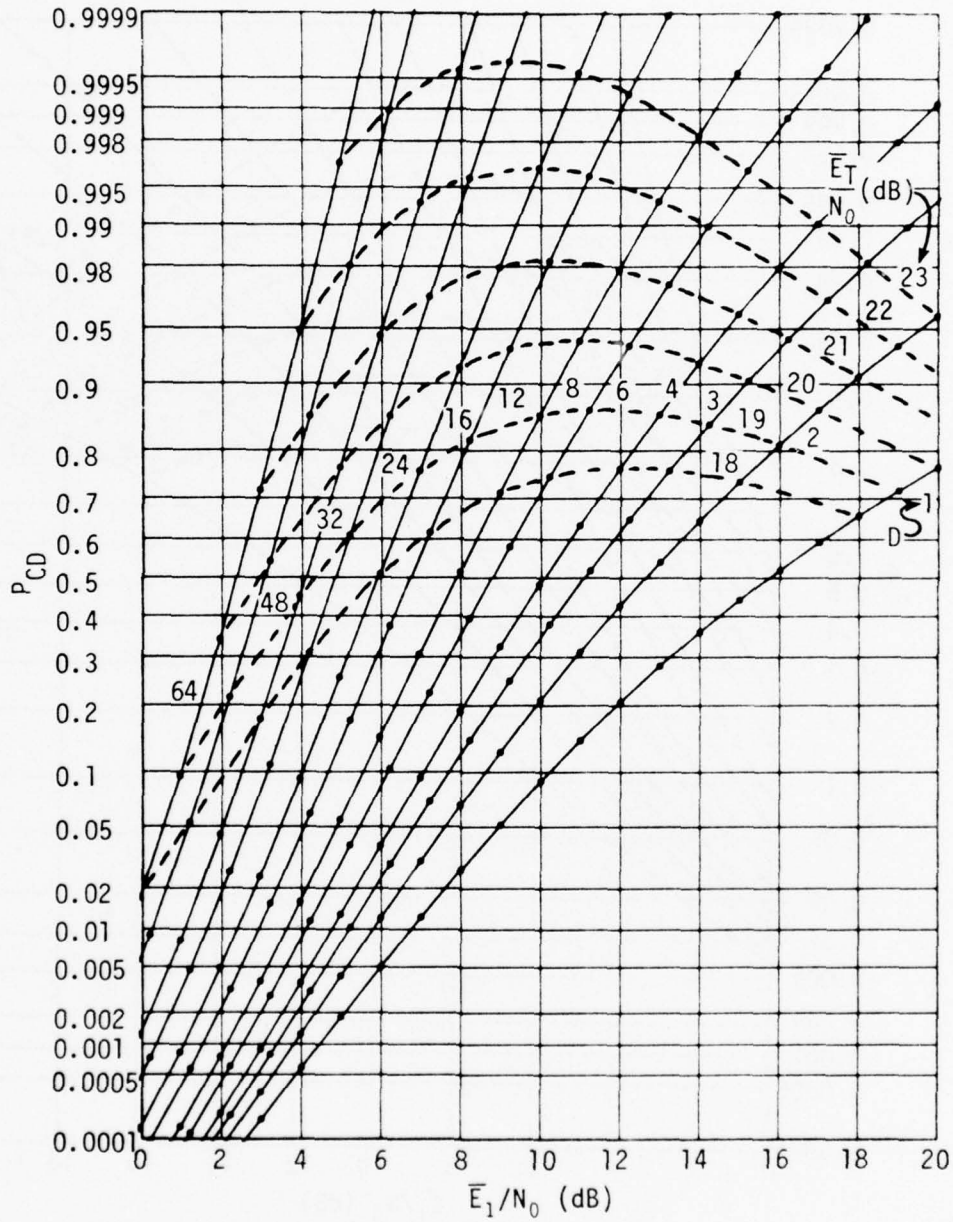


Figure 36. Detection Characteristics for $K = 4$, $M = 16$, $P_{FA} = 10^{-8}$

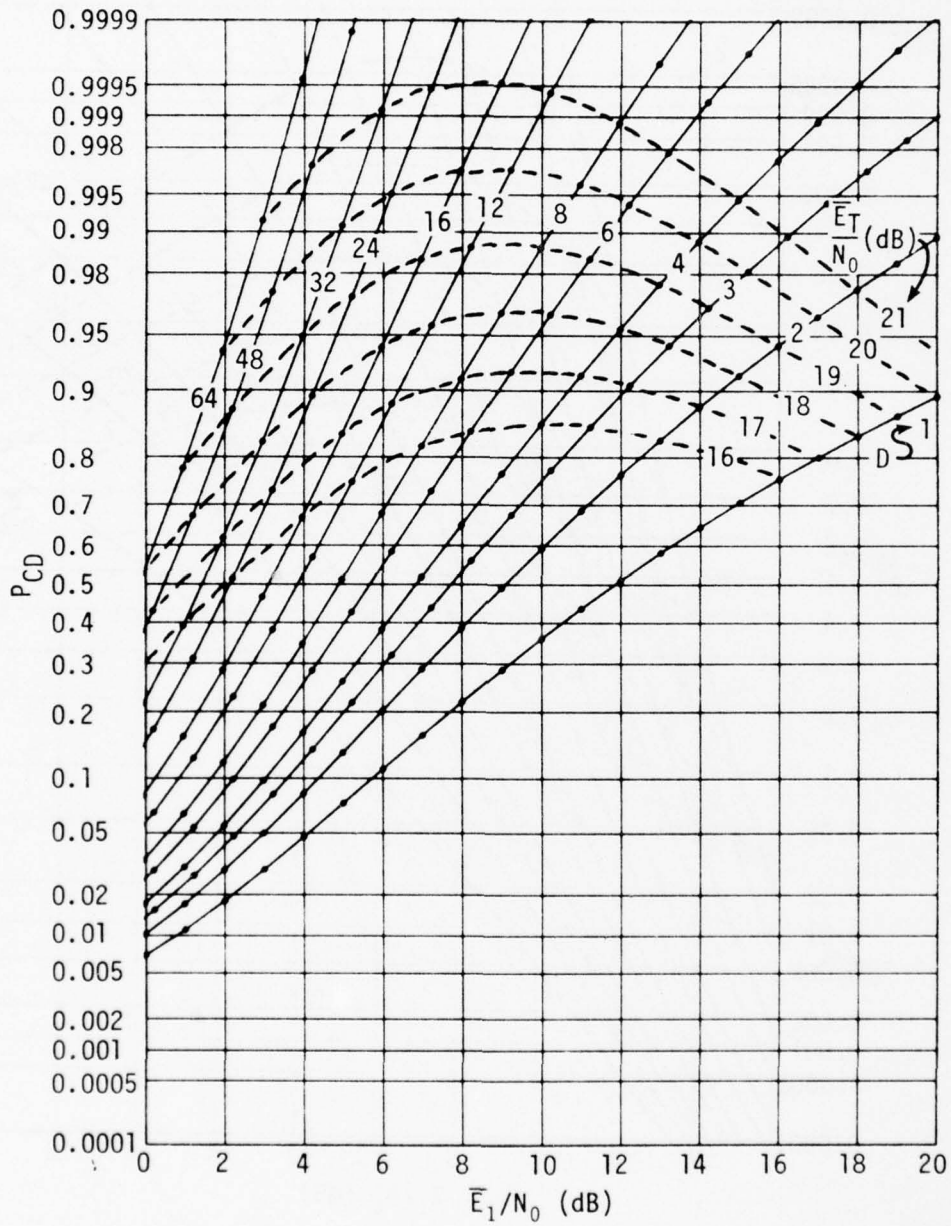


Figure 37. Detection Characteristics for $K = 5$, $M = 16$, $P_{FA} = 10^{-2}$

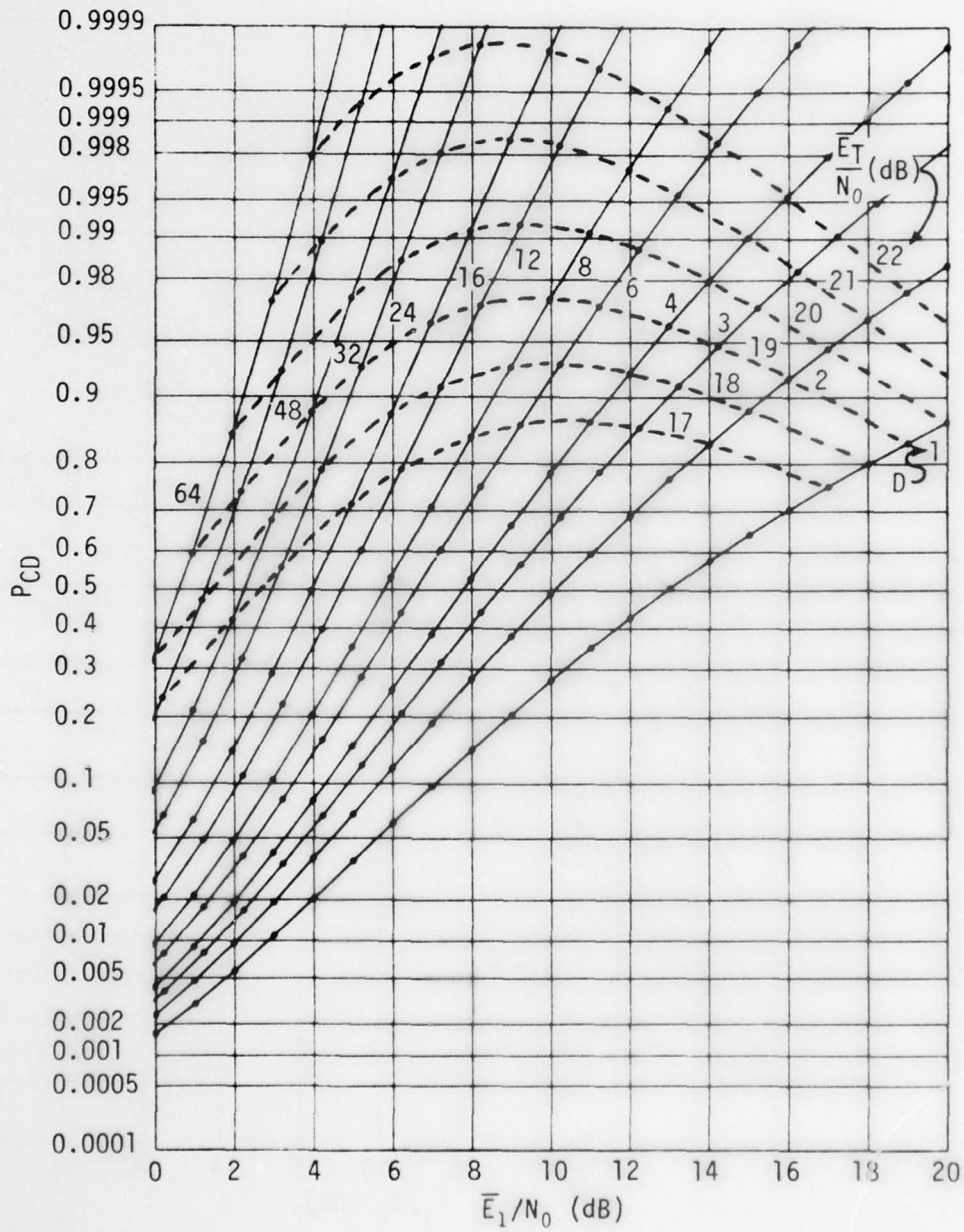


Figure 38. Detection Characteristics for $K = 5$, $M = 16$, $P_{FA} = 10^{-3}$

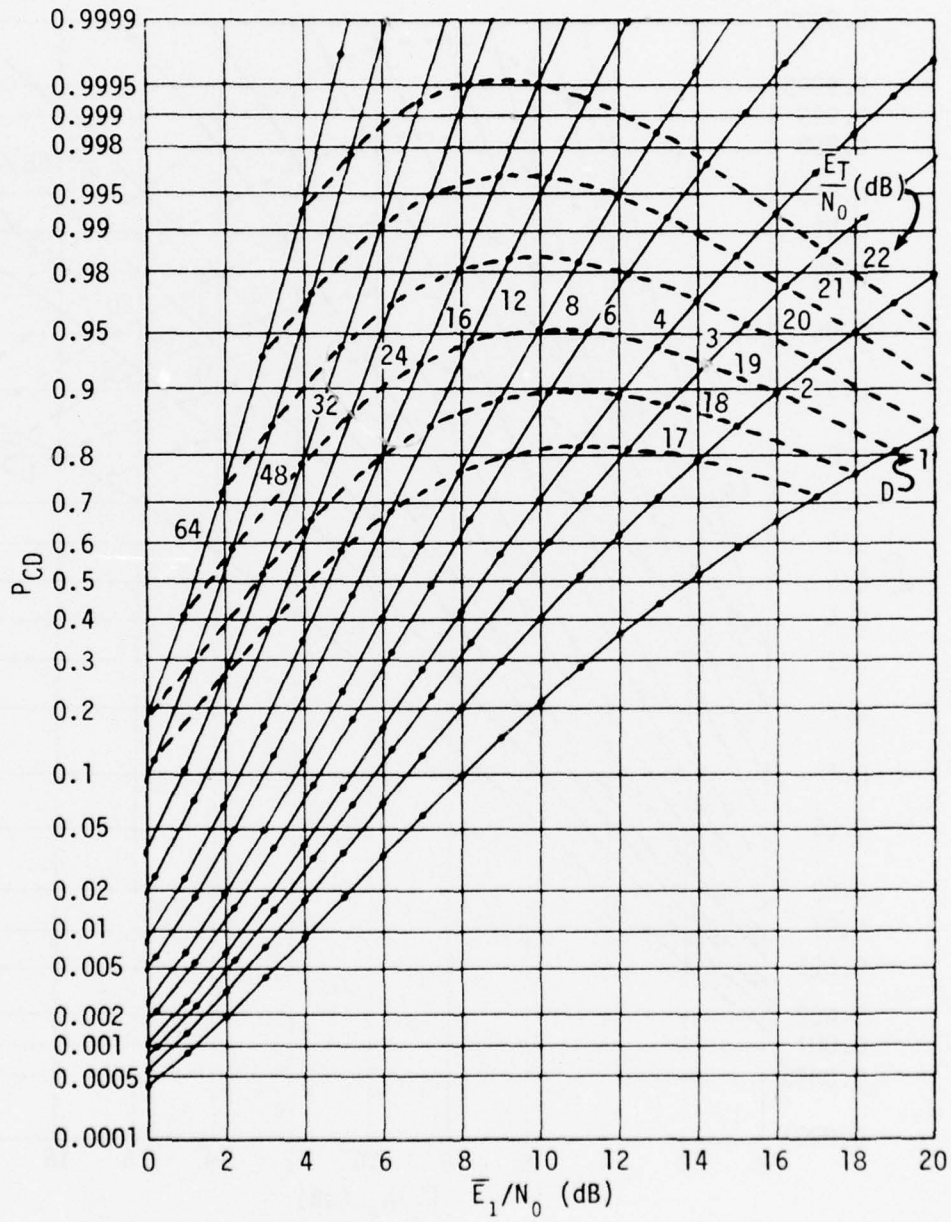


Figure 39. Detection Characteristics for $K = 5$, $M = 16$, $P_{FA} = 10^{-4}$

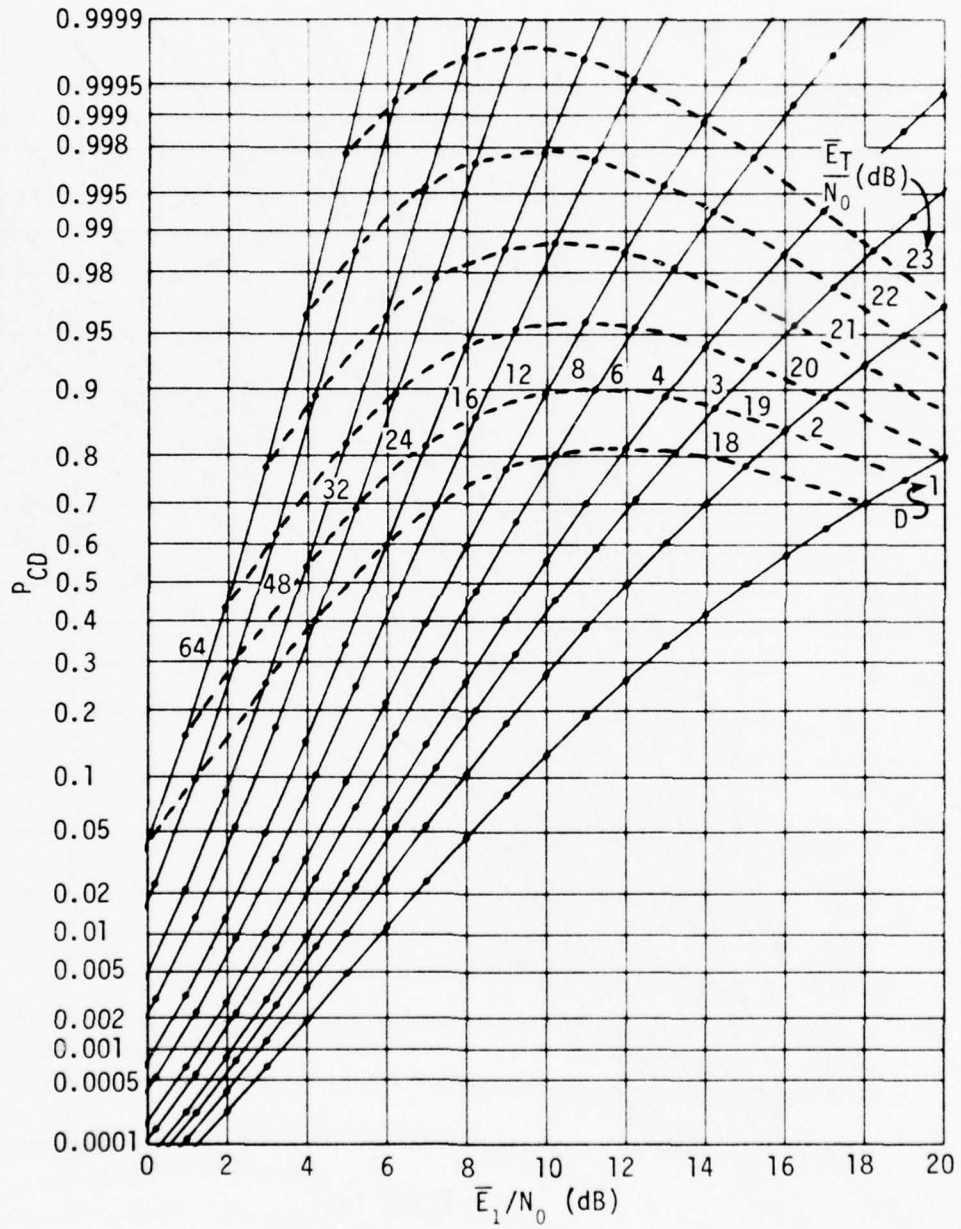


Figure 40. Detection Characteristics for $K = 5$, $M = 16$, $P_{FA} = 10^{-6}$

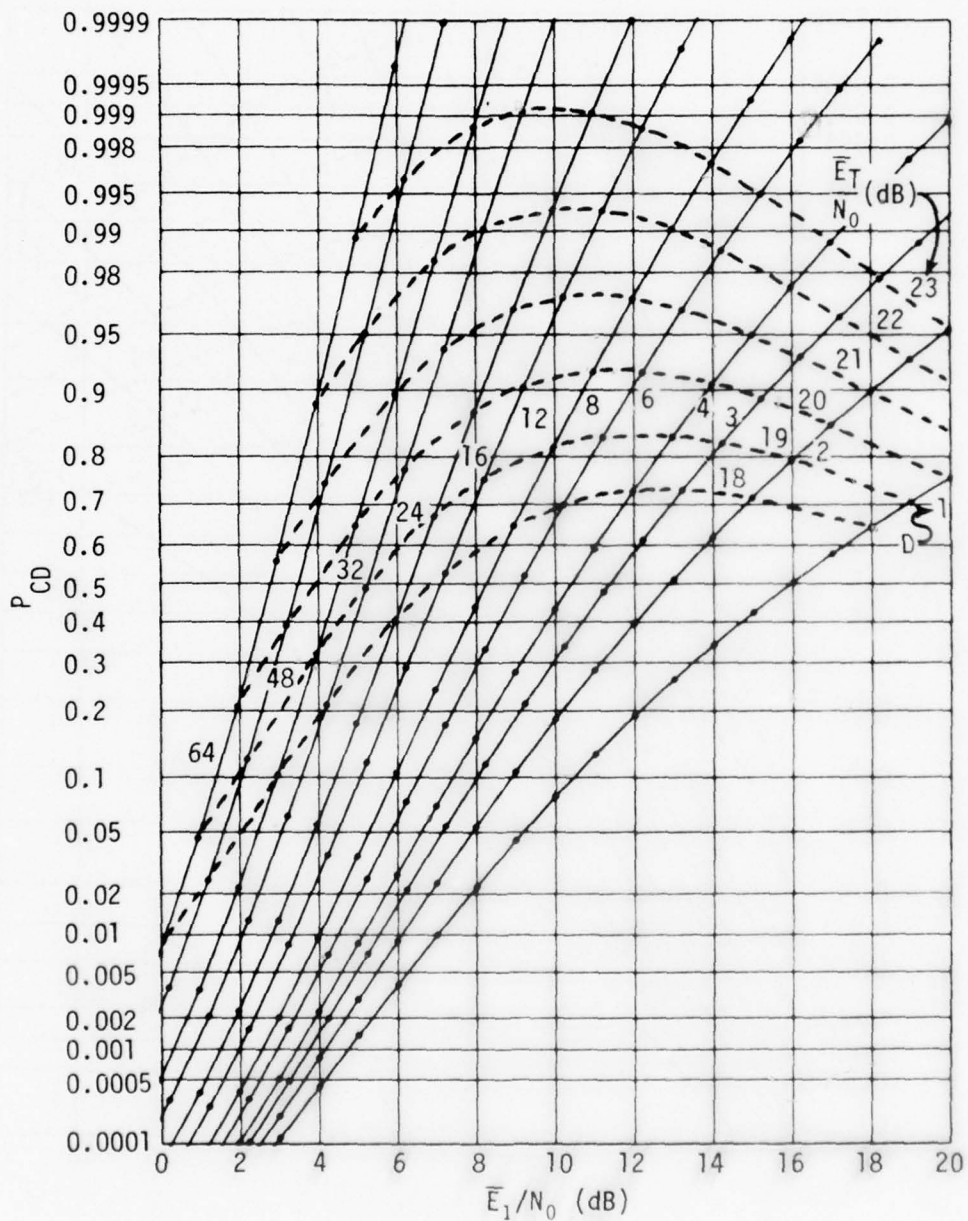


Figure 41. Detection Characteristics for $K = 5$, $M = 16$, $P_{FA} = 10^{-8}$

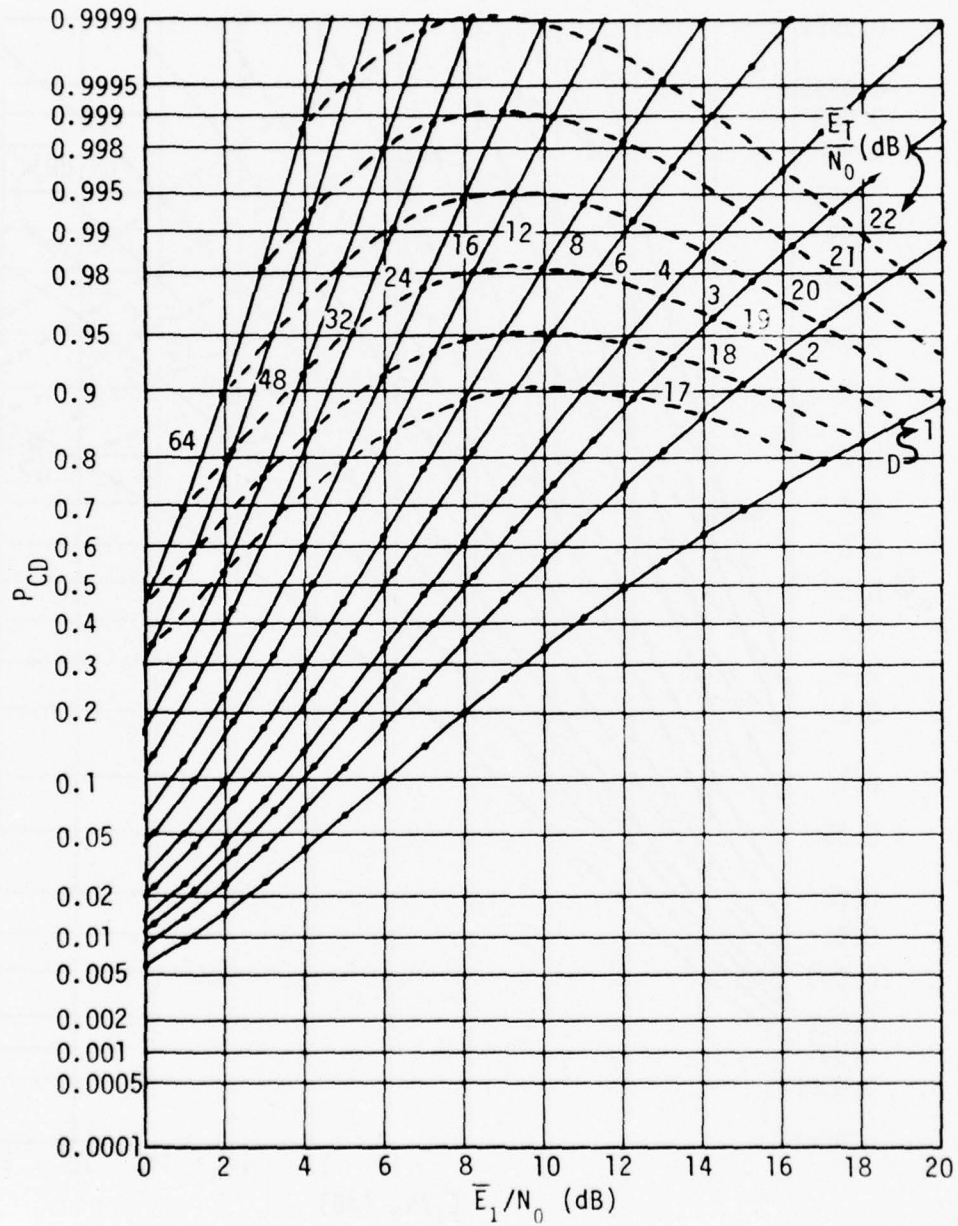


Figure 42. Detection Characteristics for $K = 6$, $M = 16$, $P_{FA} = 10^{-2}$

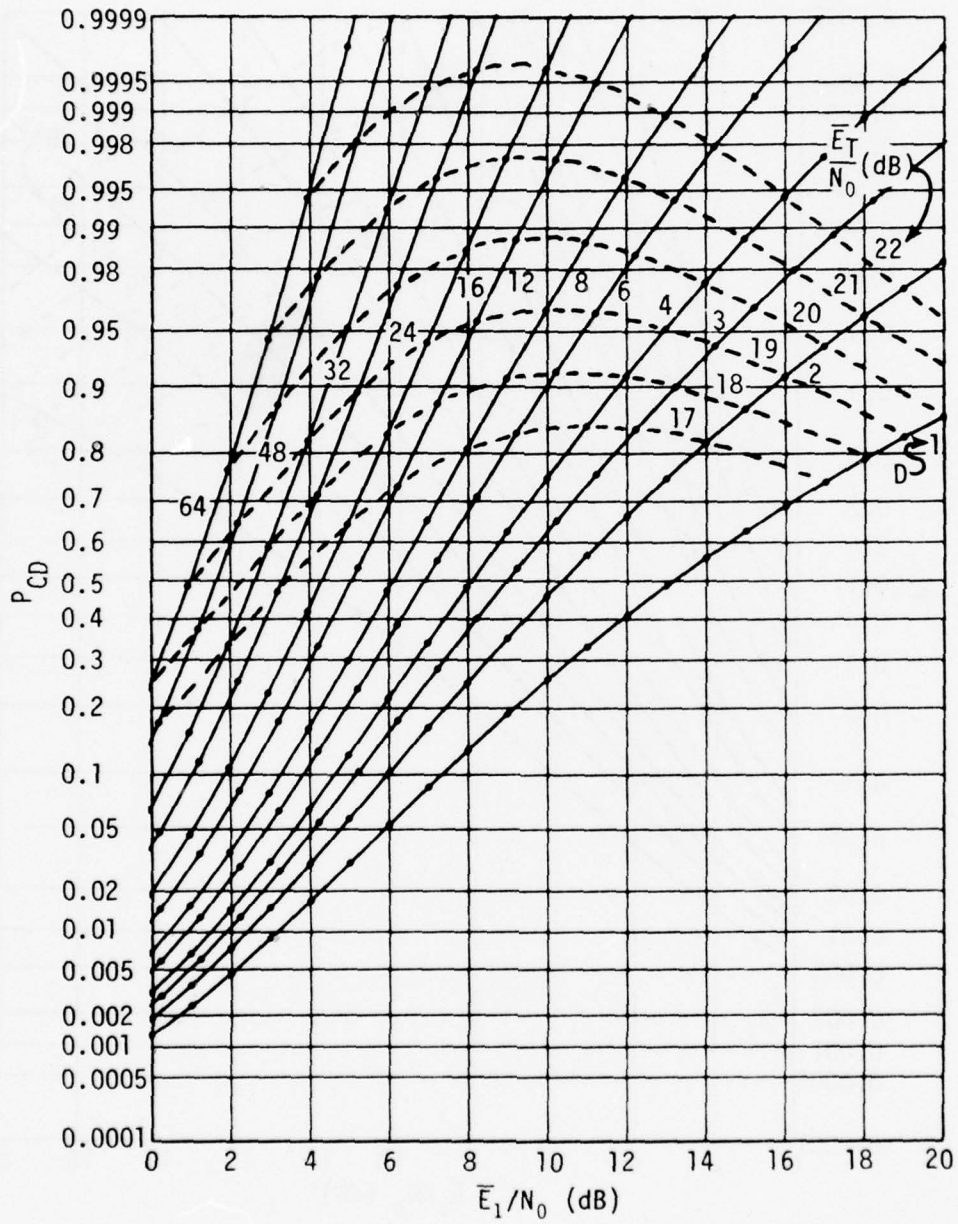


Figure 43. Detection Characteristics for $K = 6$, $M = 16$, $P_{FA} = 10^{-3}$

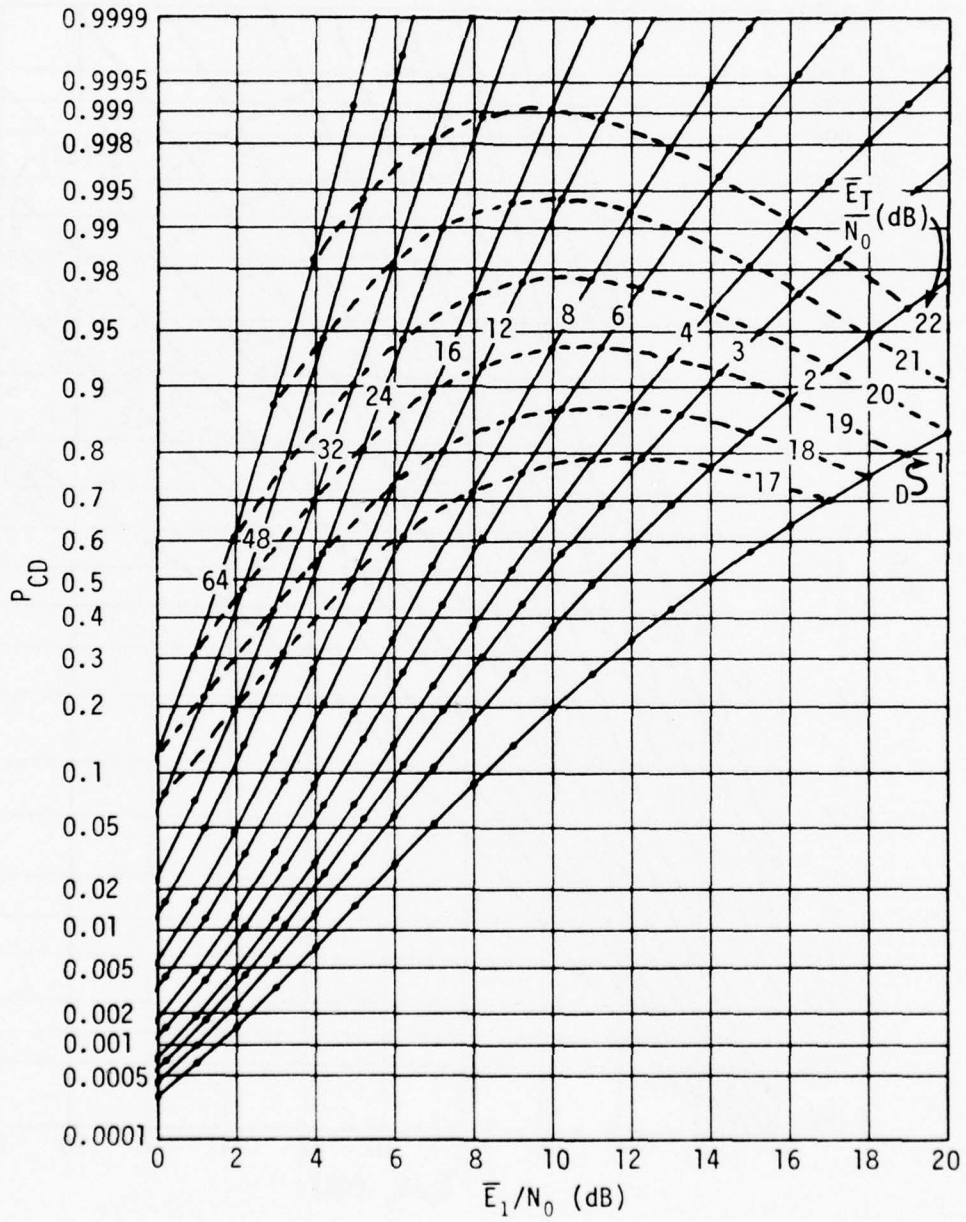


Figure 44. Detection Characteristics for $K = 6$, $M = 16$, $P_{FA} = 10^{-4}$

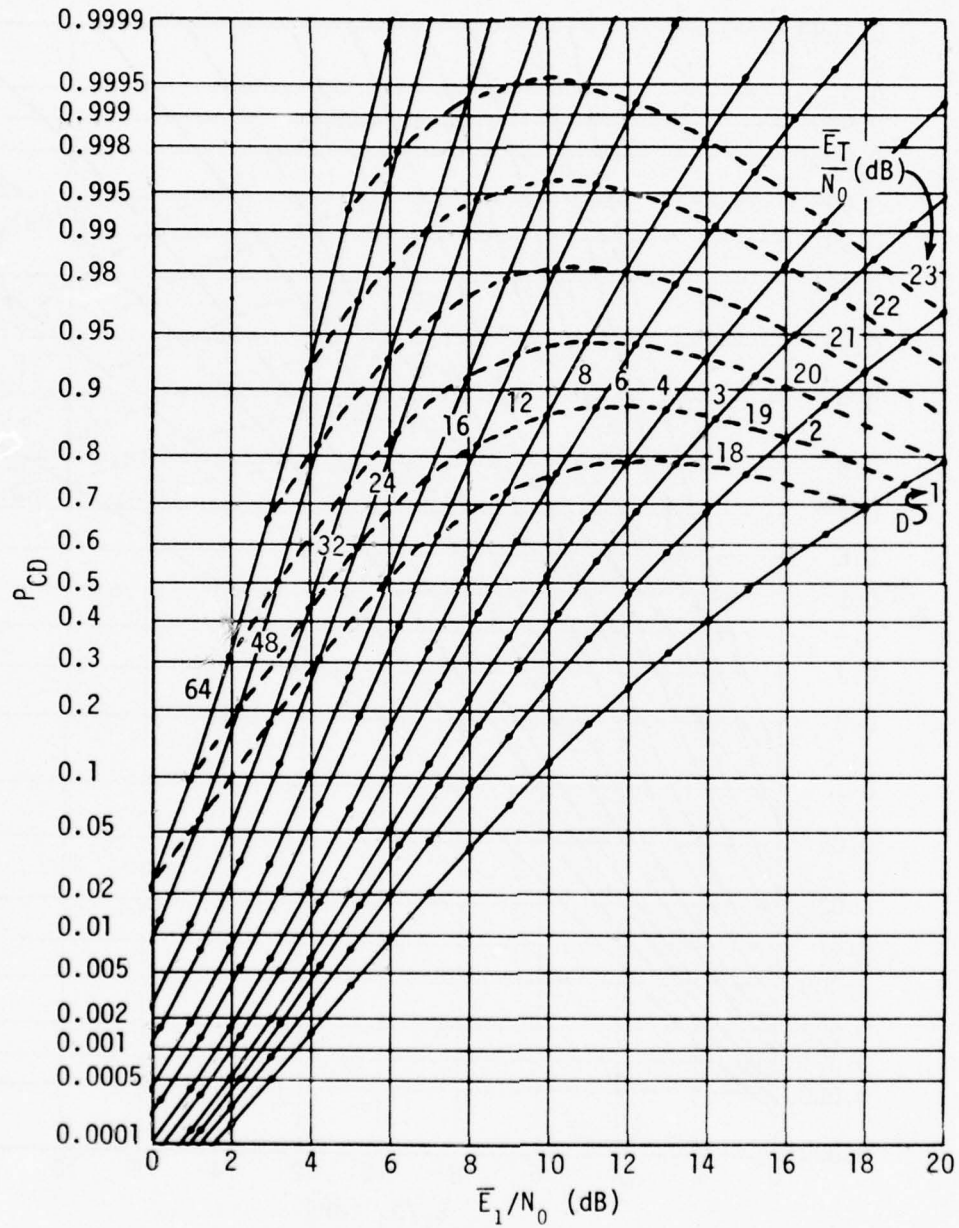


Figure 45. Detection Characteristics for $K = 6$, $M = 16$, $P_{FA} = 10^{-6}$

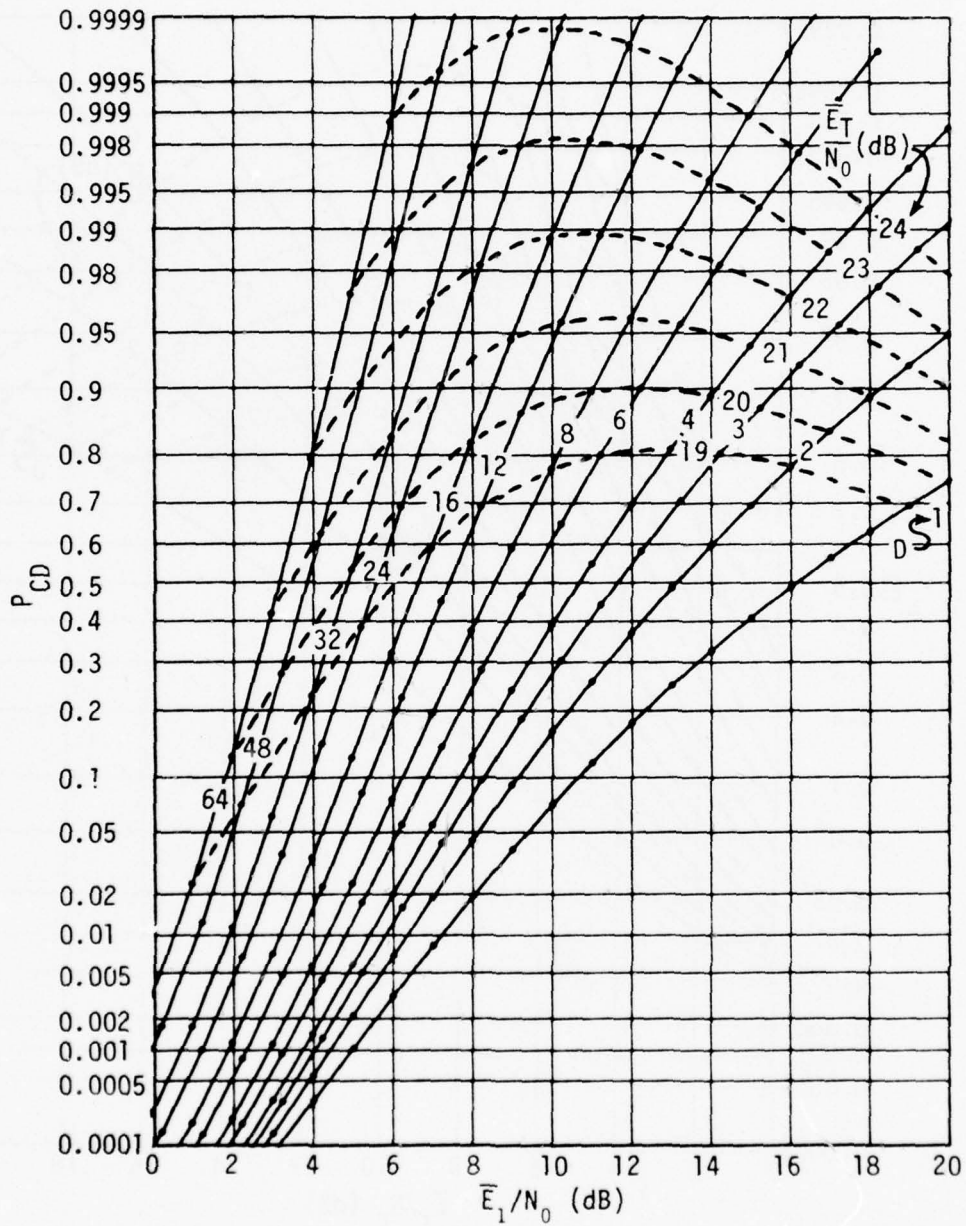


Figure 46. Detection Characteristics for $K = 6$, $M = 16$, $P_{FA} = 10^{-8}$

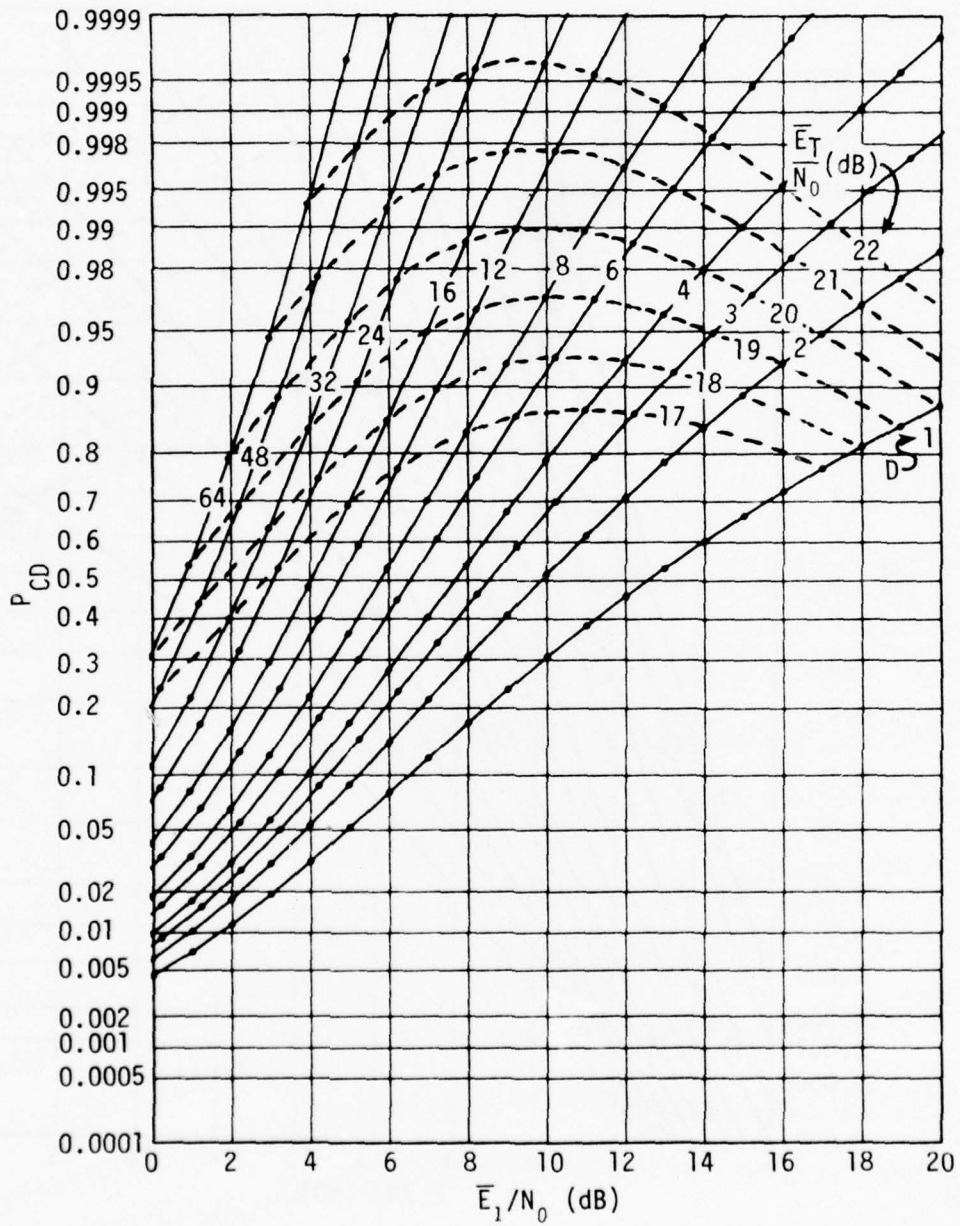


Figure 47. Detection Characteristics for $K = 8$, $M = 16$, $P_{FA} = 10^{-2}$

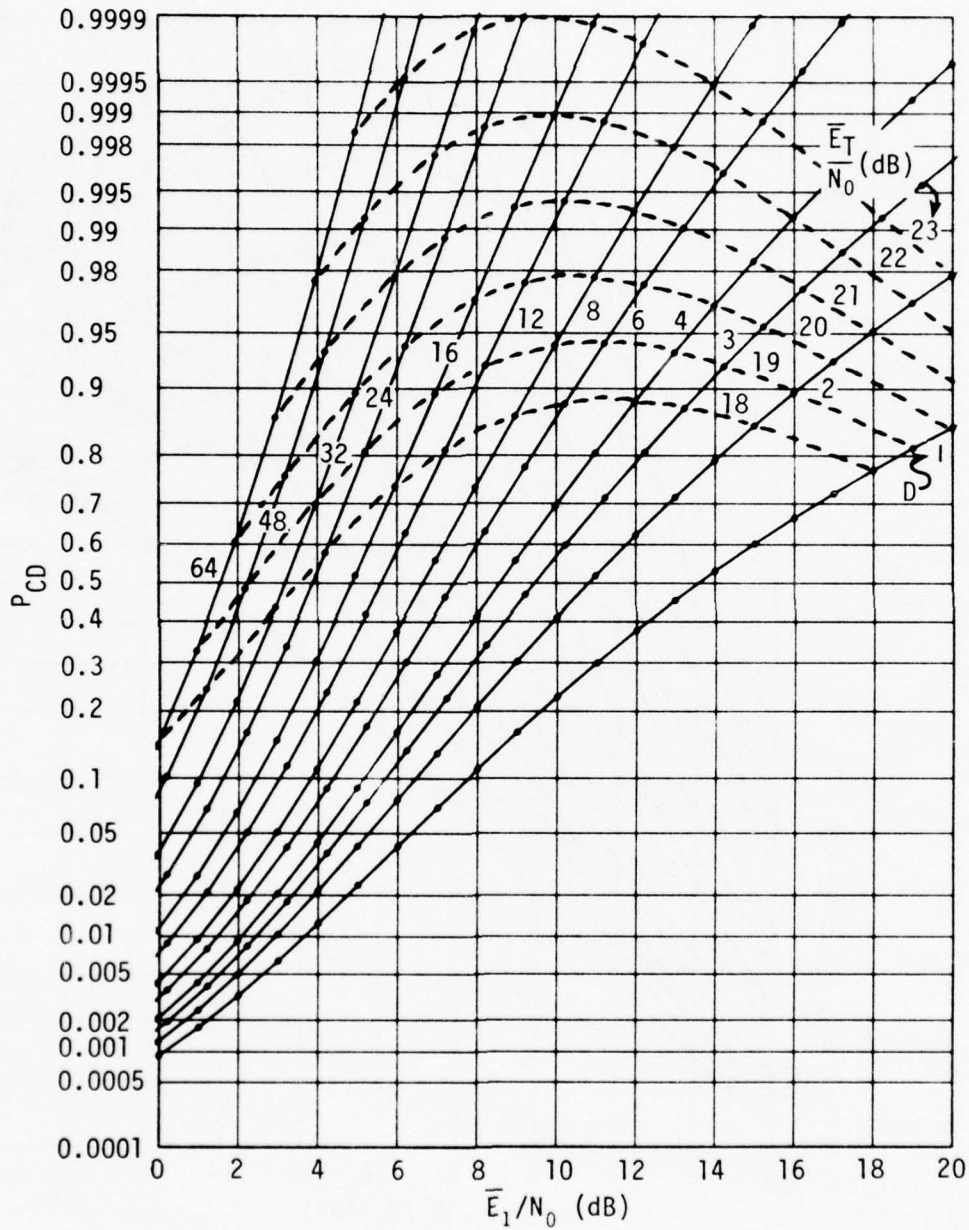


Figure 48. Detection Characteristics for $K = 8$, $M = 16$, $P_{FA} = 10^{-3}$

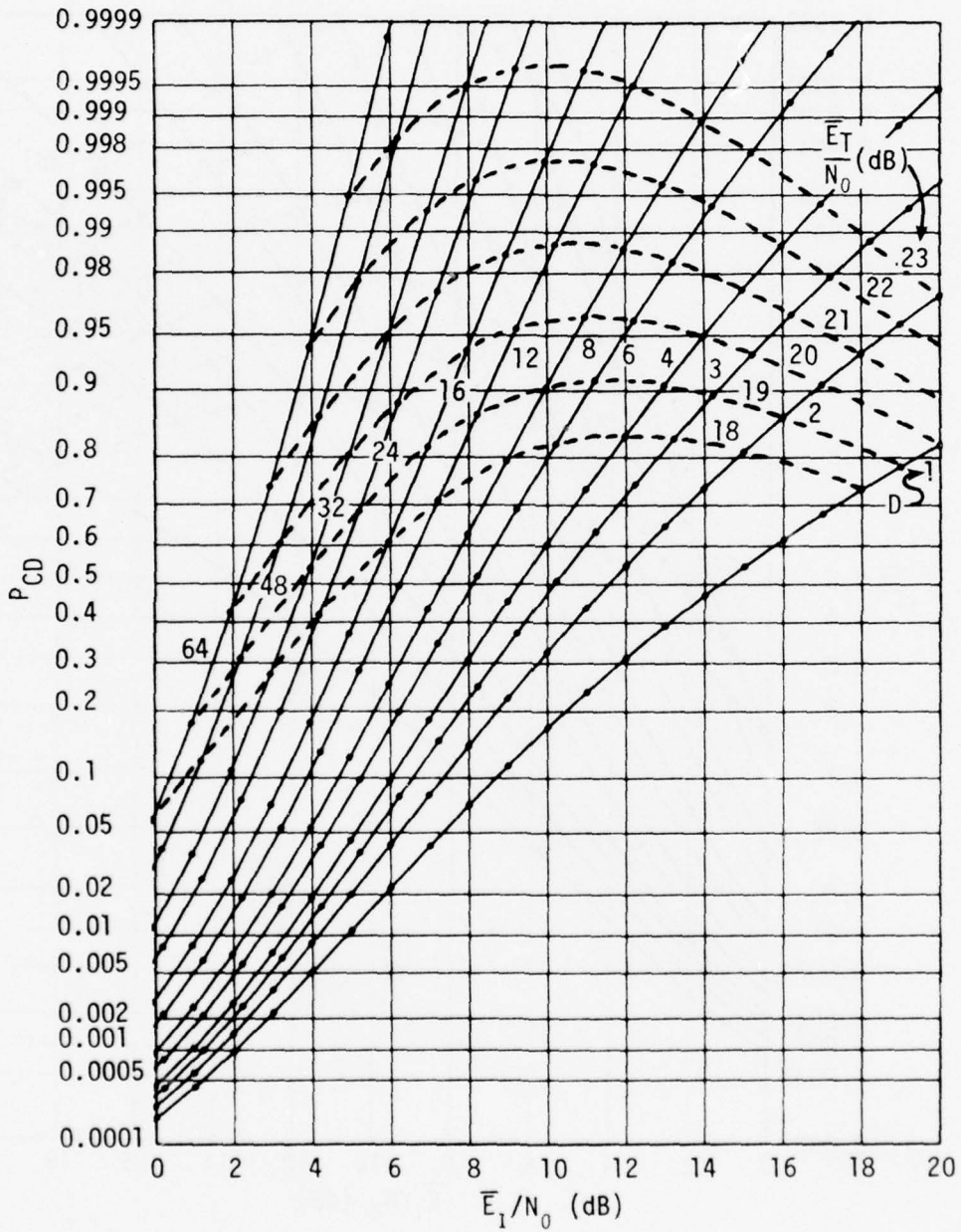


Figure 49. Detection Characteristics for $K = 8$, $M = 16$, $P_{FA} = 10^{-4}$

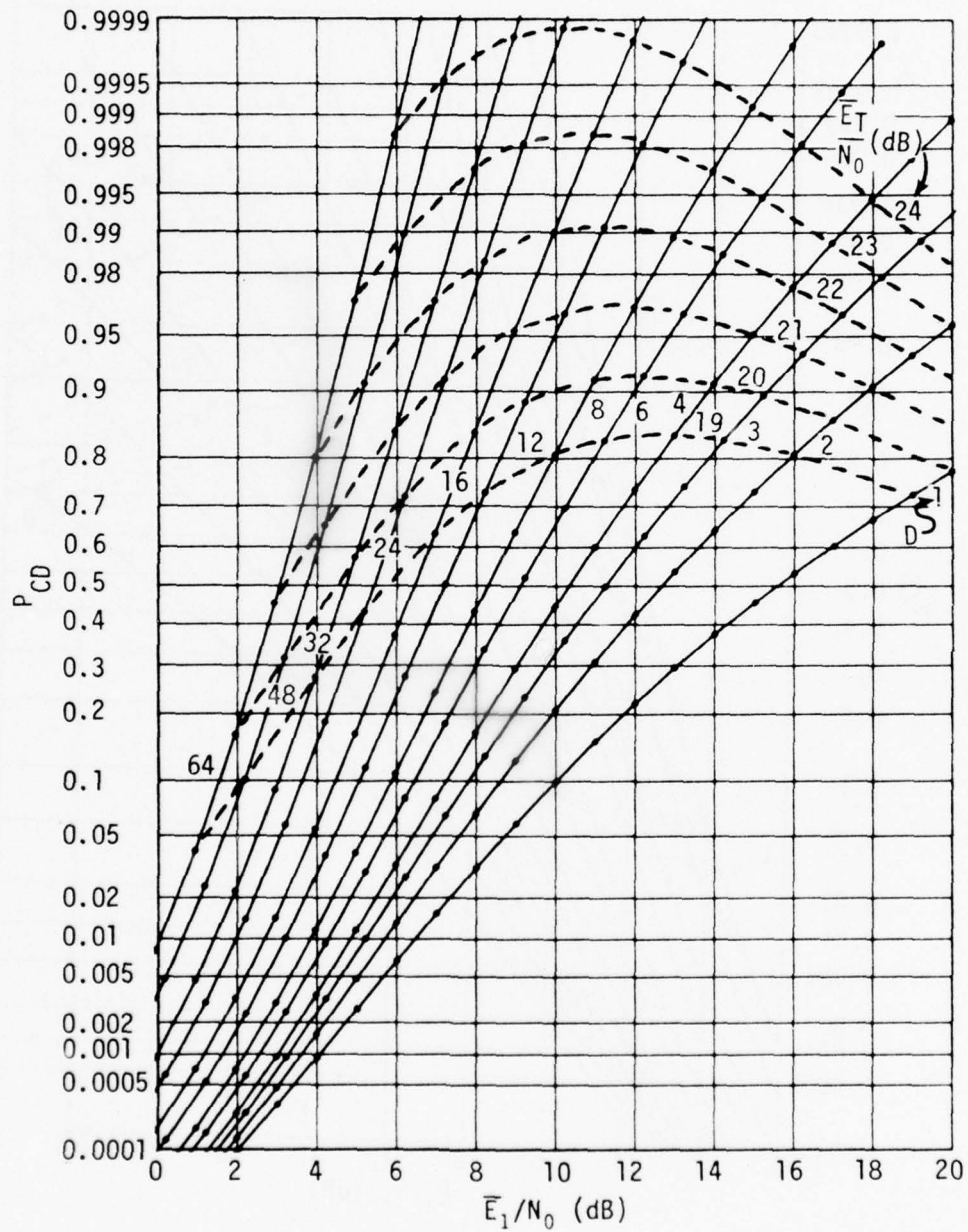


Figure 50. Detection Characteristics for $K = 8$, $M = 16$, $P_{FA} = 10^{-6}$

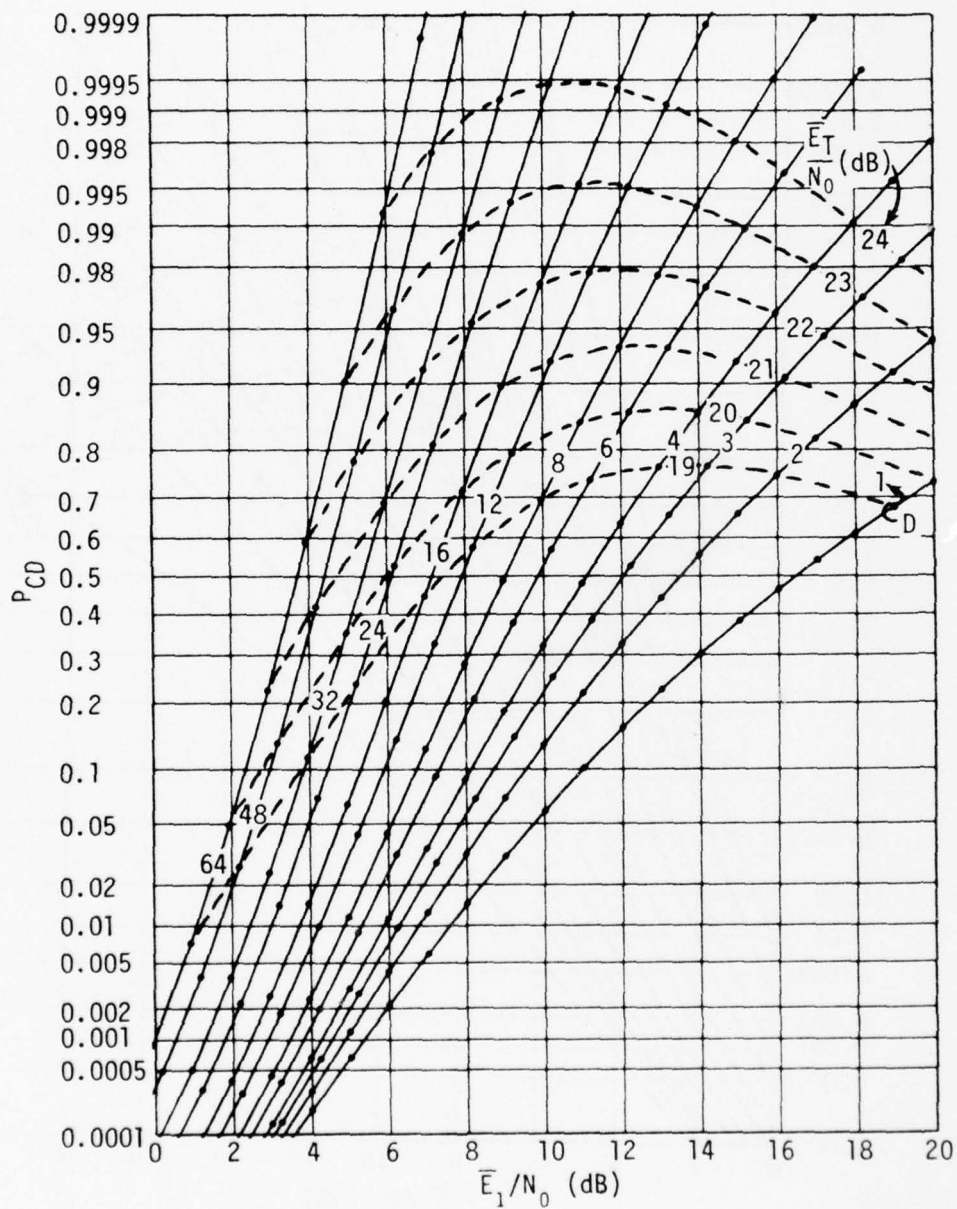


Figure 51. Detection Characteristics for $K = 8$, $M = 16$, $P_{FA} = 10^{-8}$

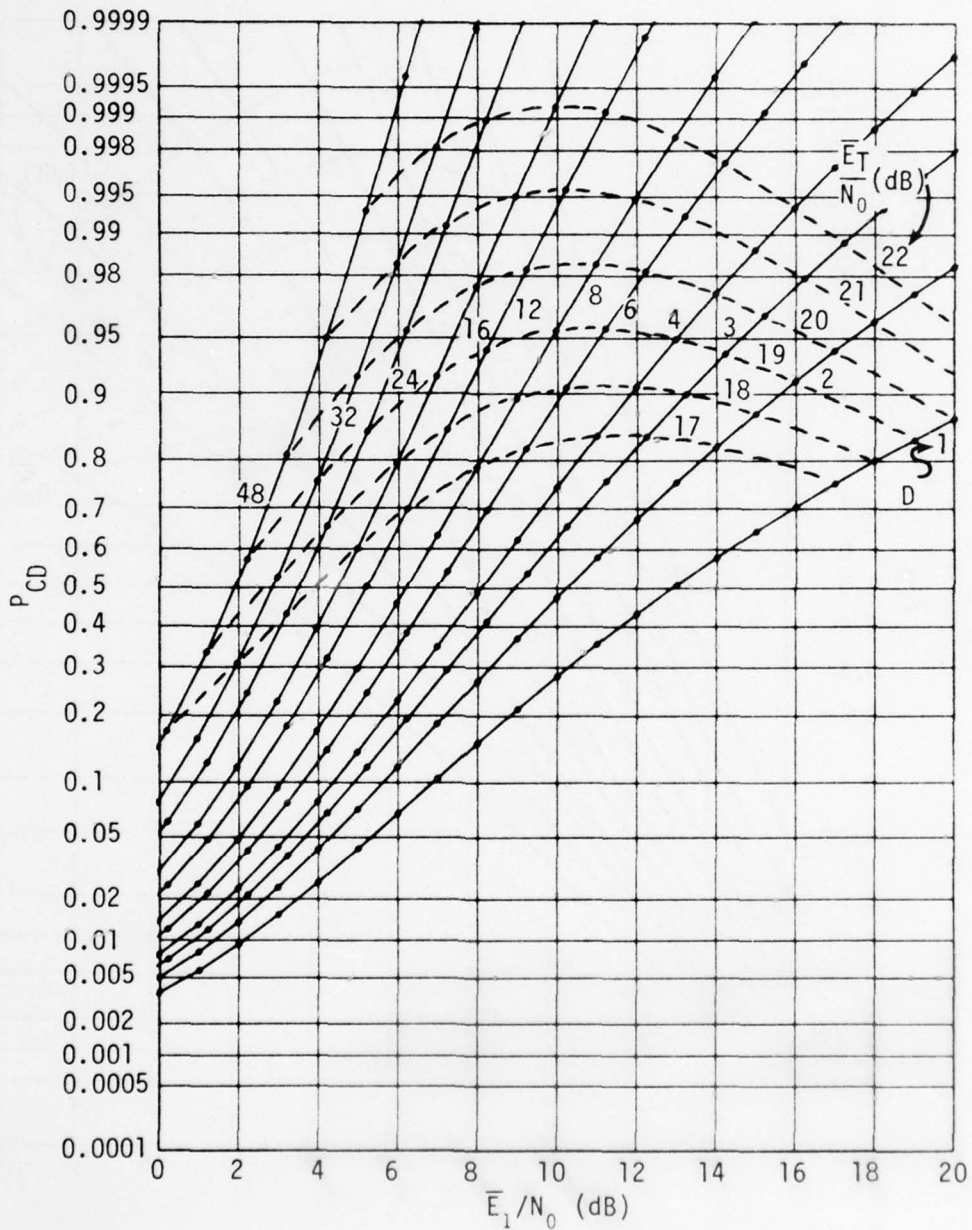


Figure 52. Detection Characteristics for $K = 10$, $M = 16$, $P_{FA} = 10^{-2}$

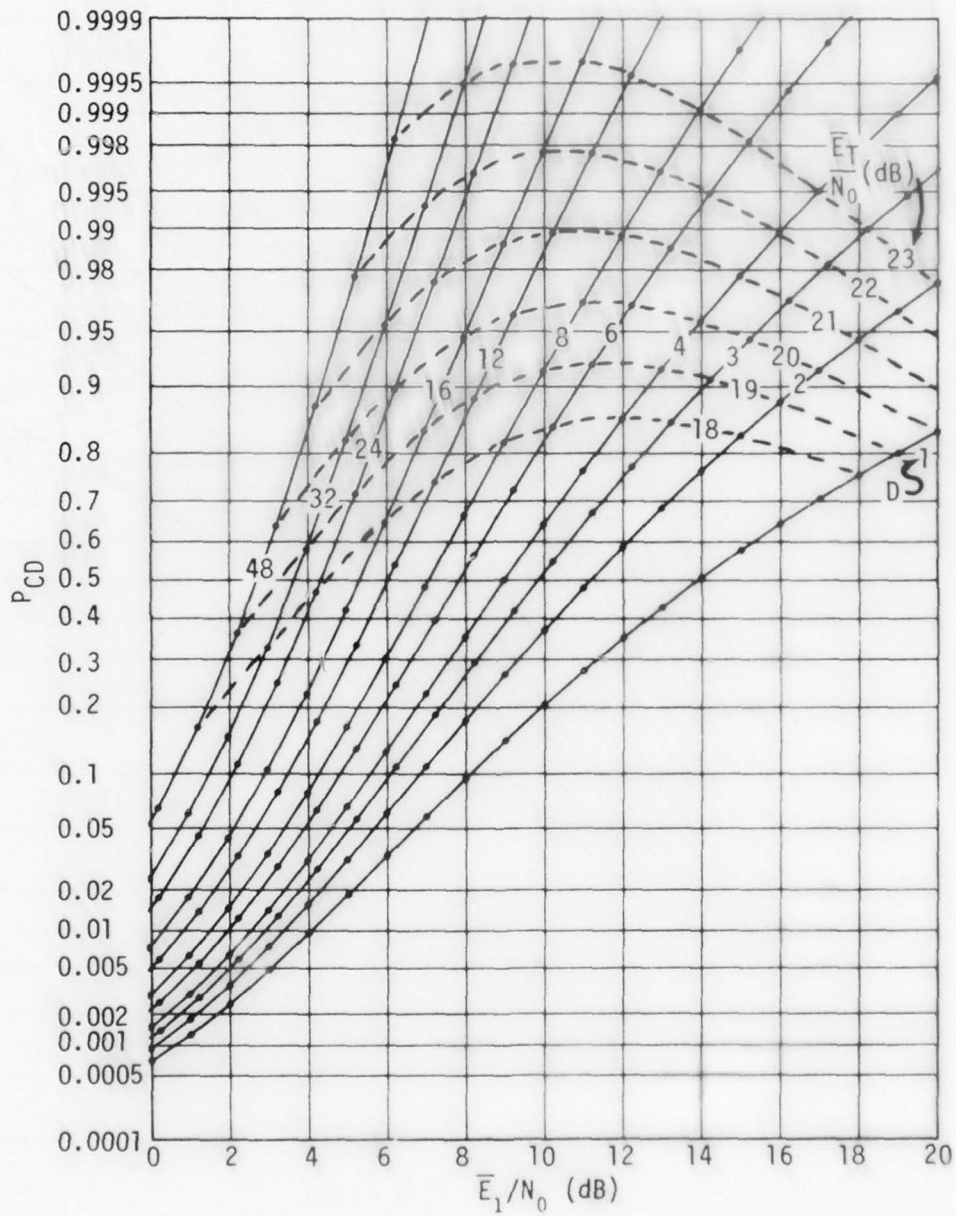


Figure 53. Detection Characteristics for $K = 10$, $M = 16$, $P_{FA} = 10^{-3}$

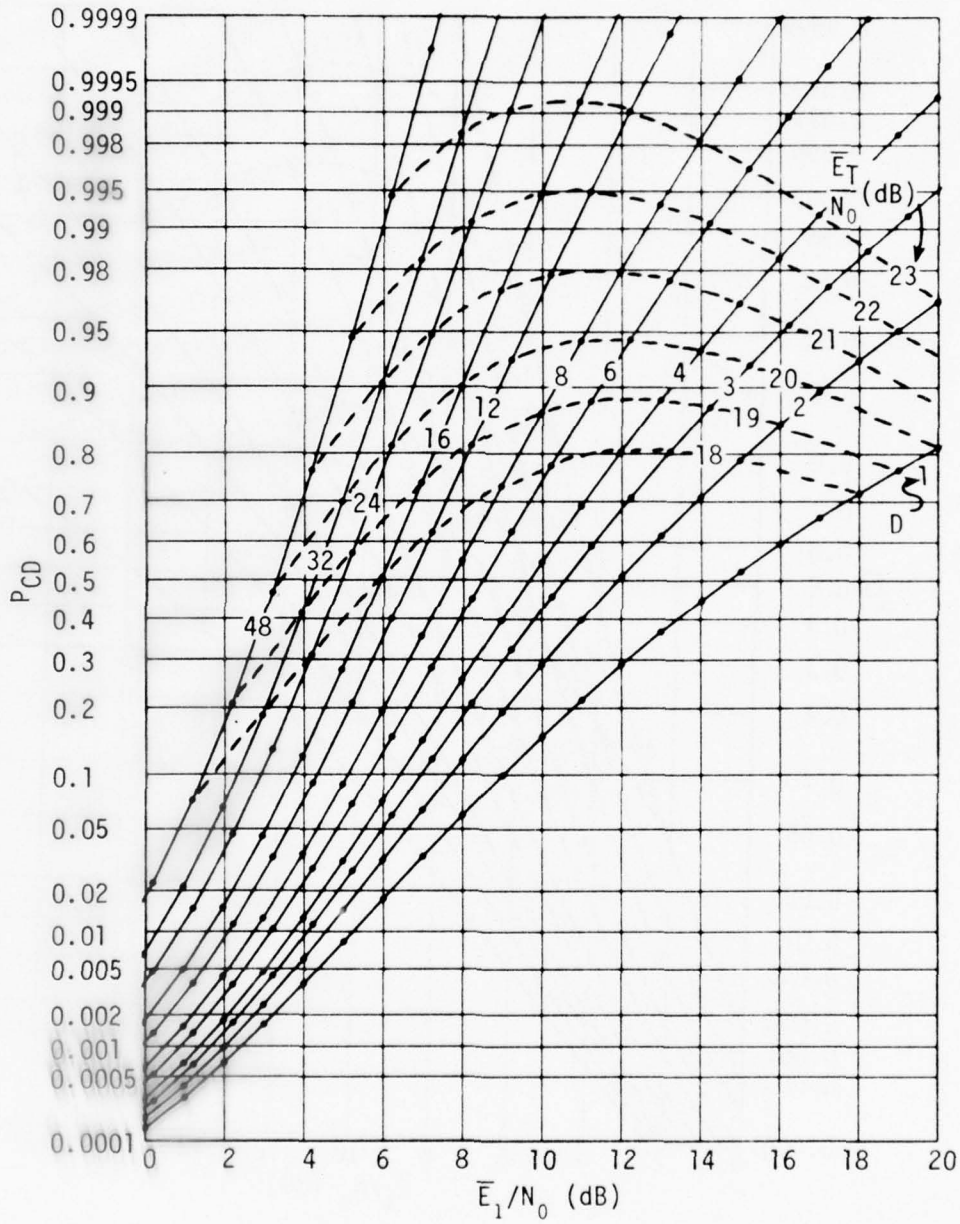


Figure 54. Detection Characteristics for $K = 10$, $M = 16$, $P_{FA} = 10^{-4}$

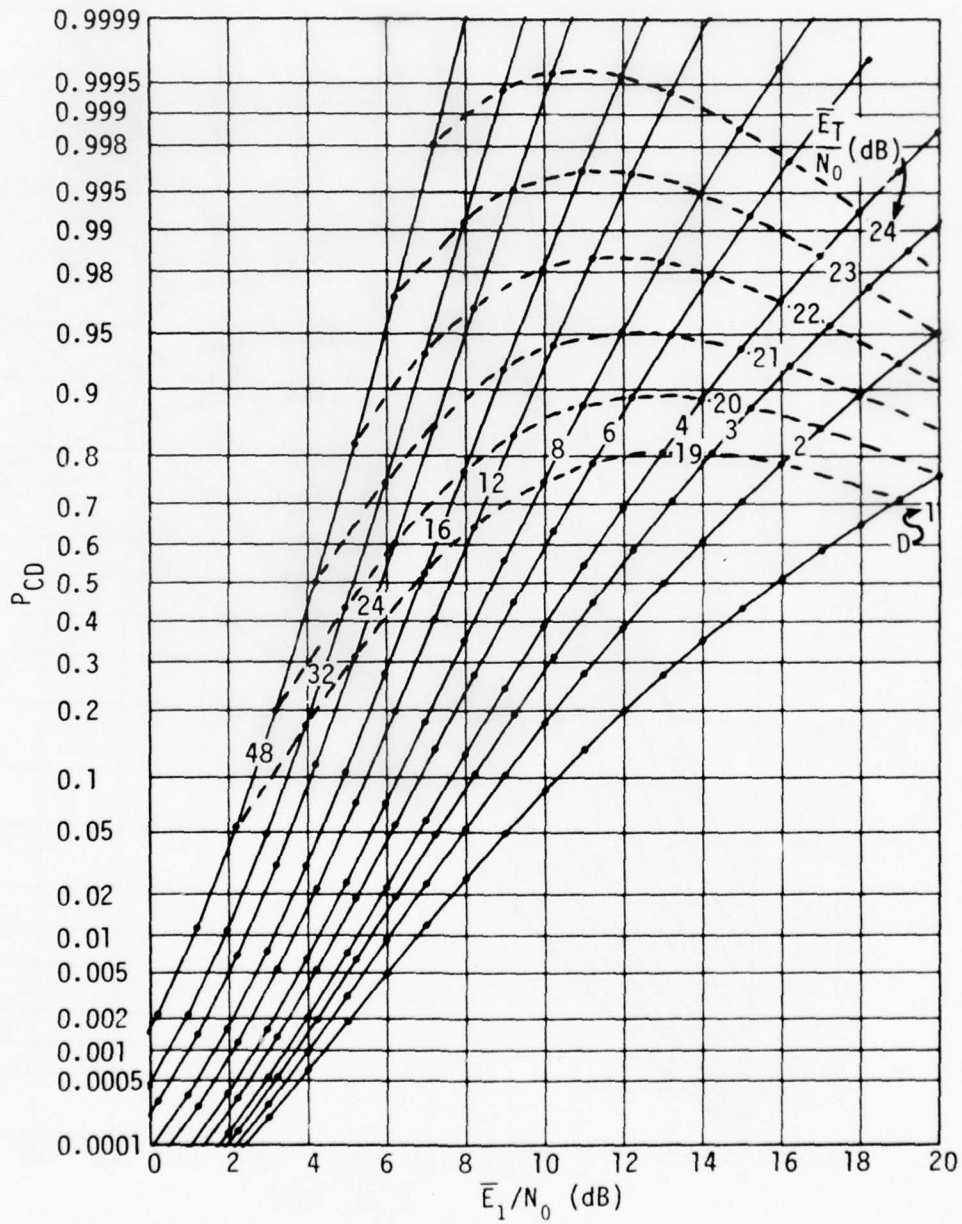


Figure 55. Detection Characteristics for $K = 10$, $M = 16$, $P_{FA} = 10^{-6}$

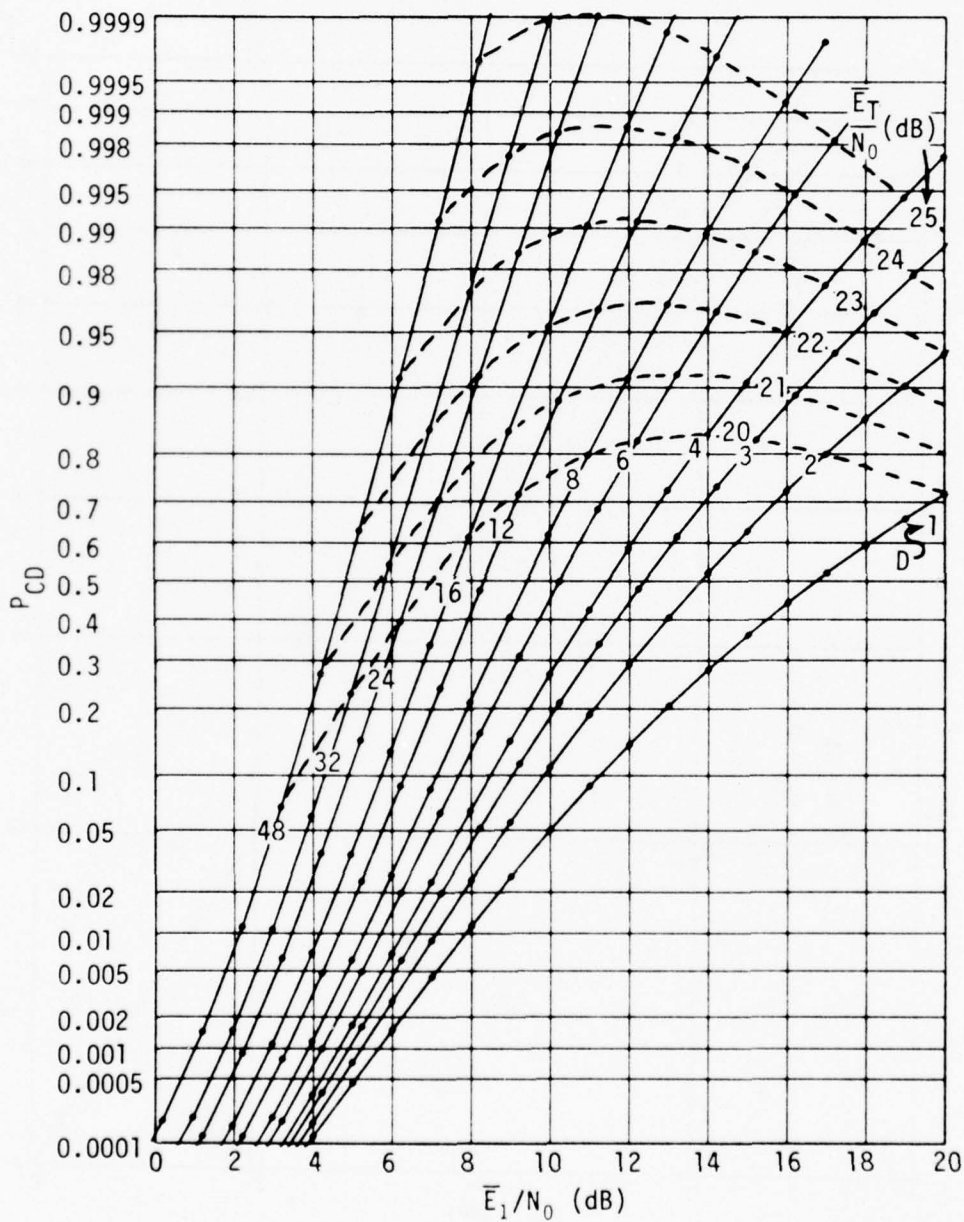


Figure 56. Detection Characteristics for $K = 10$, $M = 16$, $P_{FA} = 10^{-8}$

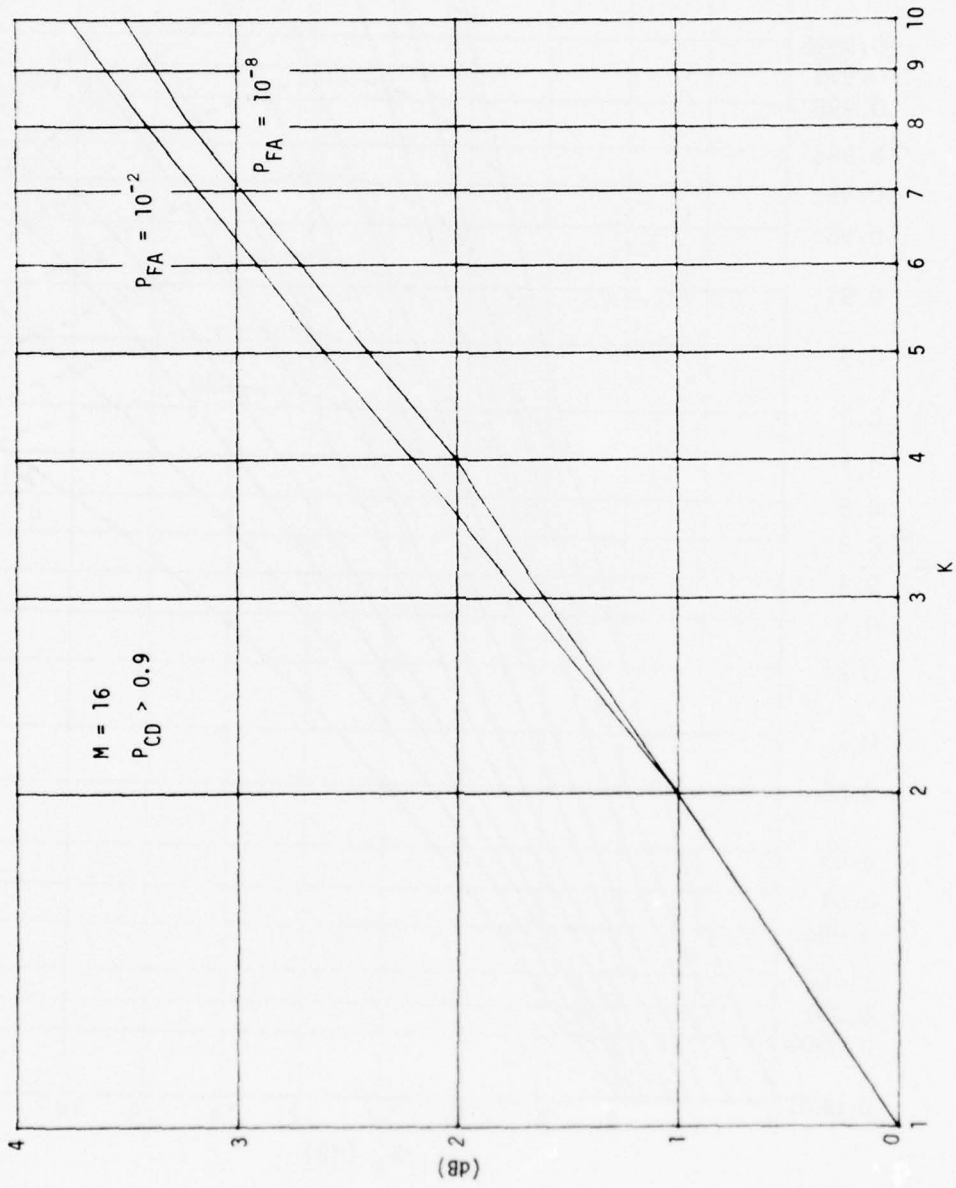


Figure 57. Additional Input Signal-to-Noise Ratio Necessary as a Function of K

Appendix A

DERIVATION OF $P_1(\Lambda)$

From equation (1), we have

$$x_1 = \sum_{d=1}^D \sum_{k=1}^K |s_d + n_{dk}^{(1)}|^2 = \sum_{d=1}^D \alpha_d, \quad (\text{A-1})$$

where

$$\alpha_d \equiv \sum_{k=1}^K |s_d + n_{dk}^{(1)}|^2. \quad (\text{A-2})$$

The D random variables $\{\alpha_d\}$ are statistically independent of each other. Our approach will be to find, first, the characteristic function of α_d , then the characteristic function of x_1 , and, finally, the probability density and cumulative distribution of x_1 .

We start by finding the characteristic function of α_d conditioned on a fixed known value of s_d ,

$$\begin{aligned} f_{\alpha_d}(\xi | s_d) &\equiv \overline{\exp(i\xi \alpha_d)}^n \\ &= \overline{\exp\left(i\xi \sum_{k=1}^K |s_d + n_{dk}^{(1)}|^2\right)}^n \\ &= \left[\overline{\exp\left(i\xi |s_d + n_{dk}^{(1)}|^2\right)} \right]^K, \end{aligned} \quad (\text{A-3})$$

using the independence of $\{n_{dk}^{(1)}\}$ and their identical statistics. Now $n_{dk}^{(1)}$ is assumed complex Gaussian with independent real and imaginary parts:

$$\begin{aligned}
 n_{dk}^{(0)} &\equiv x + iy, \\
 \bar{x} = \bar{y} &= 0, \quad \overline{xy} = 0, \quad \overline{x^2} = \overline{y^2} = \sigma^2, \\
 \overline{|n_{dk}^{(0)}|^2} &= \overline{x^2 + y^2} = 2\sigma^2 \equiv \sigma_n^2.
 \end{aligned}
 \tag{A-4}$$

Then the bracketed term in equation (A-3) is given by

$$\begin{aligned}
 &\iint dx dy (2\pi\sigma^2)^{-1} \exp\left[-\frac{x^2+y^2}{2\sigma^2}\right] \exp\left(i\xi(s_{dr}+x) + i\xi(s_{di}+y)\right) \\
 &= (1 - i2\sigma^2\xi)^{-1} \exp\left(\frac{i\xi|s_d|^2}{1 - i\xi 2\sigma^2}\right),
 \end{aligned}
 \tag{A-5}$$

where we have used the result

$$\int dx \exp(-\alpha x^2 + \beta x) = \left(\frac{\pi}{\alpha}\right)^{1/2} \exp\left(\frac{\beta^2}{4\alpha}\right), \quad \text{Re } \alpha > 0.
 \tag{A-6}$$

For later use, the probability density function corresponding to equation (A-5) is

$$p(x|s_d) = \frac{1}{2\sigma^2} \exp\left(-\frac{x+|s_d|^2}{2\sigma^2}\right) I_0\left(\frac{|s_d| x^{1/2}}{\sigma^2}\right), \quad x > 0,
 \tag{A-7}$$

which is recognized as the probability density function corresponding to the square of a Rician variate; recall that this holds for $K = 1$.

The characteristic function in equation (A-3) is now available by using equations (A-5) and (A-4):

$$f_{\alpha_d}(\xi|s_d) = (1 - i\xi\sigma_n^2)^{-K} \exp\left(\frac{i\xi K |s_d|^2}{1 - i\xi\sigma_n^2}\right).
 \tag{A-8}$$

(If the signal component s_d in equation (A-2) were different on each of the K processing intervals, equation (A-8) would be replaced by

$$f_{\alpha_d}(\xi | \{s_{dk}\}) = (1 - i\xi\sigma_n^2)^{-K} \exp\left(\frac{i\xi}{1 - i\xi\sigma_n^2} \sum_{k=1}^K |s_{dk}|^2\right). \quad (\text{A-9})$$

We will find use for this result later.)

To find the characteristic function $f_{\alpha_d}(\xi)$, we have to average equation (A-8) over the statistics of s_d . We assume that s_d is complex Gaussian with independent real and imaginary parts; then $|s_d|$ is a Rayleigh variate. Letting, as in equation (A-5),

$$\begin{aligned} s_d &= s_{dr} + i s_{di}, \\ \overline{s_{dr}} &= \overline{s_{di}} = 0, \\ \overline{s_{dr} s_{di}} &= 0, \quad \overline{s_{dr}^2} = \overline{s_{di}^2} = \sigma_s^2/2, \\ \overline{|s_d|^2} &= \sigma_s^2, \end{aligned} \quad (\text{A-10})$$

we have the average

$$\begin{aligned} \overline{\exp(\nu |s_d|^2)}^{s_d} &= \iint dx dy (\pi\sigma_s^2)^{-1} \exp\left(-\frac{x^2+y^2}{\sigma_s^2}\right) \exp(\nu(x^2+y^2)) \\ &= (1 - \nu\sigma_s^2)^{-1}. \end{aligned} \quad (\text{A-11})$$

If ν is identified as $i\xi K / (1 - i\xi\sigma_n^2)$, the average on s_d in equation (A-8) is now available as

$$\begin{aligned} f_{\alpha_d}(\xi) &= \overline{f_{\alpha_d}(\xi | s_d)}^{s_d} \\ &= \frac{1}{[1 - i\xi\sigma_n^2]^{K-1} [1 - i\xi(\sigma_n^2 + K\sigma_s^2)]}. \end{aligned} \quad (\text{A-12})$$

The characteristic function of x_1 is immediately available in equation (A-1), using the statistical independence of $\{\alpha_d\}$, as

$$f_{x_1}(\xi) = \frac{1}{[1 - i\xi\sigma_n^2]^{D(K-1)} [1 - i\xi(\sigma_n^2 + K\sigma_s^2)]^D} \quad (\text{A-13})$$

Since we know the probability density function-characteristic function pair,

$$\frac{1}{(1 - i\xi a)^J} \longleftrightarrow \frac{x^{J-1} \exp(-x/a)}{(J-1)! a^J}, \quad x > 0, \quad (\text{A-14})$$

we can write the probability density function corresponding to multiplicative characteristic function (A-13) as the convolution

$$p_1(x) = \int_0^x du \frac{u^{J-1} \exp(-u/a)}{(J-1)! a^J} \frac{(x-u)^{D-1} \exp(-\frac{x-u}{b})}{(D-1)! b^D}, \quad x > 0, \quad (\text{A-15})$$

where

$$J \equiv D(K-1), \quad a = \sigma_n^2, \quad b = \sigma_n^2 + K\sigma_s^2. \quad (\text{A-16})$$

Now, by employing reference 3, 3.383.1 and 8.384.1, equation (A-15) becomes

$$p_1(x) = \frac{\exp(-x/a) x^{D+J-1}}{a^J b^D (D+J-1)!} {}_1F_1\left(D; J+D; x\left(\frac{1}{a} - \frac{1}{b}\right)\right), \quad x > 0. \quad (\text{A-17})$$

If we scale random variable x according to

$$t = \frac{x}{a} = \frac{x}{\sigma_n^2}, \quad (\text{A-18})$$

(we can absorb the scaling in threshold Λ) we get, for the probability density function of t ,

$$\begin{aligned}
 p_i(t) &= \frac{\exp(-t) t^{DK-1}}{(DK-1)! (1+KR)^D} {}_1F_1(D; DK; \gamma t) \\
 &= \frac{\exp\left(-\frac{t}{1+KR}\right) t^{DK-1}}{(DK-1)! (1+KR)^D} {}_1F_1(DK-D; DK; -\gamma t), t > 0,
 \end{aligned}
 \tag{A-19}$$

where we have used equation (A-16) and reference 3, 9.212 1, and defined

$$R = \frac{\sigma_s^2}{\sigma_n^2}, \quad \gamma = \frac{KR}{1+KR}
 \tag{A-20}$$

As a check on equation (A-19), we have the following: for $K = 1$, equation (A-19) reduces to equation (B-3) in reference 1; and for $R = 0$, equation (A-19) reduces to equation (B-2) in reference 1.

To find the cumulative distribution function of variate t , we integrate equation (A-19):

$$\begin{aligned}
 1 - P_i(\lambda) &= \int_{\lambda}^{\infty} dt p_i(t) \\
 &= \frac{1}{(DK-1)! (1+KR)^D} \int_{\lambda}^{\infty} dt \exp(-t) t^{DK-1} {}_1F_1(D; DK; \gamma t).
 \end{aligned}
 \tag{A-21}$$

By employing the power series expansion of ${}_1F_1$ in reference 3, 9.210 1, and defining the partial exponential

$$e_j(\lambda) \equiv \sum_{k=0}^j \frac{\lambda^k}{k!} = 1 + \lambda + \dots + \frac{\lambda^j}{j!},
 \tag{A-22}$$

we find

$$1 - P_1(\lambda) = \exp(-\lambda)(1-\gamma)^D \sum_{n=0}^{\infty} \binom{D+n-1}{n} \gamma^n e_{DK-1+n}(\lambda). \quad (\text{A-23})$$

The partial exponential in equation (A-23) tends to the constant value $\exp(\lambda)$ as $n \rightarrow \infty$ and offers no help in convergence. Also, the ratio of the $n+1$ -th to n -th remaining factors tends to γ as $n \rightarrow \infty$. Therefore, equation (A-23) is always a convergent series of positive terms, since $\gamma < 1$; see equation (A-20). However, for large KR , the convergence is so slow that equation (A-23) is not very useful for numerical evaluation.

By taking the $\exp(-\lambda)$ term in equation (A-23) inside the sum, and adding and subtracting 1 from the product of the exponential and the partial exponential, we obtain

$$1 - P_1(\lambda) = 1 - (1-\gamma)^D \sum_{n=0}^{\infty} \binom{D+n-1}{n} \gamma^n \left[1 - \exp(-\lambda) e_{DK-1+n}(\lambda) \right], \quad (\text{A-24})$$

where we used the result (reference 3, 9.100 and 9.121 1),

$$\sum_{n=0}^{\infty} \binom{D+n-1}{n} \gamma^n = {}_2F_1(D, \beta; \beta; \gamma) = (1-\gamma)^{-D}. \quad (\text{A-25})$$

Now, the bracketed term in equation (A-24) tends to zero as $n \rightarrow \infty$, as do the leading factors. Thus, equation (A-24) is a more rapidly convergent series of positive terms than equation (A-23).

A problem arises in the accurate evaluation of the bracketed term in equation (A-24):

$$\begin{aligned} Q_n &\equiv 1 - \exp(-\lambda) e_{DK-1+n}(\lambda) \\ &= 1 - \exp(-\lambda) \sum_{m=0}^{DK-1+n} \lambda^m / m! \\ &= \exp(-\lambda) \sum_{m=DK+n}^{\infty} \lambda^m / m! \end{aligned} \quad (\text{A-26})$$

We note the downward recursion of positive quantities

$$Q_n = Q_{n+1} + C_n, \quad 0 \leq n, \quad (\text{A-27})$$

where

$$C_n \equiv \exp(-\lambda) \lambda^{DK+n} / (DK+n)!, \quad 0 \leq n, \quad (\text{A-28})$$

and for which

$$C_0 = \exp(-\lambda) \lambda^{DK} / (DK)!; \quad C_n = C_{n-1} \lambda / (DK+n), \quad 1 \leq n. \quad (\text{A-29})$$

Thus, if we evaluate $\{C_n\}_0^{N-1}$ and Q_N , we can then evaluate $\{Q_n\}_0^{N-1}$ via the downward recursion in equation (A-27).

In order to accomplish this, we evaluate $\{C_n\}_0^N$ by the forward recursion in equation (A-29), and then note that, from equations (A-26) and (A-28),

$$\begin{aligned} Q_N &= \exp(-\lambda) \frac{\lambda^{DK+N}}{(DK+N)!} \sum_{m=0}^{\infty} \frac{\lambda^m}{(DK+N+1)_m} \\ &= C_N \sum_{m=0}^{\infty} \frac{\lambda^m}{(DK+N+1)_m}. \end{aligned} \quad (\text{A-30})$$

This last sum is terminated for desired accuracy in Q_N .

As a check on accuracy, we note from equation (A-26) that

$$Q_0 + \sum_{m=0}^{DK-1} \exp(-\lambda) \lambda^m / m! = 1. \quad (\text{A-31})$$

But the terms in this sum are computed in the initial evaluation of C_0 ; so, if these terms are saved and combined with the final result of Q_0 obtained via downward recursion (A-27), the sum of 1 dictated by equation (A-31) should be obtained.

The procedure is summarized below:

1. C_0
2. C_1, C_2, \dots, C_N
3.
$$\sum_{m=0}^{\infty} \frac{\Lambda^m}{(DK + N + 1)_m}$$
4. Q_N
5. $Q_{N-1}, Q_{N-2}, \dots, Q_0$

At all times we are dealing with positive numbers, and no differences are formed. The only difference occurs in the final subtraction from 1 in equation (A-24).

A FORTRAN program for the evaluation and plotting of equation (A-24) by means of the procedure above is presented on pages A-9 through A-14. The accuracy of the check formula (A-31) is typically 16 decimals for the double precision routine used.

```

PARAMETER NUM=1000
DOUBLE PRECISION F, OM, PFA, T, S, V1, V2, G(12), D1, THK, CO, SO, OO
DOUBLE PRECISION C(LUM), Q(NUM), ETNODB, RK, GAMMA
INTEGER D(12), DK1, DK
EXTERNAL F

DIMENSION Z(200), PCL(27,12), YNORM(25)
COMMON DK1
DATA D/1,2,3,4,6,8,12,16,24,32,48,64/
DATA YNORM/-3.71902,-3.29053,-3.09023,-2.87816,-2.57583,-2.32635,
$-2.05375,-1.64485,-1.28155,-.84162,-.52440,-.25335,0.,.25335,.5244
$,.84162,1.28155,1.64485,2.05375,2.32635,2.57583,2.87816,3.09023,
$3.29053,3.71902/
M=16
K=5
CALL MODESG(Z,0)
CALL SUBJEG(Z,0.,YNORM(1),20.,YNORM(25))
CALL OBJCTG(Z,1150.,300.,2850.,2700.)
OM=1.00+1.00/M
DO 23 IP=2,6
PFA=10.00*(-IP)
IF(IP.EQ.5) PFA=1.0-6
IF(IP.EQ.6) PFA=1.0-8
T=PFA/M
S=T
DO 1 J=2,100
T=T*(J-OM)*PFA/J
S=S+T
IF(T.LE.1.0-9*S) GO TO 2
DK1=D(1)*K-1
V1=-LOG(S)
V2=V1+1.00
CALL ROOT(F,S,V1,V2)
G(1)=V2
PRINT 4, D(1),G(1)
DO 3 ID=2,12

```

1
2

```

DK1=D(ID)*K-1
V1=G(ID-1)+I0.
V2=V1+1.00
CALL ROOT(F,S,V1,V2)
G(ID)=V2
PRINT 4, D(ID),G(ID)
FORMAT(' D =',I3,'
DO 5 ID=1,12
D1=D(ID)-1
THR=G(ID)
DK=D(ID)*K
DK1=DK-1
CO=EXP(-THR)
SO=0.00
DO 6 J=1,DK
SO=SO+CO
CO=CO*THR/J
C(1)=CO*THR/(DK+1)
DO 7 J=2,NUM
C(J)=C(J-1)*THR/(DK+J)
IF(C(J).LT.1.0-20) GO TO 51
PRINT 52,
FORMAT(' NUM MAY NOT BE LARGE ENOUGH')
NEJ
SE=1.00
TE=1.00
DO 53 J=1,400
T=T*THR/(DK+N+J)
SES=T
IF(T.LE.S*1.0-6) GO TO 54
PRINT 55,
FORMAT(' 400 TERMS IN Q(N) MAY NOT BE LARGE ENOUGH')
G(H)=C(H)*S
N1=N-1
DO 56 J=N1,1,-1

```

3 4

6

7

52 51

53

55 54

```

56 Q(J)=Q(J+1)+C(J)
   Q0=Q(1)+C0
   S=50+Q0
   PRINT 57, S
57 FORMAT(/, S0+Q0 SHOULD EQUAL 1:,D30.18)
   PRINT 58, N,G(N)
58 FORMAT(' N =,I4,' Q(N) =,D24.18)
   DO 19 IE=1,27
   ETNODB=IE-1
   RK=10.00**(.100*ETNODB)/D(ID)
   GAMMA=RK/(1.00+RK)
   T=1.00
   S=Q0
   DO 20 J=1,N
   T=T*(01+J)*GAMMA/J
   S=S+T*Q(J)
20 IF(T*Q(J).LE.S*1.0-6) GO TO 19
   PRINT 21, IE, ID
21 FORMAT(' QUESTION AT IE, ID =,2I3)
13 V=1.00-(1.00-GAMMA)**D(ID)*S
   IE1=IE-1
   PRINT 22, IE1,D(ID),J,V
22 FORMAT(3I5,E15.9)
   V=MIN(V,.999999)
19 PCU(IE, ID)=MAX(V,1.E-6)
   CONTINUE
   CALL SETSMG(Z,30,1.)
   DO 9 J=2,18,2
   CALL LINESG(Z,0,FLOAT(J),YNORM(1))
   CALL LINESG(Z,1,FLOAT(J),YNORM(25))
   DO 10 J=2,24
   CALL LINESG(Z,0, 0.,YNORM(J))
   CALL LINESG(Z,1,20.,YNORM(J))
   CALL SETSMG(Z,30,2.)
   CALL LINESG(Z,0, 0.,YNORM(1))

```

```
CALL LINESG(Z,1, 0.,YNORM(25))
CALL LINESG(Z,1,20.,YNORM(25))
CALL LINESG(Z,1,20.,YNORM(1))
CALL LINESG(Z,1, 0.,YNORM(1))
CALL SETSMG(Z,84,'4')
DO 11 ID=1,12
  DDB=10.*LOG10(D(ID))
  P=TNORM(PCD(1,ID),$30)
  CALL LINESG(Z,0,-DDB,P)
  CALL POINTG(Z,1,-DDB,P)
  DO 11 IE=2,27
    P=TNORM(PCD(IE,ID),$30)
    CALL LINESG(Z,1,IE-1-DDB,P)
    CALL POINTG(Z,1,IE-1-DDB,P)
  CALL PAGEG(Z,0,1,1)
CONTINUE
CALL EXITG(Z)
END
```

11
37
23

```

DOUBLE PRECISION FUNCTION F(X)
DOUBLE PRECISION X,T
INTEGER DK1
COMMON DK1
F=EXP(-X)
IF(DK1.EQ.0) RETURN
T=F
DO 1 K=1,DK1
T=T*X/K
F=F+T
RETURN
END
SUBROUTINE ROOT(F,D,V1,V2)
DOUBLE PRECISION F,D,V1,V2,X(100),DA(100),B,HA
X(1)=V1
X(2)=V2
DA(1)=F(X(1))
DA(2)=F(X(2))
N1=2
DO 4 N=3,100
IF(ABS(DA(N-1)-D).LE.1.D-9*ABS(D)) GO TO 5
IF(DA(N-1)-DA(N-2)) 7,6,7
X(N)=X(N-1)*1.100
GO TO 8
X(N)=(X(N-1)*(D-DA(N-2))+X(N-2)*(DA(N-1)-L))/(DA(N-1)-DA(N-2))
B=X(N)-X(N-1)
BA=ABS(B)
X(N)=X(N-1)+MIN(BA,X(N-1)*.100)*SIGN(1.00,B)
X(N)=MAX(X(N),0.00)
N1=N
DA(N)=F(X(N))
PRINT 9, X(N1),DA(N1),N1
FORMAT(/2D30.18,I10)
V2=X(N1)
RETURN
END

```

1

6

7

8

4

5

5

Appendix B

ALTERNATIVE INTERPRETATION OF R

Let the transmitted waveform on one diversity branch during one individual processing interval ($D = 1, K = 1$) be

$$B(t) \cos[\omega_0 t + \theta(t)] = \text{Re} \{ E(t) \exp(i\omega_0 t) \}. \quad (\text{B-1})$$

Then the received waveform corresponding to this transmission is

$$\text{Re} \{ [G E(t) + N(t)] \exp(i\omega_0 t) \}, \quad (\text{B-2})$$

where

$$G = A \exp(i\phi) \quad (\text{B-3})$$

is the complex fading of the channel (assumed slow and frequency nonselective) and $N(t)$ is the complex envelope of the received noise. The noise correlation is

$$\overline{N(t_1) N^*(t_2)} = 2 N_0 \delta(t_1 - t_2), \quad (\text{B-4})$$

which corresponds to white noise of single-sided density level N_0 .

The received signal energy in one diversity branch during one processing interval is

$$E_s = \int dt \{ A B(t) \cos[\omega_0 t + \theta(t) + \phi] \}^2 = \frac{A^2}{2} \int dt B^2(t), \quad (\text{B-5})$$

and the corresponding average received signal energy is

$$\overline{E_s} = \frac{1}{2} A^2 \int dt B^2(t). \quad (\text{B-6})$$

The received signal energy on one diversity branch during all K processing intervals is

$$E_1 = E_s K, \quad (\text{B-7})$$

since the fading is completely dependent during this time. Hence, the average received signal energy on one diversity branch during all K processing intervals is

$$\overline{E}_1 = \overline{E}_s K. \quad (\text{B-8})$$

The total received signal energy over all diversity branches and processing intervals is

$$E_T = E_1 + E_2 + \dots + E_D, \quad (\text{B-9})$$

with average value

$$\overline{E}_T = \overline{E}_1 D = \overline{E}_s K D. \quad (\text{B-10})$$

This is the average total received signal energy.

For a synchronized matched filter to the transmitted signal on one diversity branch and one processing interval ($D = 1, K = 1$), the output complex envelope at the best sampling instant is (see equation (B-2))

$$y = \int dt [G E(t) + N(t)] E^*(t). \quad (\text{B-11})$$

Hence, the squared envelope output is proportional to

$$|y|^2 = \left| G \int dt |E(t)|^2 + \int dt N(t) E^*(t) \right|^2 \equiv |s + n|^2. \quad (\text{B-12})$$

Therefore (see equation (A-10)),

$$\sigma_s^2 = \overline{|s|^2} = \overline{|G|^2} \left\{ \int dt |E(t)|^2 \right\}^2 = \overline{A^2} \left\{ \int dt B^2(t) \right\}^2 \quad (\text{B-13})$$

and (see equation (A-4))

$$\sigma_n^2 = \overline{|n|^2} = 2N_0 \int dt |E(t)|^2 = 2N_0 \int dt B^2(t), \quad (\text{B-14})$$

where we have used equations (B-3), (B-1), and (B-4). As a result,

$$R = \frac{\sigma_s^2}{\sigma_n^2} = \frac{\overline{A^2}}{2N_0} \int dt B^2(t) = \frac{\overline{E_s}}{N_0}, \quad (\text{B-15})$$

using equations (A-20) and (B-6). Combining this result with equation (B-10), we have

$$\frac{\overline{E_T}}{N_0} = R K D, \quad (\text{B-16})$$

and, finally,

$$\frac{\overline{E_1}}{N_0} = \frac{\overline{E_T}/N_0}{D} = R K. \quad (\text{B-17})$$

Equation (B-16) is the average total received signal-energy-to-noise density ratio, whereas equation (B-17) is the average received signal-energy per diversity branch-to-noise density ratio.

Appendix C

DERIVATION OF OPTIMUM PROCESSOR

The a posteriori probability of alternative ℓ , given (squared-envelope) observations

$$x_{dk}^{(m)}, \quad 1 \leq d \leq D, \quad 1 \leq k \leq K, \quad 1 \leq m \leq M, \quad (\text{C-1})$$

is

$$\Pr(\ell | \{x_{dk}^{(m)}\}) = \frac{p(\{x_{dk}^{(m)}\} | \ell) \Pr(\ell)}{p(\{x_{dk}^{(m)}\})}, \quad 0 \leq \ell \leq M, \quad (\text{C-2})$$

by Bayes theorem. Using the statistical independence of all the variables in equation (C-1), we have, for $\ell = 0$ (no signal),

$$p(\{x_{dk}^{(m)}\} | 0) = \prod_{dkm} \{p_0(x_{dk}^{(m)})\}, \quad (\text{C-3})$$

where the product is over the range indicated in equation (C-1).

On the other hand, for $\ell \geq 1$, we have

$$p(\{x_{dk}^{(m)}\} | \ell) = \prod_d \{p_\ell(x_{d1}^{(\ell)}, \dots, x_{dK}^{(\ell)})\} \prod_{\substack{dkm \\ m \neq \ell}} \{p_0(x_{dk}^{(m)})\}. \quad (\text{C-4})$$

To make an optimum selection among the $M + 1$ alternatives, we only need compare the numerators of the a posteriori probabilities in equation (C-2). They are available from equations (C-3) and (C-4). By dividing these numerators by equation (C-3), the comparison is seen to be between the quantities

$$\Pr(0) \text{ and } \Pr(\ell) \prod_d \left\{ \frac{p_\ell(x_{d1}^{(\ell)}, \dots, x_{dK}^{(\ell)})}{p_0(x_{d1}^{(\ell)}) \dots p_0(x_{dK}^{(\ell)})} \right\} \text{ for } 1 \leq \ell \leq M. \quad (\text{C-5})$$

If the a priori probabilities are all equal, $\Pr(1) = \Pr(2) = \dots = \Pr(M)$, the comparison is between

$$\frac{Pr(0)}{Pr(1)} \text{ and } \prod_d \left\{ \frac{p_i(x_{d1}^{(l)}, \dots, x_{dK}^{(l)})}{p_0(x_{d1}^{(l)}, \dots, x_{dK}^{(l)})} \right\} \text{ for } 1 \leq l \leq M. \quad (C-6)$$

Ability to evaluate this expression depends on the form of the density $p_i(x_{d1}^{(l)}, \dots, x_{dK}^{(l)})$.

In the rest of this appendix, we restrict consideration to $K = 2$. From equations (A-7) and (A-4), for one sample of a squared-envelope, we have

$$p_i(x | |s_d| = r) = \frac{1}{\sigma_n^2} \exp\left(-\frac{x+r^2}{\sigma_n^2}\right) I_0\left(\frac{2r\sqrt{x}}{\sigma_n^2}\right), \quad x > 0. \quad (C-7)$$

But the probability density function of r is available from equations (A-10) and (A-11) as

$$p_{s_d}(r) = \frac{2}{\sigma_s^2} r \exp\left(-\frac{r^2}{\sigma_s^2}\right), \quad r > 0. \quad (C-8)$$

Therefore, using a shorthand notation,

$$p_i(x_1, x_2) = \int dr p_{s_d}(r) p_i(x_1 | r) p_i(x_2 | r). \quad (C-9)$$

Substituting equations (C-7) and (C-8) into equation (C-9) and employing reference 3, 6.633 2, we obtain

$$p_i(x_1, x_2) = \frac{1}{\sigma_n^4 (1+2R)} \exp\left(-\frac{1+R}{1+2R} \frac{x_1+x_2}{\sigma_n^2}\right) I_0\left(\frac{R}{1+2R} \frac{2\sqrt{x_1 x_2}}{\sigma_n^2}\right), \quad x_1, x_2 > 0. \quad (C-10)$$

Therefore, the desired ratio is

$$\frac{p_i(x_1, x_2)}{p_0(x_1) p_0(x_2)} = \frac{1}{1+2R} \exp\left(\frac{R}{1+2R} \frac{x_1+x_2}{\sigma_n^2}\right) I_0\left(\frac{R}{1+2R} \frac{2\sqrt{x_1 x_2}}{\sigma_n^2}\right). \quad (C-11)$$

Then the right-hand term of equation (C-6) is given by

$$(1+2R)^{-D} \exp\left(\frac{R}{1+2R} \frac{1}{\sigma_n^2} \sum_{d=1}^D (X_{d1}^{(\ell)} + X_{d2}^{(\ell)})\right) \prod_{d=1}^D I_0\left(\frac{R}{1+2R} \frac{2}{\sigma_n^2} \sqrt{X_{d1}^{(\ell)} X_{d2}^{(\ell)}}\right), \quad (C-12)$$

and its natural logarithm is

$$-D \ln(1+2R) + \frac{R}{1+2R} \frac{1}{\sigma_n^2} \sum_{d=1}^D (X_{d1}^{(\ell)} + X_{d2}^{(\ell)}) + \sum_{d=1}^D \ln I_0\left(\frac{R}{1+2R} \frac{2}{\sigma_n^2} \sqrt{X_{d1}^{(\ell)} X_{d2}^{(\ell)}}\right). \quad (C-13)$$

Finally, the comparison dictated by equation (C-6) can be summarized as

$$\max_{1 \leq \ell \leq M} \left\{ \sum_{d=1}^D (\alpha_{d1}^{(\ell)} + \alpha_{d2}^{(\ell)}) + \sum_{d=1}^D \ln I_0\left(2\sqrt{\alpha_{d1}^{(\ell)} \alpha_{d2}^{(\ell)}}\right) \right\} \geq \Lambda, \quad (C-14)$$

where

$$\alpha_{dk}^{(\ell)} \equiv \frac{R}{1+2R} \frac{X_{dk}^{(\ell)}}{\sigma_n^2}. \quad (C-15)$$

If the maximum on the left side exceeds threshold Λ , we state that signal alternative is present; otherwise, we state no signal present. The value of Λ is adjusted to realize a specified value of false alarm probability.

It is of interest to know what values the argument $2\sqrt{\alpha_{d1}^{(\ell)} \alpha_{d2}^{(\ell)}}$ takes on, because we may be able to simplify the $\ln I_0(\cdot)$ operation if the argument is often very small or very large. To this aim, we compute the average value of $\sqrt{X_{d1}^{(\ell)} X_{d2}^{(\ell)}}$ for an alternative with signal present. Since, from equation (C-10),

$$\rho_i(x_1, x_2) = A \exp(-B(x_1 + x_2)) I_0(C\sqrt{x_1 x_2}), \quad x_1, x_2 > 0, \quad (C-16)$$

where

$$\begin{aligned}
 A &= \frac{1}{1+2R} \frac{1}{\sigma_n^4} \\
 B &= \frac{1+R}{1+2R} \frac{1}{\sigma_n^2} \\
 C &= \frac{R}{1+2R} \frac{2}{\sigma_n^2} ,
 \end{aligned} \tag{C-17}$$

we have

$$m \equiv \overline{\sqrt{x_1 x_2}} = \iint_0^\infty dx_1 dx_2 \sqrt{x_1 x_2} A \exp(-B(x_1 + x_2)) I_0(C\sqrt{x_1 x_2}). \tag{C-18}$$

By letting $x_2 = t^2$, equation (C-18) is converted into

$$m = 2 \iint_0^\infty dx_1 dt \sqrt{x_1} t^2 A \exp(-B(x_1 + t^2)) I_0(C\sqrt{x_1} t). \tag{C-19}$$

Employment of reference 3, 6.631 1, enables the evaluation of the integral on t and yields

$$m = \frac{\sqrt{\pi}}{2} \frac{A}{B^{3/2}} \int_0^\infty dx_1 \sqrt{x_1} \exp(-Bx_1) F_1\left(\frac{3}{2}; 1; \frac{C^2}{4B} x_1\right). \tag{C-20}$$

Then, we employ reference 3, 7.621 4, to obtain

$$\begin{aligned}
 m &= \frac{\pi}{4} \frac{A}{B^3} F\left(\frac{3}{2}, \frac{3}{2}; 1; \frac{C^2}{4B^2}\right) \\
 &= \frac{\pi}{4} \sigma_n^2 \frac{(1+2R)^2}{(1+R)^3} F\left(\frac{3}{2}, \frac{3}{2}; 1; \left(\frac{R}{1+R}\right)^2\right).
 \end{aligned} \tag{C-21}$$

The last step is by use of equation (C-17). Then reference 3,

9.131 1, yields

$$m = \frac{\pi}{4} \sigma_n^2 (1+R) F\left(-\frac{1}{2}, -\frac{1}{2}; 1; \left(\frac{R}{1+R}\right)^2\right). \quad (C-22)$$

That is,

$$\overline{\sqrt{X_{d1}^{(l)} X_{d2}^{(l)}}} = \left\{ \begin{array}{l} \frac{\pi}{4} \sigma_n^2 \text{ if no signal in alternative } l \\ \frac{\pi}{4} \sigma_n^2 (1+R) F\left(-\frac{1}{2}, -\frac{1}{2}; 1; \left(\frac{R}{1+R}\right)^2\right) \text{ if signal in} \\ \text{alternative } l \end{array} \right\}. \quad (C-23)$$

There follows immediately, by means of equation (C-15), that the average value of the argument of $\ln I_0$ in equation (C-14) is given by

$$\overline{2\sqrt{\alpha_{d1}^{(l)} \alpha_{d2}^{(l)}}} = \left\{ \begin{array}{l} \frac{\pi}{2} \frac{R}{1+2R} \text{ if no signal in alternative } l \\ \frac{\pi}{2} \frac{R(1+R)}{1+2R} F\left(-\frac{1}{2}, -\frac{1}{2}; 1; \left(\frac{R}{1+R}\right)^2\right) \text{ if signal in} \\ \text{alternative } l \end{array} \right\}. \quad (C-24)$$

From this result, we conclude that if $R \ll 1$, all the mean values in equation (C-24) are much less than 1, and the expansion in equation (18) is valid. Alternatively, if $R \gg 1$, since the F function approaches $4/\pi$ as $R \rightarrow \infty$ (reference 3, 9.122 1), we conclude that the mean value for the signal-present alternative is much larger than 1, whereas the mean value for the other alternatives is $\pi/4$. Although this latter value is not larger than 1, we don't know a priori which alternative contains the signal, and we must, therefore, go along with the signal-bearing alternative and use the approximation in equation (21) for all alternatives, for large R. Considering the fact that for large R the variable dominating the maximum comparison in equation (C-14) virtually always will be the signal-bearing alternative anyway (if signal present), the approximate rule of equation (22) is virtually optimum, for large R.

Appendix D

DERIVATION OF CHARACTERISTIC FUNCTION
FOR PARTIALLY DEPENDENT SIGNAL FADING

The starting point for this derivation is the conditional characteristic function (A-9) for different signal samples on the K intervals:

$$f_{\alpha_d}(\xi | \{s_{dk}\}) = (1 - i\xi\sigma_n^2)^{-K} \exp\left(\frac{i\xi}{1 - i\xi\sigma_n^2} \sum_{k=1}^K |s_{dk}|^2\right). \quad (D-1)$$

We express collection $\{s_{dk}\}$ in terms of their real and imaginary parts according to

$$\sum_{k=1}^K |s_{dk}|^2 = \sum_{k=1}^K (x_k^2 + y_k^2), \quad (D-2)$$

and assume that the real and imaginary parts, $\{x_k\}$ and $\{y_k\}$, are samples of two independent zero-mean Gaussian processes $x(t)$ and $y(t)$. Because of the independence, the average of the exponential in (D-1) can be expressed as

$$\overline{\exp\left(\nu \sum_{k=1}^K |s_{dk}|^2\right)} = \overline{\exp\left(\nu \sum_{k=1}^K (x_k^2 + y_k^2)\right)}$$

$$= \left[\int \dots \int dx_1 \dots dx_K \exp\left(\nu \sum_{k=1}^K x_k^2\right) p(x_1, \dots, x_K) \right]^2, \quad (D-3)$$

where

$$\nu \equiv \frac{i\xi}{1 - i\xi\sigma_n^2}. \quad (D-4)$$

AD-A047 289

NAVAL UNDERWATER SYSTEMS CENTER NEW LONDON CONN NEW --ETC F/G 17/2
OPERATING CHARACTERISTICS FOR DETECTION OF A FADING SIGNAL WITH--ETC(U)
OCT 77 A H NUTTALL
NUSC-TR-5739

UNCLASSIFIED

NL

2 of 2
ADA047289



END
DATE
FILMED
1 -78
DDC

Now, for Gaussian $\{x_k\}$,

$$p(x_1, \dots, x_k) = (2\pi)^{-k/2} (\det C)^{-1/2} \exp\left[-\frac{1}{2} X^T C^{-1} X\right], \quad (D-5)$$

where column matrix

$$X = [x_1, \dots, x_k]^T \quad (D-6)$$

and square matrix

$$C = \left[\begin{array}{cc} x_k & x_l \\ x_k & x_l \end{array} \right]_1^k \quad (D-7)$$

Then, equation (D-3) becomes

$$\overline{\exp\left(\nu \sum_{k=1}^k |s_{dk}|^2\right)} =$$

$$\left\{ \int dX (2\pi)^{-k/2} (\det C)^{-1/2} \exp\left[-\frac{1}{2} X^T (C^{-1} - 2\nu I) X\right] \right\}^2 \quad (D-8)$$

Upon employment of the integral

$$\int dX \exp\left[-\frac{1}{2} X^T M X\right] = (2\pi)^{k/2} / (\det M)^{1/2}, \quad (D-9)$$

(which follows from equation (D-5) when we remember that p must have unit volume for any positive definite matrix C), equation (D-8) becomes

$$\overline{\exp\left(\nu \sum_{k=1}^k |s_{dk}|^2\right)} = \left[\det(I - 2\nu C) \right]^{-1}. \quad (D-10)$$

Now

$$\det(C - \lambda I) = \prod_{k=1}^k (\lambda_k^{(k)} - \lambda), \quad (D-11)$$

where $\{\lambda_k^{(x)}\}$ are the eigenvalues of C. Therefore,

$$\det(I - 2\nu C) = (-2\nu)^K \det\left(C - \frac{1}{2\nu} I\right) = \prod_{k=1}^K (1 - 2\nu \lambda_k^{(x)}). \quad (D-12)$$

Combining equations (D-1), (D-4), and (D-10), we get

$$\begin{aligned} f_{x_d}(\xi) &= (1 - i\xi\sigma_n^2)^{-K} / \prod_{k=1}^K \left(1 - \frac{i\xi 2}{1 - i\xi\sigma_n^2} \lambda_k^{(x)}\right) \\ &= \left[\prod_{k=1}^K \left\{ 1 - i\xi (\sigma_n^2 + 2\lambda_k^{(x)}) \right\} \right]^{-1}. \end{aligned} \quad (D-13)$$

Then, from equation (A-1),

$$f_{x_1}(\xi) = \left[\prod_{k=1}^K \left\{ 1 - i\xi (\sigma_n^2 + 2\lambda_k^{(x)}) \right\} \right]^{-D}, \quad (D-14)$$

which is the characteristic function of the decision variable with signal present in it. This result includes equation (A-13) as a special case.

REFERENCES

1. A. H. Nuttall, Operating Characteristics for Detection of a Fading Signal in M Alternative Locations with D-Fold Diversity, NUSC Technical Report 4793, 20 August 1974.
2. A. H. Nuttall, Alternate Forms and Computational Considerations for Numerical Evaluation of Cumulative Probability Distributions Directly from Characteristic Functions, NUSC Technical Report 3012, 12 August 1970.
3. I. S. Gradshteyn and I. M. Ryzhik, Table of Integrals, Series, and Products, Academic Press, New York, 1965.

INITIAL DISTRIBUTION LIST

Addressee	No. of Copies
ONR, Code 480, 410	3
CNO, OP-941, -96	2
CNM, MAT-03B, -03L4, -0302	3
NRL	1
NAVOCEANO, Code 02, 7200	2
NAVELEX, Code 03, PME-117, -108	3
NAVSEA, SEA-03C, -032, -06H1-31, -06H2, -09G3(4), -661E	9
NAVAIRDEVCEN (R. DaFrico)	1
NAVWPNSCEN	1
NAVCOASTSYSLAB	1
NELC	1
NOSC, (D. Marsh)	2
NAVSEC, SEC-6034	1
NISC	1
NAVPGSCOL	1
APL/UW, Seattle	1
ARL/PENN STATE, State College	1
CENTER FOR NAVAL ANALYSES (ACQUISITION UNIT)	1
DDC, Alexandria	12
DEFENSE INTELLIGENCE AGENCY	1
MARINE PHYSICAL LAB, Scripps	1
NOAA/ERL	1
NATIONAL RESEARCH COUNCIL (COMMITTEE UNDERSEA WARFARE)	1
WEAPON SYSTEM EVALUATION GROUP	1
WOODS HOLE OCEANOGRAPHIC INSTITUTION	1